

**ADVERTIMENT.** L'accés als continguts d'aquesta tesi doctoral i la seva utilització ha de respectar els drets de la persona autora. Pot ser utilitzada per a consulta o estudi personal, així com en activitats o materials d'investigació i docència en els termes establerts a l'art. 32 del Text Refós de la Llei de Propietat Intel·lectual (RDL 1/1996). Per altres utilitzacions es requereix l'autorització prèvia i expressa de la persona autora. En qualsevol cas, en la utilització dels seus continguts caldrà indicar de forma clara el nom i cognoms de la persona autora i el títol de la tesi doctoral. No s'autoritza la seva reproducció o altres formes d'explotació efectuades amb finalitats de lucre ni la seva comunicació pública des d'un lloc aliè al servei TDX. Tampoc s'autoritza la presentació del seu contingut en una finestra o marc aliè a TDX (framing). Aquesta reserva de drets afecta tant als continguts de la tesi com als seus resums i índexs.

**ADVERTENCIA.** El acceso a los contenidos de esta tesis doctoral y su utilización debe respetar los derechos de la persona autora. Puede ser utilizada para consulta o estudio personal, así como en actividades o materiales de investigación y docencia en los términos establecidos en el art. 32 del Texto Refundido de la Ley de Propiedad Intelectual (RDL 1/1996). Para otros usos se requiere la autorización previa y expresa de la persona autora. En cualquier caso, en la utilización de sus contenidos se deberá indicar de forma clara el nombre y apellidos de la persona autora y el título de la tesis doctoral. No se autoriza su reproducción u otras formas de explotación efectuadas con fines lucrativos ni su comunicación pública desde un sitio ajeno al servicio TDR. Tampoco se autoriza la presentación de su contenido en una ventana o marco ajeno a TDR (framing). Esta reserva de derechos afecta tanto al contenido de la tesis como a sus resúmenes e índices.

**WARNING.** The access to the contents of this doctoral thesis and its use must respect the rights of the author. It can be used for reference or private study, as well as research and learning activities or materials in the terms established by the 32nd article of the Spanish Consolidated Copyright Act (RDL 1/1996). Express and previous authorization of the author is required for any other uses. In any case, when using its content, full name of the author and title of the thesis must be clearly indicated. Reproduction or other forms of for profit use or public communication from outside TDX service is not allowed. Presentation of its content in a window or frame external to TDX (framing) is not authorized either. These rights affect both the content of the thesis and its abstracts and indexes.



Departament d'Enginyeria Química, Biològica i Ambiental

Escola d'Enginyeria

GICOM (Composting Research Group)

PhD in Environmental Science and Technology

# **Production of Biostimulant and Biopesticide through Solid-State Fermentation Using Green Waste**

PhD Thesis

Golafarin Ghoreishi

Supervised by

Xavier Font

Raquel Barrena

Bellaterra, Barcelona

September 2024



Xavier Font Segura, catedràtic laboral del Departament d'Enginyeria Química, Biològica i Ambiental de la Universitat Autònoma de Barcelona i Raquel Barrena Gómez, professora agregada del Departament d'Enginyeria Química, Biològica i Ambiental de la Universitat Autònoma de Barcelona,

Certifiquem:

que GOLAFARIN GHOREISHI ha realitzat sota la nostra direcció el treball “**Production of Biostimulant and Biopesticide through Solid-State Fermentation Using Green Waste**”, que es presenta en aquesta memòria i que constitueix la seva Tesi per optar al Grau de Doctor.

I, per a que se'n tingui coneixement i consti als efectes oportuns, firmem el present document.

Bellaterra, setembre de 2024

Dr. Xavier Font Segura.

Dra. Raquel Barrena Gómez

هرچيز که در جستجوي آني آني

*“What you seek is seeking you”*

Rumi

## **Acknowledgement**

I officially thank the Composting Research Group (GICOM), especially Antoni Sánchez for providing the financial support to conduct the thesis (Project Fertilab, PLEC2022-009252, Ministerio de Ciencia e Innovacion, Spain).

I am close to the end of the strangest period of my life. A time filled with challenges, new and exciting experiences, yet also moments of fear and pain. It was a time full of change and growth. This journey was not just about pursuing a PhD for me, which in itself carries a lot of difficulty. Along with starting my PhD, I also began the experience of moving away from home and adapting to life in a new country. Despite the many hardships, as I stand at the close of this chapter, I feel a deep sense of joy and accomplishment. I am deeply grateful for all the bittersweet experiences that contributed to my personal growth. I am thankful to God for placing kind people in my path throughout this journey, whose presence provided me with encouragement and strength. Their support has been the greatest blessing of all.

I would like to express my gratitude to my supervisors, Xavi and Raquel, for their guidance, support and encouragement during these four years. Having nice and supportive supervisors makes the PhD journey much more enjoyable and I was really lucky to have mentors like you. Your patience and understanding to help me learn from my mistakes have been invaluable. Thank you for making this experience one that I will carry with me for the rest of my life.

Working in GICOM has been a wonderful experience filled with learning, a strong sense of community, and lasting friendships. It has been an honor to be part of this incredible team. I would like to take this opportunity to express my thanks to the head of the group, Toni for his helpful

guidance as well as to Professors Adriana, Teresa, and Javi for their support throughout my time here.

During this journey I have met a lot of kind people whose friendship have the toughest moments of PhD pleasant. I have shared a countless memorable moment with them which I will never forget. At this point I want to thank all of them. Ahmad, thank you for teaching me HPLC and thank you for all your help and guidance, it was an honor working with you. Arnau, thank you for teaching me to work with Trichoderma and answering my endless questions during my stay in Copenhagen. I always appreciate your understanding and empathy. Esther, thank you for always being helpful and considerate. I am grateful to have your friendship. Nathaly, we started PhD together and having all the difficult moments together and your courage and passion inspired me a lot. My lab mates of GICOM: Anna, Nico, José, Carlos, Ali, Jana, Elena, Marta, Michel, David, Laila, Natalia, and Fabiola, thank you all for making lab work more fun. My friends in the office: Pili, Pia, CongCong, and Mengqi, thank you for making pleasant memories in the office. Shamim, I am really happy to have a friend like you. Talking to you has always been a source of comfort for me.

I would also like to thank the laboratory technicians of the department Manuel, Pili, and Rosi for their help and guidance and all the people of the department, the students, the professors and the staff. Working in such a warm and welcoming environment was a great chance.

Finally, I would like to thank my family for their unconditional love, encouragement, and inspiration. Being far from you was difficult, but it strengthened my belief that you would never stop supporting me. To my parents for always being there to cheer me up. Your sacrifices have been the foundation of my success, and I am forever indebted to you. To my brothers and their wives, thank you for your support and for always reminding me to find joy in the little moments.

A heartfelt thank you to the best friend in my life, my husband, Mohammad Reza. Without you, I would not be where I am today. I am deeply grateful for your unwavering support, understanding, and patience.

## Thesis Summary

This thesis focuses on the use solid state fermentation (SSF) as an approach to produce plant biostimulant and biopesticide using green waste. This study has been conducted in Composting Research Group (GICOM) at Universitat Autònoma de Barcelona (UAB) and is the first work focusing on the production of biostimulant within the research group and, as well as the first work reported green waste valorization through SSF in literature. The research utilized green waste, including grass clippings and tree pruning collected from the UAB campus, as substrates. *Trichoderma harzianum* was used as the inoculum to produce the biostimulant indole-3-acetic acid (IAA) and the biopesticide in the form of conidial spores through SSF.

The first part of the results, presented in Chapter 4, corresponds to the preliminary tests to validate and optimize the process. Experiments in this chapter were conducted using 0.5 L packed bed reactors. Initially, the feasibility of SSF using *T.harzianum* to produce IAA and spores on grass and pruning waste was assessed. Subsequently, various parameters, including the proportions of grass and pruning waste, moisture content, and tryptophan concentration (as the precursor of IAA production in the SSF) were analyzed to develop a model for optimizing the simultaneous production of IAA and spores. The model's optimized conditions were grass content at 56% and pruning waste at 44% of dry matter (DM), moisture at 74%, and tryptophan (Trp) concentration at 0.43% (w/w). Additionally, the effects of temperature and fermentation time on bioproducts obtention were investigated. The time-course experiments revealed that maximum IAA production occurred on day 3 of fermentation, reaching 101.4  $\mu\text{g g}^{-1}$  DM, while spore production peaked on day 7 at  $3.0 \times 10^9$  spores  $\text{g}^{-1}$  DM. Further experiments showed that the produced IAA can be consumed by *T.harzianum*. Finally, a preliminary germination test was conducted and presented the effectiveness of the SSF final product on the germination of cucumber (*Cucumis sativus*) seeds.



Chapter 5 presents the second part of the results, focusing on SSF for the production of IAA and conidia at bench scale using a 22 L packed bed reactor, and also exploring the use of a sequential batch operation (SBO) as an operational strategy. The process was conducted under the same conditions established for the 0.5 L reactor. However, preliminary SSF results at the 22 L scale indicated that pruning waste was not a suitable bulking agent, as it failed to provide adequate porosity. When pruning waste was used, the production of IAA and spores was  $62.3 \mu\text{g g}^{-1} \text{DM}$  and  $9.5 \times 10^8 \text{ spores g}^{-1} \text{DM}$ , respectively. In contrast, substituting pruning waste with wood chips as a bulking agent increased porosity to nearly 70%, which substantially improved productivity, with IAA and spore production rising to  $119.9 \mu\text{g g}^{-1} \text{DM}$  and  $1.3 \times 10^9 \text{ spores g}^{-1} \text{DM}$ , respectively. These findings suggest that porosity is a critical factor in SSF performance at larger scales. Additionally, the use of the sequential batch operation strategy was unsuccessful, highlighting the need for new strategies to reduce contamination issues arising from the use of real waste and the complex composition of green waste. Furthermore, a series of experiments were conducted to monitor the spore germination of *T.harzianum* with different concentrations of IAA and Trp. According to the obtained results, the germination rate of spores increased slightly with lower concentrations of IAA, while in higher concentrations of IAA, spore germination did not occur. Similar results obtained when different concentrations of Trp was applied.

The third part of the results (Chapter 6) presents the outcome of IAA and conidia production in the tray bioreactor. In this configuration, IAA production reached  $201.3 \mu\text{g g}^{-1} \text{DM}$ , which is higher than the levels achieved in the 22 L packed bed reactor. The maximum conidia production in the tray bioreactor was  $1.1 \times 10^9 \text{ spores g}^{-1} \text{DM}$ . A comparison between the tray and 22 L bioreactors suggested that the tray bioreactor is a more advantageous configuration for fungal SSF biostimulant production using green waste, due to the different aeration system in the tray setup.

However, there was variability in the results between experiments carried out under same conditions. To better understand this variability, principal component analysis (PCA) was used to examine the relationship between key process parameters. The analysis revealed that the temperature, particularly in the latter stages of the process, was related to the final IAA levels. As a result, a process strategy based on an initial temperature of 25-21°C and followed by a lower temperature regimen (18°C), was developed to prevent IAA degradation and enhance production.

Overall, the outcome of this thesis represents a new approach to valorize GW to produce biostimulant and biopesticide agents in the framework of circular bioeconomy.

## Resumen de la tesis

Esta tesis se centra en el uso de la fermentación en estado sólido (FES) como un enfoque para producir bioestimulantes y biopesticidas a partir de residuos verdes. El estudio se llevó a cabo en el Grupo de Investigación en Compostaje (GICOM) de la Universitat Autònoma de Barcelona (UAB) siendo el primer trabajo del grupo enfocado en la producción de bioestimulantes así como el primer trabajo reportado en la literatura sobre la valorización del residuo verde o vegetal (RV) a través de FES. En la investigación se utilizaron residuos verdes, incluyendo restos césped y poda de árboles del campus de la UAB, como sustratos. Se usó *Trichoderma harzianum* como inóculo para producir el bioestimulante ácido indol-3-acético (IAA) y el biopesticida en forma de esporas conidiales mediante FES.

La primera parte de los resultados, presentada en el Capítulo 4, corresponde a las pruebas preliminares para validar y optimizar el proceso. Los experimentos en este capítulo se realizaron utilizando reactores de lecho empacado de 0.5 L. Inicialmente, se evaluó la viabilidad de la FES utilizando *T.harzianum* para producir IAA y esporas en residuos de césped y poda. Posteriormente, se analizaron diversos parámetros, incluidos las proporciones de residuo de césped y poda, el contenido de humedad y la concentración de triptófano (utilizado como precursor de la producción de IAA en la FES), para desarrollar un modelo que optimizara la producción simultánea de IAA y esporas. Las condiciones optimizadas del modelo fueron: contenido de residuo de césped al 56% y poda al 44% de materia seca (MS), humedad al 74% y concentración de triptófano (Trp) al 0.43% (p/p). Además, se investigaron los efectos de la temperatura y el tiempo de fermentación en la obtención de los bioproductos objeto de estudio. Los experimentos mediante un seguimiento a lo largo del tiempo del proceso, revelaron que la producción máxima de IAA tuvo lugar el día 3 de

fermentación, alcanzando  $101.4 \mu\text{g g}^{-1} \text{MS}$ , mientras que la producción de esporas alcanzó su pico el día 7 con  $3.0 \times 10^9$  esporas  $\text{g}^{-1} \text{MS}$ . Experimentos adicionales mostraron que el IAA producido puede ser consumido por *T.harzianum*. Finalmente, se llevó a cabo una prueba preliminar de germinación que mostró la efectividad del producto final de FES en la germinación de semillas de pepino (*Cucumis sativus*).

El Capítulo 5 presenta la segunda parte de los resultados, centrándose en la FES para la producción de IAA y conidios a bench scale utilizando un reactor de lecho empacado de 22 L, y también explorando la operación del reactor en modo de lotes secuenciales como estrategia de operación. El proceso se realizó bajo las mismas condiciones establecidas para el reactor de 0.5 L. Sin embargo, los resultados preliminares de la FES a escala de 22 L indicaron que los residuos de poda no eran un agente estructurante adecuado, ya que no proporcionaban la porosidad suficiente y eran más propensos a la contaminación. Cuando se utilizaron residuos de poda, la producción de IAA y esporas fue de  $62.3 \mu\text{g g}^{-1} \text{MS}$  y  $9.5 \times 10^8$  esporas  $\text{g}^{-1} \text{MS}$ , respectivamente. En cambio, la sustitución de los residuos de poda por virutas de madera como agente estructurante aumentó la porosidad a casi el 70%, lo que mejoró sustancialmente la productividad, con la producción de IAA y esporas llegando a alcanzar los valores de  $119.9 \mu\text{g g}^{-1} \text{MS}$  y  $1.3 \times 10^9$  esporas  $\text{g}^{-1} \text{MS}$ , respectivamente. Estos hallazgos sugieren que la porosidad es un factor crítico en el rendimiento de la SSF a escalas mayores. Por su parte, el uso de la estrategia de lote secuencial no tuvo éxito, lo que resalta la necesidad de nuevas estrategias para reducir los problemas de contaminación derivados de trabajar con residuos reales y heterogéneos como el residuo verde. Asimismo, se realizaron una serie de experimentos para determinar la germinación de esporas de *T.harzianum* con diferentes concentraciones de IAA y Trp. Según los resultados obtenidos, la tasa de germinación de esporas aumentó ligeramente con concentraciones más bajas de IAA, mientras que

a concentraciones más altas de IAA, no se observó la germinación de esporas. Se obtuvieron también resultados similares al aplicar diferentes concentraciones de Trp.

La tercera parte de los resultados (Capítulo 6) presenta los resultados de la producción de IAA y conidios en un reactor de bandejas. En esta configuración, la producción de IAA alcanzó  $201.3 \mu\text{g g}^{-1}$  MS, valor superior a los niveles alcanzados en el reactor de lecho empacado de 22 L. La producción máxima de conidios en el reactor de bandejas fue de  $1.1 \times 10^9$  esporas  $\text{g}^{-1}$  MS. La comparación entre los reactores de bandejas y lecho empacado de 22 L sugiere que el de bandejas es una configuración más adecuada para la producción de bioestimulantes fúngicos mediante SSF usando residuos verdes, debido al diferente sistema que ofrece la configuración de bandejas. Sin embargo, se observó cierta variabilidad en los resultados entre las repeticiones de las fermentaciones. Para comprender mejor esta variabilidad, se utilizó un análisis de componentes principales (PCA) para examinar la relación entre los parámetros clave del proceso. El análisis reveló que la temperatura, especialmente en las etapas finales del proceso, estaba relacionada con los niveles finales de IAA. Como resultado, se desarrolló una estrategia de proceso basada en un régimen de temperatura inicial de  $25\text{-}21^\circ\text{C}$  y controlada posteriormente a una temperatura inferior ( $18^\circ\text{C}$ ) para prevenir la degradación de IAA y mejorar su producción.

Los resultados de esta tesis representan un nuevo enfoque para la valorización del residuo verde con el objetivo de producir productos con propiedades bioestimulantes y biopesticidas en el marco de la bioeconomía circular.

## Resum de la tesi

Aquesta tesi se centra en l'ús de la fermentació en estat sòlid (FES) com un enfocament per produir bioestimulants i biopesticides a partir de residus verds. L'estudi es va dur a terme en el Grup de Recerca en Compostatge (GICOM) de la Universitat Autònoma de Barcelona (UAB) sent el primer treball del grup enfocat en la producció de bioestimulants així com el primer treball reportat en la literatura sobre la valorització del residu verd o vegetal (RV) a través de FES. En la investigació es van utilitzar residus verds, incloent restes gespa i poda d'arbres del campus de la UAB, com a substrats. Es va utilitzar *Trichoderma harzianum* com a inòcul per produir el bioestimulant àcid indol-3-acètic (IAA) i el biopesticida en forma d'espores conidials mitjançant FES.

La primera part dels resultats, presentada en el Capítol 4, correspon a les proves preliminars per validar i optimitzar el procés. Els experiments en aquest capítol es van realitzar utilitzant reactors de llit empaquetat de 0.5 L. Inicialment, es va avaluar la viabilitat de la FES utilitzant *T.harzianum* per produir IAA i espores en residus de gespa i poda. Posteriorment, es van analitzar diversos paràmetres, inclosos les proporcions de residu de gespa i poda, el contingut d'humitat i la concentració de triptòfan (utilitzat com a precursor de la producció d'IAA a la FES), per desenvolupar un model que optimitzés la producció simultània d'IAA i espores. Les condicions optimitzades del model van ser: contingut de residu de gespa al 56% i poda al 44% de matèria seca (MS), humitat al 74% i concentració de triptòfan (Trp) al 0.43% (p/p). A més, es van investigar els efectes de la temperatura i el temps de fermentació en l'obtenció dels bioproductes objecte d'estudi. Els experiments mitjançant un seguiment al llarg del temps del procés, van revelar que la producció màxima d'IAA va tenir lloc el dia 3 de fermentació, assolint  $101.4 \mu\text{g g}^{-1}$  MS, mentre que la producció d'espores va assolir el seu pic el dia 7 amb  $3.0 \times 10^9$  espores  $\text{g}^{-1}$  MS. Experiments

addicionals van mostrar que l'IAA produït pot ser consumit per *T.harzianum*. Finalment, es va dur a terme una prova preliminar de germinació que va mostrar l'efectivitat del producte final de FES en la germinació de llavors de cogombre (*Cucumis sativus*).

El Capítol 5 presenta la segona part dels resultats, centrant-se en la FES per a la producció d'IAA i amb un reactor de llit empaquetat de 22 L, també explorant l'operació del reactor en mode de lots seqüencials com a estratègia d'operació. El procés es va realitzar sota les mateixes condicions establertes per al reactor de 0.5 L. No obstant això, els resultats preliminars de la FES a escala de 22 L van indicar que el residu de poda no eren un agent estructurant adequat, ja que no proporcionaven la porositat suficient i a més a més era més propens a la contaminació. A l'utilitzar residu de poda, la producció d'IAA i espores va ser de  $62.3 \mu\text{g g}^{-1} \text{MS}$  y  $9.5 \times 10^8$  esporas  $\text{g}^{-1} \text{MS}$ , respectivament. En canvi, la substitució dels residus de poda per encenalls de fusta com a agent estructurant va augmentar la porositat a gairebé el 70%, la qual cosa va millorar substancialment la productivitat, amb la producció d'IAA i espores arribant a assolir els valors de  $119.9 \mu\text{g g}^{-1} \text{MS}$  y  $1.3 \times 10^9$  esporas  $\text{g}^{-1} \text{MS}$ , respectivament. Aquestes troballes suggereixen que la porositat és un factor crític en el rendiment de la SSF a escales majors. Per la seva banda, l'ús de l'estratègia de lot seqüencial no va tenir èxit, cosa que ressalta la necessitat de noves estratègies per reduir els problemes de contaminació derivats de treballar amb residus reals i heterogenis com el residu verd. Així mateix, es van realitzar una sèrie d'experiments per determinar la germinació d'espores de *T.harzianum* amb diferents concentracions d'IAA i Trp. Segons els resultats obtinguts, la taxa de germinació d'espores va augmentar lleugerament amb concentracions més baixes d'IAA, mentre que a concentracions més altes d'IAA, no es va observar la germinació d'espores. Es van obtenir també resultats similars en aplicar diferents concentracions de Trp.

La tercera part dels resultats (Capítol 6) presenta els resultats de la producció d'IAA i conidis en un reactor de safates. En aquesta configuració, la producció d' IAA va assolir  $201.3 \mu\text{g g}^{-1}$  MS, valor superior als nivells assolidor en el reactor de llit empaquet de 22 L. La producció màxima de conidis al reactor de safates va ser de  $1.1 \times 10^9$  esporas  $\text{g}^{-1}$  MS. La comparació entre els reactors de safates i llit empaquet de 22 L suggereix que el de safates és una configuració més adequada per a la producció de bioestimulants fúngics mitjançant SSF usant residus verds, a causa del diferent sistema que ofereix la configuració de safates. Tanmateix, es va observar certa variabilitat en els resultats entre les repeticions de les fermentacions. Per comprendre millor aquesta variabilitat, es va utilitzar una anàlisi de components principals (PCA) per examinar la relació entre els paràmetres clau del procés. L'anàlisi va revelar que la temperatura, especialment en les etapes finals del procés, estava relacionada amb els nivells finals d'IAA. Com a resultat, es va desenvolupar una estratègia de procés basada en un règim de temperatura inicial dels  $25\text{-}21^\circ\text{C}$  i controlada posteriorment a una temperatura inferior ( $18^\circ\text{C}$ ) per prevenir la degradació d'IAA i millorar la seva producció.

Els resultats d' aquesta tesi representen un nou enfocament per a la valorització del residu verd amb l' objectiu de produir productes amb propietats bioestimulants i biopesticides en el marc de la bioeconomia circular.



# SOLID STATE FERMENTATION

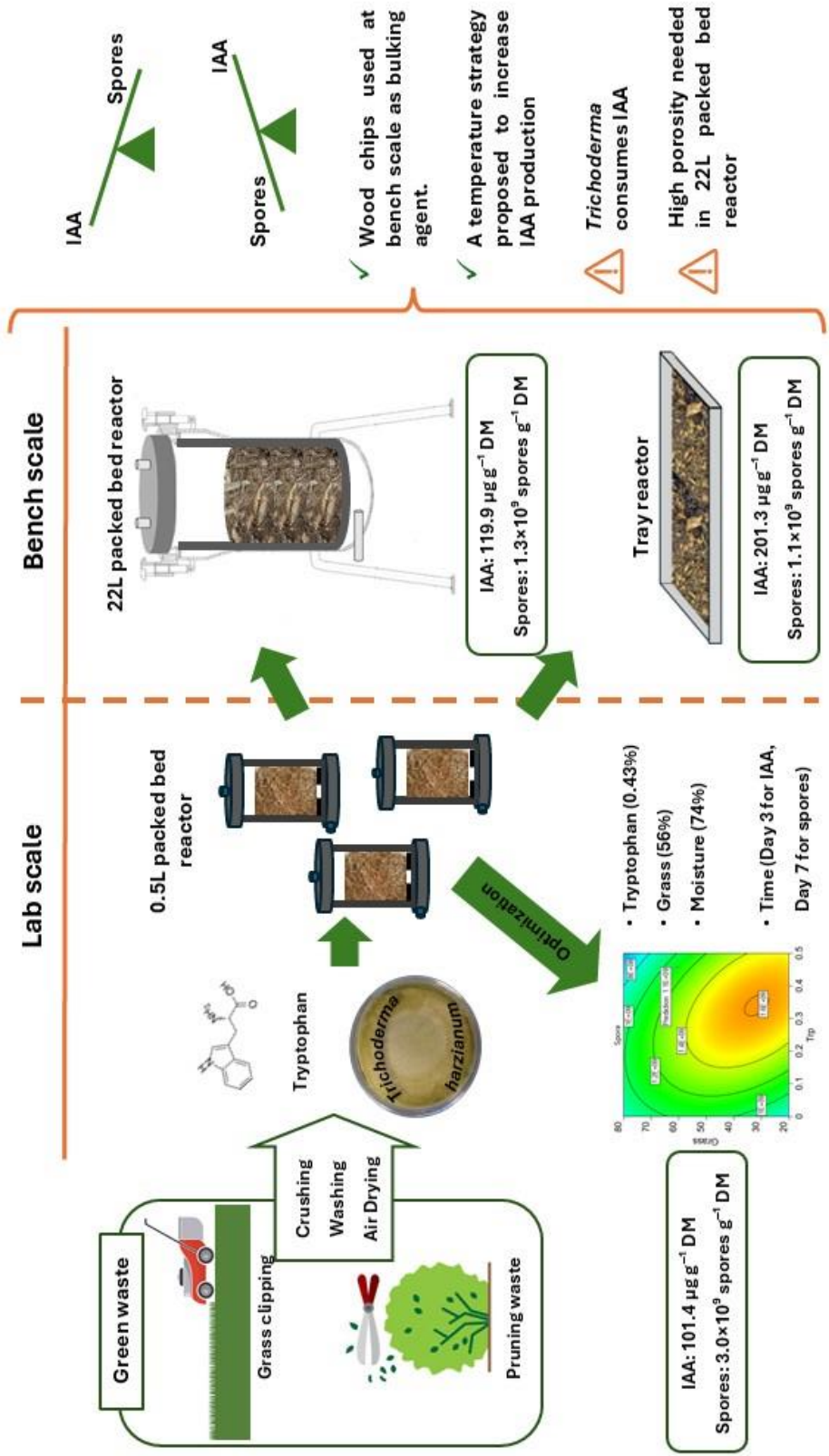


# Table of Contents

Chapter 1	Introduction .....	31
1.1	Circular economy .....	32
1.2	The potential of green waste .....	32
1.2.1	Green Waste Composition.....	33
1.2.2	Strategies to valorize GW.....	35
1.2.3	Pretreatment of GW .....	37
1.3	Biostimulant and its promising role in sustainable agriculture .....	38
1.3.1	Biostimulant categorization.....	40
1.3.2	Indole-3-acetic acid.....	43
1.3.3	Trichoderma and its role as biostimulant and biopesticide .....	45
1.4	The advantages of solid-state fermentation to produce biopesticide and biostimulant .....	46
1.4.1	Reactor Configuration.....	48
Chapter 2	Objectives.....	52
Chapter 3	Materials and Methods.....	54
3.1	Materials.....	55
3.1.1	Substrates.....	55
3.1.2	Fungal strains.....	57
3.2	Solid-State Fermentation (SSF).....	58
3.2.1	0.5 L packed bed reactor setup .....	58
3.2.2	22 L packed bed reactor setup .....	61
3.2.3	Tray bioreactor setup .....	64
3.3	Seed Germination test.....	65
3.4	Germination of fungal spores.....	66
3.5	Analytical methods .....	67
3.5.1	Analysis of oxygen consumption.....	67
3.5.2	Spore counting.....	69
3.5.3	IAA and Trp analysis .....	70
3.5.4	Gas measurements .....	72
3.5.5	Monitoring the contamination .....	72
3.5.6	Microbial identification.....	72

3.5.7	Moisture, dry matter and organic matter.....	73
3.5.8	pH and conductivity .....	74
3.5.9	Porosity, water holding capacity and C/N analysis .....	74
3.5.10	Statistical analysis.....	76
Chapter 4	Green Waste as a Substrate to Produce Biostimulant and Biopesticide Products through Solid-State Fermentation.....	77
4.1	Overview.....	78
4.2	The materials and conditions of the experiments.....	78
4.3	Experiments.....	79
4.3.1	The effect of green waste conditioning procedures on solid state fermentation ...	79
4.3.2	The feasibility of TH growth and sporulation on grass and pruning waste .....	81
4.3.3	The effect of tryptophan on spore and IAA production.....	83
4.3.4	Optimization of IAA and spore production through SSF (a design of experiment) 85	
4.3.5	The effect of temperature on spore and IAA production .....	89
4.3.6	The effect of fermentation time on IAA and spore production .....	91
4.3.7	The fate of added IAA in SSF .....	95
4.3.8	Germination test.....	97
4.4	Conclusion.....	101
Chapter 5	Solid-State Fermentation to Produce Biostimulant Agents from Green Waste at Bench-Scale (22 L) .....	102
5.1	Overview.....	103
5.2	The materials and condition of the experiments .....	103
5.3	Experiments.....	104
5.3.1	Bench-scale SSF performance.....	104
5.3.2	SSF in sequential batch bench-scale strategy .....	122
5.3.3	Analysis of the SSF products: IAA degradation.....	127
5.3.4	The effect of temperature, IAA, and Trp on spore germination of <i>T. harzianum</i> 128	
5.4	Conclusion.....	134
Chapter 6	Enhancing the Production of Biostimulant through SSF in Tray Bioreactors .....	136
6.1	Overview.....	137
6.2	The materials and conditions of the experiments.....	137

6.3	Experiments.....	138
6.3.1	Experimental setups in tray bioreactor.....	138
6.3.2	SSF in tray experiments with low temperature .....	154
6.4	The comparison of the results obtained in 22 L packed bed reactor and tray reactor .	162
6.5	Conclusion.....	167
Chapter 7	Conclusions and Future Remarks .....	168
7.1	General conclusions.....	169
7.2	Future Works.....	171
Chapter 8	References .....	172

## List of Figures

Figure 1.1. Classification of lignocellulosic pretreatment methods (Kucharska et al., 2018). ....	37
Figure 1.2. The effects of biostimulants on plants.....	39
Figure 1.3. Trp-dependent and Trp-not-dependent biosynthesis pathways of microorganisms. TAM: tryptamine; IPA: indole-3-pyruvic acid; IAM: indole-3-acetamide; IAOx: indole-3-acetaldoxime; IAN: indole-3-acetonitrile Tang et al., 2023).....	44
Figure 1.4. The biostimulant effects of <i>Trichoderma</i> on plants via fungal-root communication. <i>Trichoderma</i> metabolites like volatile organic compounds (VOCs), auxins and ethylene regulate root development including lateral root (LR). <i>T. atroviride</i> induces the activation of plant mitogen activated protein 6 (MPK6) that translates fungal signals into root cellular responses. The stomatal aperture is affected by <i>Trichoderma</i> metabolites. The nutrient uptake increases by <i>Trichoderma</i> root stimulation and improve plant growth and productivity (López-Bucio et al., 2015). ....	46
Figure 1.5. Various reactor configurations are usually applied in SSF. (a) packed bed reactor; (b) tray reactor; (c) rotating drum reactor. ....	49
Figure 3.1 The different grass clippings and pruning waste collecting in different times of the year. a) fresh grass; b) aged grass; c) a pile of grass clipping; d) fresh pruning waste; e) aged pruning waste .....	56
Figure 3.2 a) The compost shredder used to chop the grass clipping; b,c) air drying the grass in a biodrying reactor .....	56
Figure 3.3 <i>Trichoderma harzianum</i> a) plate; b) spores.....	57
Figure 3.4. The system of SSF with 0.5L packed bed reactors .....	59
Figure 3.5 The 0.5L reactor a) set up and b) appearance. ....	60

Figure 3.6. SSF set up in 22 L reactor.....	62
Figure 3.7 Schematics photo of 22 L reactor and the distribution of sampling areas and temperature sensors from different heights. ....	63
Figure 3.8. The tray reactor. a) a schematic of the system; b) the appearance of set up.....	65
Figure 3.9. oCelloScope system for real-time monitoring of microbial growth .....	67
Figure 3.10. The peaks of Trp and IAA in the chromatography that observed in minutes 3 and 11 respectively. ....	71
Figure 4.1. Different conditioning procedures for the grass. (a) the effect of conditionings on spore production and pH. (b) The respiration profiles for the conditioning procedures. The experiments were carried out in triplicate and the error bars present standard deviations....	80
Figure 4.2. (a) Spore counts in different percentages of grass and pruning waste. (b) Respiration profile of different percentages of grass and pruning waste. The experiments were carried out in triplicate and the error bars present standard deviations.....	82
Figure 4.3. The effect of Trp (0.5%) on IAA concentration and spores. The experiments were carried out in triplicate and the error bars are standard deviations. Data from two other Trp treatments were not presented as no IAA and spore production observed.....	84
Figure 4.4. The contour profile of the predicted optimized point by the model. The moisture was set at 74%.....	89
Figure 4.5. The effect of temperature on (a) sOUR and (b) spores and IAA production. The experiments were replicated three times and error bars are standard deviation. ....	90
Figure 4.6. The results of a 10-day time course experiment for <i>T. harzianum</i> without Trp. The error bars are standard deviations of the triplicated samples taken from a single reactor.....	91

Figure 4.7. The results of a 10-day time course experiment for <i>T. harzianum</i> . The error bars are standard deviations of the triplicated samples taken from a single reactor. ....	92
Figure 4.8. The results of a 10-day time course experiment for <i>T. viride</i> . The error bars are standard deviations of the triplicated samples taken from a single reactor. ....	94
Figure 4.9. The fate of IAA added to the fermentation and its effect on TH sporulation.....	96
Figure 4.10. sOUR profile in the presence and absence of IAA. ....	96
Figure 4.11. the germinated seed with different treatments after 5 days. a) treatment A, b) treatment B, c) treatment C, d) treatment IAA1, e) treatment IAA2, f) distillate water. ....	99
Figure 4.12. a) seed germinated under treatment IAA 1 with short and thick roots. b) seed germinated under treatment C. c) seed germinated with distillate water .....	100
Figure 5.1. The results of the preliminary experiment in the 22 L reactor with pruning waste as bulking agent. The error bars are the standard deviation of the samples taken from different zones of the reactor.....	105
Figure 5.2. The contamination observed in the reactor. a) The plate prepared from the samples on day 3 of fermentation, b) The plate prepared from the samples on day 7 of fermentation, c) The SSF at day 7. ....	106
Figure 5.3. a) The location of the sensors, b) The temperature profiles of the fermentation in different zones of the reactor. ....	106
Figure 5.4. The culture of the isolated colonies.....	107
Figure 5.5. 22 L reactor SSF performance using pruning waste. The error bars are the standard deviation of the samples taken from different zones of the reactor. ....	110
Figure 5.6. 22 L reactor SSF performance using wood chips. The error bars are the standard deviation of the samples taken from different zones of the reactor. ....	114

Figure 5.7. Performance of 22 L reactor SSF using different concentrations of Trp. a) Production of IAA, b) Sporulation, c) Specific oxygen uptake rate (sOUR), d) pH, e) Maximum temperature, and f) Final moisture. Different letters indicate significant differences between the zones of the reactor sampled ( $p < 0.05$ ) based on Tukey analysis. .... 119

Figure 5.8. Performance of SBO SSF strategy: (a) The profiles of IAA production, number of spores, specific oxygen uptake rate (sOUR), and temperature. The red, orange, yellow, and green dashed curves respectively correspond to the temperature profile of batch 1, batch 2, batch 3, and batch 4, while the red, orange, yellow, and green solid curves correspond to sOUR profile of batch 1, batch 2, batch 3, and batch 4, respectively. (b) Production of IAA and (c) Spores count in distinct parts of the reactor. Different letters indicate significant differences between the zones of the reactor sampled ( $p < 0.05$ ) based on Tukey analysis. .... 123

Figure 5.9. The photos of sequential batch experiment at the end of each batch and the microbial culture prepared from each batch. A1) Batch 1, A2) A normal culture of *Trichoderma harzianum* with no contamination, B1) Batch 2, B2) Plate cultured from batch 2, C1) Batch 3, C2) Plate cultured from batch 3, D1) Batch 4, D2) Plate cultured from batch 4. .... 125

Figure 5.10. IAA degradation in SSF product at room temperature. The error bars are the standard deviation of the samples taken for HPLC. .... 128

Figure 5.11. (a) Photos of *T.harzianum* spores germinating in the presence of  $1 \text{ g L}^{-1}$  IAA. After 12 hours, most of the spores disappeared and the rest accumulated in one spot. (b) Photos of *T.harzianum* spores germinating in the presence of  $0.5 \text{ g L}^{-1}$  IAA. Most of the spores disappeared after 14 hours and a few germinated after 24 hours. .... 129

Figure 5.12. Photos of *T.harzianum* spores germinating during 22 hours. .... 130



Figure 5.13. The germination percentage of <i>T.harzianum</i> spores in the presence of different concentrations of Trp and IAA at 25°C. The error bars are the standard deviation of the triplicate germination data. ....	131
Figure 5.14. The germination percentage of <i>T.harzianum</i> spores in the presence of different concentrations of Trp and IAA at 28°C. The error bars are the standard deviation of the triplicate germination data. ....	132
Figure 5.15. The germination percentage of <i>T.harzianum</i> spores in the presence of different concentrations of Trp and IAA at 30°C. The error bars are the standard deviation of the triplicate germination data. ....	133
Figure 6.1. The profiles of IAA, spores, Trp, and temperature of Experiment A. The error bars correspond to the standard deviation of sample replications taken from a single tray. ....	139
Figure 6.2 SSF in tray bioreactor. a) Initial material of the fermentation, b) Fermented material after 10 days of process, c) Fermented material from a closer view to observe <i>Trichoderma</i> . ....	139
Figure 6.3. The profiles of IAA, spores, Trp, NH <sub>3</sub> , and temperature of Experiment B. The error bars are the standard deviation of sample replications taken from a single tray. The Trp values lower than 0.5 mg g <sup>-1</sup> DM presented as zero in the graph.....	141
Figure 6.4. The profiles of IAA, spores, Trp, NH <sub>3</sub> , and temperature of Experiment C. The error bars are the standard deviation of sample replications taken from a single tray. The Trp values lower than 0.5 mg g <sup>-1</sup> DM presented as zero in the graph.....	142
Figure 6.5. The profiles of IAA, spores, Trp, and temperature of Experiment D. The error bars are the standard deviation of sample replications taken from a single tray. The Trp values lower than 0.5 mg g <sup>-1</sup> DM presented as zero in the graph.....	144

Figure 6.6. The profiles of NH <sub>3</sub> , and oxygen from points A and B of the incubator for experiment with no Trp and experiment D. ....	145
Figure 6.7. The profiles of IAA, spores, and temperature of experiment with no Trp. The error bars are the standard deviation of sample replications taken from a single tray. ....	145
Figure 6.8. All profiles of IAA, number of spores, Trp, and temperature for experiments A, B, C, and D. a) IAA, b) Number of spores, c) Trp, d) Temperature. The error bars are the standard deviation of sample replications taken from a single tray. The Trp values lower than 0.5 mg g <sup>-1</sup> DM presented as zero in the graph.....	147
Figure 6.9 The biplot of the first two components of PCA. The data have been separated based on maximum temperature: blue circles, maximum temperature of 22°C; red squares, 22.5°C; green diamonds, 23°C; and purple triangles, 23.5°C. ....	150
Figure 6.10. The linear regressions of a) IAA and spores, b) IAA and consumed Trp, c) IAA and maximum temperature, d) spores and maximum temperature, e) spores and consumed Trp, and f) maximum temperature and consumed Trp. ....	152
Figure 6.11 Performing SSF in one tray with conditions. a) SSF with 0.2% Trp, b) SSF with 0.2% (left) and 0.43 (right) % Trp, c) Final appearance of SSF tray reactor. ....	155
Figure 6.12. The profiles of IAA, spores, Trp, and temperature of experiment with 0.43% (w/w) Trp under temperature regimen 1. The error bars are the standard deviation of sample replications taken from distinct parts of the tray for an individual experiment.....	156
Figure 6.13. The profiles of IAA, spores, Trp, and temperature of experiment with 0.2% (w/w) Trp under temperature regimen 1. The error bars are the standard deviation of sample replications taken from distinct parts of the tray for an individual experiment.....	157

Figure 6.14. The profiles of NH<sub>3</sub> and oxygen from points A and B of the incubator of the experiment under temperature regimen 1. .... 158

Figure 6.15. The results of SSF under temperature regimen 2. a) The profiles of IAA, spores, Trp, and temperature. b) The profiles of NH<sub>3</sub> and oxygen from point A and B of the incubator. The error bars are the standard deviation of sample replications taken from a single tray. .... 160

## List of Tables

Table 1.1. Plant biostimulants and their mechanisms of action. PGPM: plant growth promoting microorganisms. ....	41
Table 4.1 The characteristics of the grass clipping and pruning waste used in the following experiments .....	78
Table 4.2. The treatments and results of the Box-Behnken experimental design. ....	86
Table 4.3. The p-value of the model and the parameters for spore and IAA. The created model for spore production is modified quadratic, and for IAA production was a linear model (p-value < 0.05 is significant).....	88
Table 4.4. The list of treatments used for cucumber seed germination. Each treatment was tested with three replications .....	98
Table 4.5. The results of germination tests. SG%: seed germinated percentage; RSG: relative seed germination; RGG: relative radicle growth; GI: germination index. ....	98
Table 5.1. The characteristics of the substrates used in the current chapter. G1: grass clipping batch 1; G2: grass clipping batch 2; PW: pruning waste; WC: wood chips.....	104
Table 5.2. The identification of the three isolated colonies. ....	107
Table 5.3. Different parameters were measured for the fermentation in 0.5 L and 22 L reactors PW and WC as bulking agent. IAA, Indole-3-acetic acid; sOUR, specific oxygen uptake rate; COC, cumulative oxygen consumption. <sup>a</sup> The presented values of IAA and spore productions were the maximum observed (day 3 for IAA and day 7 for spores). ....	111
Table 5.4. Characterization and the specific oxygen uptake rate (sOUR) of the substrates used in fermentation. ....	115
Table 6.1 The characteristics of the grass clipping used in the tray experiments.....	137

Table 6.2 The values of IAA, number of spores, Trp, and temperature obtained from experiments A, B, C, and D. All the values have one replication. All the values of Trp consumed that are more than 90% considered 100% for PCA and regression analysis. ....	149
Table 6.3 The eigenvalues and variance percentage of each component in PCA .....	149
Table 6.4. The R <sup>2</sup> and P value of the different regressions performed with the data from tray reactors.....	153
Table 6.5 Values obtained from fermentations conducted in the tray reactor and the 22 L reactor. ....	164
Table 6.6 The moisture content of all the tray experiments. ....	166

## List of Abbreviations

---

<b>Abbreviation</b>	<b>Definition</b>
AFP	Air filled porosity
C/N	Carbon/nitrogen ratio
CECT	Spanish Type Culture Collection
COC	Cumulative oxygen consumption
DM	Dry matter
EBIC	The European Biostimulant Industry Council
G	Grass
GI	Germination index
GW	Green Water
IAA	Indole-3-acetic acid
PCA	Principal component analysis
PGPM	Plant growth promoting microorganisms
PW	Pruning waste
RRG	Relative radicle growth
RSG	Relative seed germination
SBO	Sequential batch operation
SG	Seed germination
sOUR	Specific oxygen uptake rate
SSF	Solid state fermentation
T	Temperature

---

---

TH	<i>Trichoderma harzinum</i>
Trp	Tryptophan
TV	<i>Trichoderma viridae</i>
USD	United states dollar
WC	Wood chips

---

# Chapter 1

## Introduction

---



## 1.1 Circular economy

The concepts of circular economy and bioeconomy have been introduced as an alternative for linear economy in response to population growth, followed by an increase in demand for raw materials (Salmenperä et al., 2021; Tan and Lamers, 2021). This approach aims to extend product value, minimize waste, and keep resources within the economic cycle. In this regard, waste management, including solid waste, plays an important role in transitioning to a circular economy, shifting the perception of waste from a problem to a resource (Mujtaba et al., 2023; Salmenperä et al., 2021). Various strategies have been applied to process the waste through microbial fermentation such as solid-state fermentation and submerged fermentation. In these biological processes, municipal, industrial and agricultural solid organic wastes are used as a substrate to produce end products like enzymes, biopesticides, biosurfactants many other products that are useful in the industrial and pharmaceutical sectors (Ghoreishi et al., 2023; Leite et al., 2020; Sala et al., 2020).

## 1.2 The potential of green waste

Lignocellulosic biomass is considered the most abundant renewable raw material. It presents an attractive area of work for both industries and researchers, offering a substantial renewable feedstock for various industrial sectors such as food, energy, and chemicals. Lignocellulosic biomass includes plants and their residues from agriculture, forestry, recycling stations, and the paper, wood, and pulp industries (Blasi et al., 2023; Mujtaba et al., 2023).

One source of lignocellulose biomass that has gained less attention to be valorized within the framework of circular bioeconomy is green waste (GW), whose generation has been increasing in recent decades as the expansion of urbanization (Langsdorf et al., 2021). The scope of GW varies

## Chapter 1

by location; in some areas, it includes plant waste collected from municipal parks but not from private gardens, while in others, it encompasses waste from fruit and vegetable markets. Generally, GW is categorized as municipal waste, excluding waste generated in forests, woodlands, farms, etc. (Liu et al., 2023). Thus, GW is also known as garden waste, yard waste, or tree waste. In general, it is a mixture of plant residues collected from public municipal green spaces and private gardens including grass, leaves, branches, weeds, dead flowers, etc. that sometimes include plant roots and soil fragments (Inghels et al., 2016).

There is a lack of clear global data on GW generation due to the absence of a unified method for estimating urban green spaces worldwide. However, a report stated that in 2017, global municipal solid waste was estimated to be 2 billion tons, with GW comprising 11% of the total (Liu et al., 2023). The increasing volume of GW necessitates effective strategies for sustainable management, while offering a profitable opportunity through its valorization.

### **1.2.1 Green Waste Composition**

The composition of GW is variable depending on the geographical location, the season of collection, and the type of plants that compose the mixture. For example, the biggest fraction of GW in spring is pruning waste while in summer it mostly consists of grass clipping and in autumn and winter, more leaves are collected as GW (Liu et al., 2023). This variation causes a big heterogenicity in the physicochemical characteristics of GW that makes the recycling processes complicated. However, there are some characteristics commonly shared between all types of GW:

- High C/N ratio usually more than 25
- Low content of heavy metals such as Cd, Pb, and Ni.
- Low content of essential nutrients like N, P, K

- High content of organic matters mainly as lignocellulose (Liu et al., 2023; Reyes-Torres et al., 2018)

The main components of lignocellulose biomass, including GW, are cellulose (30–60% of dry matter), lignin (7–25% of dry matter), and hemicellulose (14–40% of dry matter) that depending on the substrate the composition of them would be considerably different (Kucharska et al., 2018; Langsdorf et al., 2021). For example, the content of cellulose and hemicellulose are high in lawn grass (41% and 36%, respectively), but the lignin content is low (8%) (Guo et al., 2015). While, the dead leaves, stalks, and pruning branches usually contain higher lignin and lower cellulose and hemicellulose. For example, the pruning of olive trees was reported to have 39% cellulose, 16% Hemicellulose, and 17% lignin (Langsdorf et al., 2021; Maria et al., 2012).

Cellulose is a linear polymer composed of D-glucose monomers linked by  $\beta$ -1,4-glycosidic bonds. These monomers form a crystalline structure that is resistant to swelling in water and enzymatic degradation. However, under high temperature and pressure, water can break the hydrogen-bonded crystalline structure and hydrolyze the  $\beta$ -1,4-glycosidic bonds, producing glucose monomers. In contrast, hemicellulose does not have a linear structure and contains fewer  $\beta$ -1,4-glycosidic bonds compared to cellulose. Its more random structure makes it less crystalline and less resistant. Hemicellulose is composed of various monomers, including D-xylose, D-mannose, D-galactose, D-glucose, L-arabinose, 4-O-methyl-glucuronic acid, D-galacturonic acid, and D-glucuronic acid, which are linked by both  $\beta$ -1,4-glycosidic and  $\beta$ -1,3-glycosidic bonds.

Lignin is an aromatic polymer synthesized from phenylpropanoid precursors. It consists of the monomers coniferyl alcohol, sinapyl alcohol, and p-coumaryl alcohol, with the relative composition varying significantly depending on the source. Within the cell wall, lignin provides

structural support, acts as a permeability barrier, and offers resistance against microbial attacks and oxidative stress (Kucharska et al., 2018; Langsdorf et al., 2021; Mujtaba et al., 2023).

As a consequence, GW presents a fraction with a high content of lignin material that makes its biodegradation slow (Langsdorf et al., 2021; Liu et al., 2023), but also a variable fraction that can be more easily degraded (Reyes-Torres et al., 2018). The resistant components of GW composition usually lead to a slow biodegradation process that if not well-managed often occurs with the emission of greenhouse gases. Therefore, it is crucial to consider sustainable approaches for the management of this waste stream (Reyes-Torres et al., 2018).

### **1.2.2 Strategies to valorize GW**

In many places, GW is disposed of in landfills or incinerated. One problem associated with GW is the significant release of greenhouse gases when not properly managed. One alternative method to recycle GW that is more environmentally friendly and is very conventional is composting (Langsdorf et al., 2021; Yang and Zhang, 2022). Composting is an aerobic process that transforms organic matter, including GW, into compost, a mixture used to enhance soil structure and nutrient content. Efficient composting requires proper moisture levels, an optimal carbon-to-nitrogen (C/N) ratio, and adequate aeration. However, GW's nutrient deficiency and high lignocellulose content can impact the maturation time and quality of the compost. Depending on the physical characteristics and lignocellulosic composition of GW, it can serve as a bulking agent in composting (Kumar et al., 2021; Liu et al., 2023).

As a good source of lignocellulosic biomass, GW can be utilized in the same way as other lignocellulosic wastes. A significant advantage of GW over energy crops is that it does not require arable land, as it is generated naturally. Consequently, the feedstock production costs are zero,

excluding the costs associated with the cultivation and care of plants and lawns, as well as the collection and pretreatment of the green waste (Langsdorf et al., 2021). One common way of GW valorization is the hydrolysis of lignin, cellulose, and hemicellulose into fermentable compounds. Moreover, GW contains further valuable compounds such as proteins, organic acids, lipids, and phenolic compounds that can be recovered. The use of hydrolyzed GW as a substrate in various biofuel production processes has also been extensively studied (Kumar et al., 2021). For example, a GW consisting of pruning trees, leaves, and grass clipping was utilized to produce bioethanol and biogas through anaerobic digestion (Sofokleous et al., 2022). It has also been used for biohydrogen production through dark or photo fermentations using fallen dead leaves and shrub waste respectively (Ramprakash and Incharoensakdi, 2022; Yue et al., 2021).

More recently, GW has been employed in the generation of bioenergy through methods like anaerobic digestion (Inghels et al., 2016; Yang and Zhang, 2022). However, using GW for anaerobic digestion has some challenges such as complex structure, high C/N ratio, and the necessity for pretreatment (Paul and Dutta, 2017). Besides, it could be converted into materials such as wood-plastic composites (Inghels et al., 2016; Yang and Zhang, 2022).

At both research and industrial levels, fermenting GW through microbial processes is one of the profitable approaches for the management of this organic waste to obtain bioproducts for industry, medicine, and agriculture. Among the marproducts, enzymes, biostimulants, and antibiotics can be named (Solano Porrás et al., 2023).

### 1.2.3 Pretreatment of GW

One of the limitations of GW like the other lignocellulosic residues, is the low efficiency of lignocellulose hydrolysis to sugars for the fermentation, especially in the biofuel production processes. Another disadvantage of GW, as mentioned earlier, is the varied composition which makes it a less popular feedstock. Pretreatment and conditioning can minimize this variability resulting in a more homogeneous waste. The main purpose of pretreatment is to disintegrate the hard structure of lignocellulosic complexes and to increase the availability of various complex compounds to degrade into cellulose (Kucharska et al., 2018). Various pretreatment techniques have been developed that can be divided into physical, chemical, physicochemical, and biological techniques. Based on the GW components, one or a mix of techniques is applied. Figure 1.1 shows different pretreatments used for lignocellulosic materials.

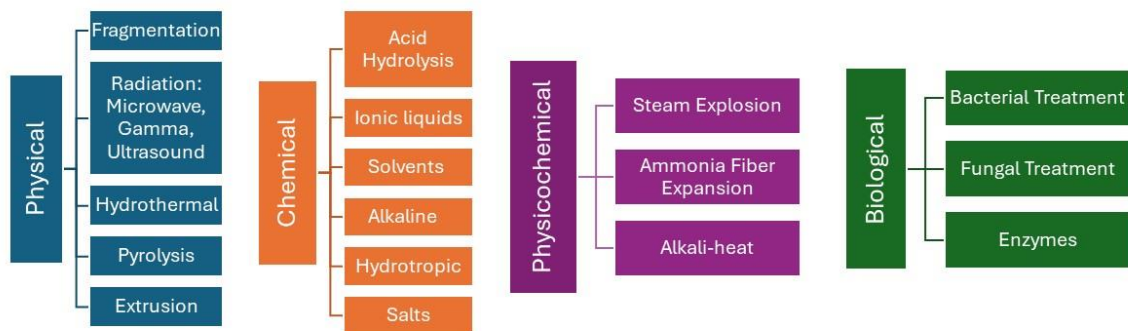


Figure 1.1. Classification of lignocellulosic pretreatment methods (Kucharska et al., 2018).

Physical pretreatments include mechanical and radiation-based techniques to reduce the particle size, decrease the crystallinity of cellulose, and increase the surface area. However, the lignin is not degraded when just physical pretreatments are applied. In chemical pretreatments, chemical reagents such as acids, alkalis, and salts are used to degrade lignocellulosic compounds. These techniques usually have effective results however, they are costly and have a more negative impact on the environment. Biological pretreatments that include employing biological agents and molecules are also effective and sometimes more economical. However, the problem with these techniques is that the process of pretreatment requires a long time. Physicochemical methods, a combination of physical and chemical pretreatments, for pretreatment have also been applied to lignocellulose. Usually, more than one single pretreatment technique is employed to improve lignocellulose degradation. The selected method for the pretreatment has a significant impact on the final cost of GW valorization because in most cases, it is the most expensive part of the process (Betiku and Ishola, 2023; Zhao et al., 2022).

### **1.3 Biostimulant and its promising role in sustainable agriculture**

Due to climate change and the increasing world population, the demand for plant biostimulants is rising as they play a promising role in shifting agricultural systems toward sustainability. Biostimulants, which are natural compounds or microorganisms distinct from fertilizers, enhance the development, quality, yield, and growth of plants through physiological stimulation (du Jardin, 2015; Rouphael and Colla, 2020). They help crops cope with stress periods and reduce the need for chemical fertilizers and pesticides in cropping systems. Modern agriculture requires such alternatives to chemicals to sustainably achieve food security while minimizing environmental impacts on ecosystems and human health (Ramawat and Bhardwaj, 2022). Biostimulants promote

## Chapter 1

plant growth and productivity through various mechanisms, such as enhancing nutrient use efficiency, increasing stress tolerance, and improving nutrient availability in the soil or rhizosphere (Figure 1.2). Since biostimulants do not supply nutrients directly, they are not considered fertilizers (Baltazar et al., 2021; Ramawat and Bhardwaj, 2022).

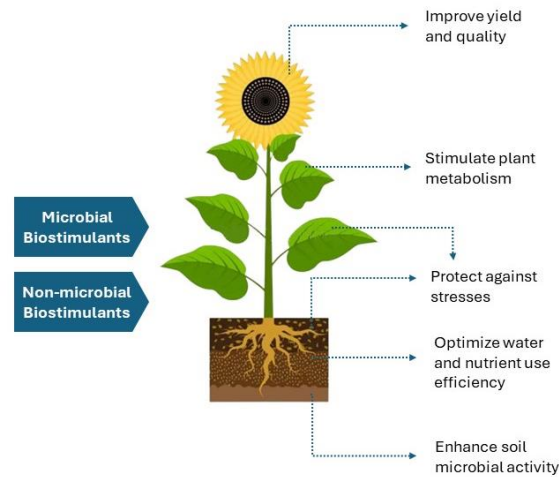


Figure 1.2. The effects of biostimulants on plants.

Although biostimulants have been used in commercial agriculture for decades, their availability and use by growers have considerably increased in recent years. Various kinds of commercial biostimulants now exist in the market. The global market for these products was estimated at USD 2.6 billion in 2019, with a projected value of over USD 4 billion by 2025 (Ramawat and Bhardwaj, 2022; Sible et al., 2021). The European Biostimulant Industry Council (EBIC) estimates the market share of biostimulants will be around 1.5-2 billion USD in 2022 with an annual growth rate of around 10-12% (Baltazar et al., 2021). The rapid growth of the biostimulants market is caused by several key factors:

- The increasing availability of novel biostimulant products



- The necessity to enhance the efficiency and effectiveness of synthetic chemicals and mineral fertilizers
- The rising frequency of environmental conditions affecting crop growth and productivity due to climate change (Ramawat and Bhardwaj, 2022; Rouphael and Colla, 2018; Sible et al., 2021).

### **1.3.1 Biostimulant categorization**

Biostimulants can be categorized based on their origin of production, mode of action, or their active ingredient. Considering the origin of production, biostimulants can be divided into two main groups: microbial and non-microbial. Table 1.1 presents the list of microbial and non-microbial biostimulants with their mechanisms of action.

#### ***1.3.1.1 Non-microbial biostimulants***

This group of biostimulants includes natural substances such as humic acids, protein hydrolysates, and seaweed extracts. Humic substances, such as humic and fulvic acids, are natural organic molecules in the soil resulting from the interaction between organic matter, microbes, and plant roots. The effect of humic substances on plant growth and productivity is very diverse due to the environmental conditions, the receiving plant, and the dose and mode of humic application.

Protein hydrolysates are mixtures of amino acids, oligopeptides, and polypeptides, resulting from the chemical or enzymatic hydrolysis of different protein sources. Source of protein hydrolysates are agro-industrial by-products from livestock and the food industry and have been divided into animal and vegetable sources (du Jardin, 2015; Ramawat and Bhardwaj, 2022). The animal sources of protein hydrolysates are feathers, collagen, leather by-products, blood meal, fish by-

Table 1.1. Plant biostimulants and their mechanisms of action. PGPM: plant growth promoting microorganisms.

	<i>Biostimulant</i>	<i>Mechanism of action</i>
<i>Non-Microbial</i>	Humic substances	<ul style="list-style-type: none"> <li>• Improve soil structure</li> <li>• Increase cation exchange</li> <li>• Neutralize soil pH</li> <li>• Improve solubility of phosphorus</li> <li>• Improve lateral root induction and hair growth due to the auxin-like activity</li> <li>• Stimulate nitrate assimilation</li> </ul>
	Protein hydrolysates	<ul style="list-style-type: none"> <li>• Stimulate key enzymes in N assimilation and C metabolism</li> <li>• Enhance auxin- and gibberellin-like activities</li> <li>• Increase pigment biosynthesis and production of secondary metabolites</li> <li>• Increase macro and micronutrients</li> </ul>
	Seaweed extract	<ul style="list-style-type: none"> <li>• Increase of rhizobacteria and mycorrhizae activities</li> <li>• Delay senescence</li> <li>• Enhance water use efficiency by improving stomatal conductance</li> <li>• Increase availability of micronutrients</li> </ul>
	Chitosan	<ul style="list-style-type: none"> <li>• Involve in signaling responses against stresses</li> </ul>
<i>Microbial</i>	PGPMs and their products	<ul style="list-style-type: none"> <li>• Hormonal regulation</li> <li>• Balance of cell oxidative status</li> <li>• Improve water use efficiency</li> </ul>

products, and casein (Malécange et al., 2023). While the plant-based protein hydrolysates are legume seeds and alfalfa.

The use of fresh seaweed as a source of organic matter and fertilizer has been traditionally used in agriculture in some regions, but its biostimulant effects have only been documented recently (du Jardin, 2015). Brown macroalgae, particularly from the *Ascophyllum* spp., *Ecklonia* spp., *Fucus* spp., *Laminaria* spp., and *Sargassum* spp. genera are extensively used in crops for their plant-growth-promoting benefits, resistance to abiotic stress, and enhancement of postharvest quality. For example, a seaweed extract derived from *Gracilaria* was found to increase sugarcane yield by 8%. Additionally, these biostimulants improve nitrogen use efficiency (Singh et al., 2023). The main components of commercial seaweed extract are polysaccharides, phenolics, vitamin precursors, osmolytes (such as mannitol), phytohormones, and hormone-like compounds (Rouphael and Colla, 2018).

Chitosan is a deacetylated form of chitin, produced naturally and industrially. Poly- and oligomers of variable, controlled sizes are used in the food, cosmetic, medical, and agricultural sectors. The physiological effects of chitosan oligomers in plants are the results of the capacity of this polycationic compound to bind a wide range of cellular components, including DNA, plasma membrane, and cell wall constituents, but also to bind specific receptors involved in defense gene activation, in a similar way as plant defense elicitors (Rouphael and Colla, 2020)

### ***1.3.1.2 Microorganism-based Biostimulants***

Microorganisms can affect positively plant physiological processes by interacting with the plants. These microorganisms include bacteria and fungi that are generally called plant growth promoting microorganisms (PGPM) and serve as microbial-based biostimulants. Plant growth promoting

## Chapter 1

bacteria (PGPB) includes free living bacteria in the soil as well as rhizobacteria that colonize the rhizosphere (Castiglione et al., 2021). Some species of PGPB are *Azotobacter* spp., *Bacillus* spp., *Clostridium* spp., *Enterobacter* spp., *Streptomyces* spp., *Klebsiella* spp., *Pseudomonas* spp., *Rhodococcus* spp. and, *Rhizobium* spp. Among the fungi, arbuscular mycorrhizal fungi (AMF), *Trichoderma* spp., *Aspergillus* spp., and *Beauveria* spp. are well-known biostimulants (Rouphael et al., 2017; Woo and Pepe, 2018). There is scientific evidence that suggests they have an important role in promoting plant growth. Besides their direct impact on plant growth, PGPM improves the soil microbial diversity and positively affects the phyllosphere, rhizosphere, and endosphere of the plants. AMFs are fungi belonging to the *Glomeromycota* phylum, that are interesting as biostimulants due to their ability to colonize plant roots through endomycorrhizal symbioses (Castiglione et al., 2021; Woo and Pepe, 2018).

### **1.3.2 Indole-3-acetic acid**

Indole-3-acetic acid (IAA), the main form of auxins, is a well-known phytohormone involved in various aspects of plant growth and development, including apical dominance, vascular tissue differentiation, the initiation of roots, cell division, and tropic responses to gravity and light (J. Luo et al., 2018). It can be produced by plants and microorganisms and acts as an important signal molecule mediating the interaction between plants and microorganisms to develop symbiosis (Duca and Glick, 2020). For this reason, auxins are considered one of the groups of biostimulant compounds that play a key role in plant growth regulation, with Indole-3-acetic acid (IAA) being the main member.

The biosynthesis of IAA by microorganisms can be categorized based on whether the pathway depends on Tryptophan (Trp) as a precursor or not. Beyond the dependency on Trp, IAA metabolic



(Kulkarni et al., 2013). It has been found that IAA production in some bacteria is affected by environmental factors including pH and temperature. Additionally, evidence suggests that IAA acts as a virulent factor in some pathogenic microorganisms. However, the mechanism of IAA action in many of these processes remains unknown and requires more in-depth studies (Tang et al., 2023).

### **1.3.3 Trichoderma and its role as biostimulant and biopesticide**

*Trichoderma* spp. is a filamentous fungus commonly found in soil ecosystems across a wide range of climatic conditions (López-Bucio et al., 2015). Although it is a well-known biocontrol agent against phytopathogens due to its antagonistic capacity, it has also the potential to serve as a biostimulant. It enhances plant resistance against stresses such as salinity and drought by promoting plant growth and reprogramming gene expression in roots and shoots. The fungus's capacity to sense, invade, and destroy other fungi has been the main reason for its commercial success as biopesticides. Additionally, *Trichoderma* secretes compounds, including IAA, that improve the plant's root network, thereby enhancing nutrient and water availability (Illescas et al., 2021; López-Bucio et al., 2015; Sala et al., 2020). The most studied *Trichoderma* species for their biopesticide activity include *T. asperellum*, *T. atroviride*, *T. harzianum*, *T. virens*, and *T. viride*. Some of the species such as *T. harzianum*, *T. viride* and *T. virens* exhibit both biocontrol and biostimulant behavior (López-Bucio et al., 2015). The mechanisms of *Trichoderma* to affect the plants' growth is shown in Figure 1.4.

Another notable characteristic of *Trichoderma* species is their ability to release extracellular hydrolytic enzymes, such as xylanases and cellulases (Li et al., 2022). This capability enhances the availability of cellulose from lignocellulosic material. While lignocellulose degradation by

*Trichoderma* has been extensively studied, most research incorporates various pretreatments along with the use of the fungus (Adav et al., 2012; Chen et al., 2020; Li et al., 2022).

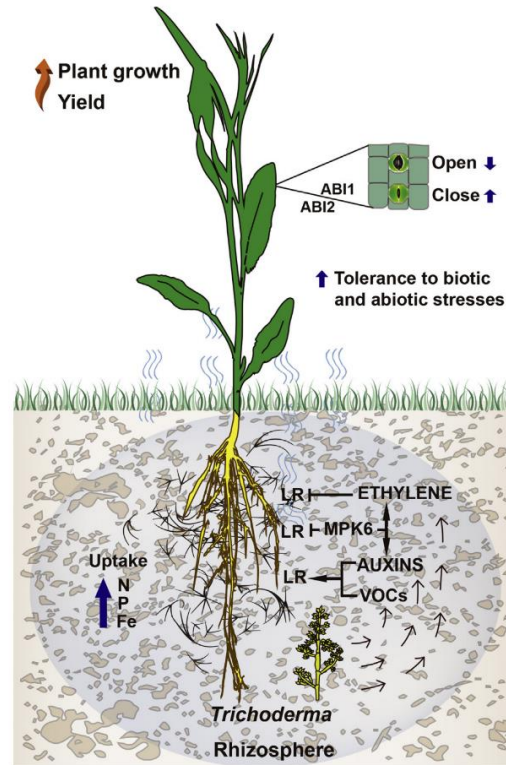


Figure 1.4. The biostimulant effects of *Trichoderma* on plants via fungal-root communication. *Trichoderma* metabolites like volatile organic compounds (VOCs), auxins and ethylene regulate root development including lateral root (LR). *T. atroviride* induces the activation of plant mitogen activated protein 6 (MPK6) that translates fungal signals into root cellular responses. The stomatal aperture is affected by *Trichoderma* metabolites. The nutrient uptake increases by *Trichoderma* root stimulation and improve plant growth and productivity (López-Bucio et al., 2015).

## 1.4 The advantages of solid-state fermentation to produce biopesticide and biostimulant

The microbial production of IAA has been extensively studied using various fermentation systems. Numerous studies have focused on IAA production in liquid fermentation at the lab scale, employing Erlenmeyer flasks as bioreactors under strictly controlled conditions, which are not

## Chapter 1

representative of realistic conditions. For instance, IAA was produced by *Rhodospiridium paludigenum* using batch and fed-batch fermentation strategies in a stirred tank fermenter (Nutaratat et al., 2016). Additionally, IAA has been successfully produced at a pilot scale (100 L) through liquid fermentation (Bunsangiam et al., 2021). However, many of these processes utilize culture media containing laboratory-grade chemicals as substrates. The use of renewable materials, particularly in solid form, introduces additional complexities, resulting in fewer studies on IAA production using solid substrates (Zanoni do Prado et al., 2019a). Solid-state fermentation (SSF) presents an interesting option for this purpose.

SSF is a process in which microorganisms grow on solid substrates in the absence or near absence of free water. This method is a promising bioprocessing technology within the framework of the circular economy, as it utilizes low-cost, renewable materials such as solid waste, transforming them into marketable products (Oiza et al., 2022; Yazid et al., 2017). SSF has been employed in the production of various marketable bioproducts, including enzymes, biosurfactants, biopesticides, biostimulants, and other valuable products for the industrial, agricultural, and pharmaceutical sectors (Eras-Muñoz et al., 2023; Jiménez-Peñalver et al., 2019; Mejias et al., 2018; Sala et al., 2021b).

SSF appears to be an ideal process for the valorization of solid lignocellulosic waste, such as GW, especially through fungal fermentation. Because many filamentous fungi can grow on substrates with a low water content. The selection of appropriate microorganisms and substrates is crucial for improving SSF efficiency (Li et al., 2022). Fungi like *Trichoderma* spp., which can degrade lignocellulose, are preferred for processing GW. In that sense, GW can serve both as a carbon source and a support for fungal growth. It is worth mentioning that the quality and longevity of



aerial (conidial) spores are notably higher when they are produced through SSF (Chilakamarry et al., 2022; Sala et al., 2019; Yazid et al., 2017).

For a successful and efficient SSF, it is crucial to optimize various process variables, including moisture, pH, temperature, particle size, aeration, agitation, and the initial concentration of inoculum, according to the selected microorganism, substrate and target product. However, due to its heterogeneous nature, maintaining and monitoring these optimized parameters during all the fermentation can be challenging (Oiza et al., 2022; Sala et al., 2019; Yazid et al., 2017).

#### **1.4.1 Reactor Configuration**

From a practical point of view, SSF involves using a bioreactor filled with a solid substrate and inoculated with a specific strain to produce the target bioproduct. Therefore, choosing the right reactor design is important for a successful SSF. One notable challenge is the complexity of scaling up SSF, as heat accumulation inside the reactor is a common issue due to the low heat transfer capacity of organic matrices (Mitchell et al., 1999). However, by providing effective aeration and a proper porosity to allow heat to be transferred and released, the problem can be partially solved or at least minimized (Chilakamarry et al., 2022; López-Bucio et al., 2015). Selecting a suitable reactor configuration can help overcome some of the drawbacks of SSF depending on the specific characteristics of substrates, inoculum and products. When analyzing various types of bioreactors for SSF, it is important to consider that each design has unique characteristics including advantages and disadvantages. Various reactor configurations are available for SSF, including simple bags, tray reactors, stirred and rotating drum bioreactor, air pressure pulsation bioreactors, and packed bed reactors (Arora et al., 2018; Rodríguez-Durá et al., 2023; Sentís-Moré et al., 2023). Figure 1.5

## Chapter 1

illustrates the different designs of bioreactors used for SSF. Here, the major reactor designs applied for SSF are briefly described.

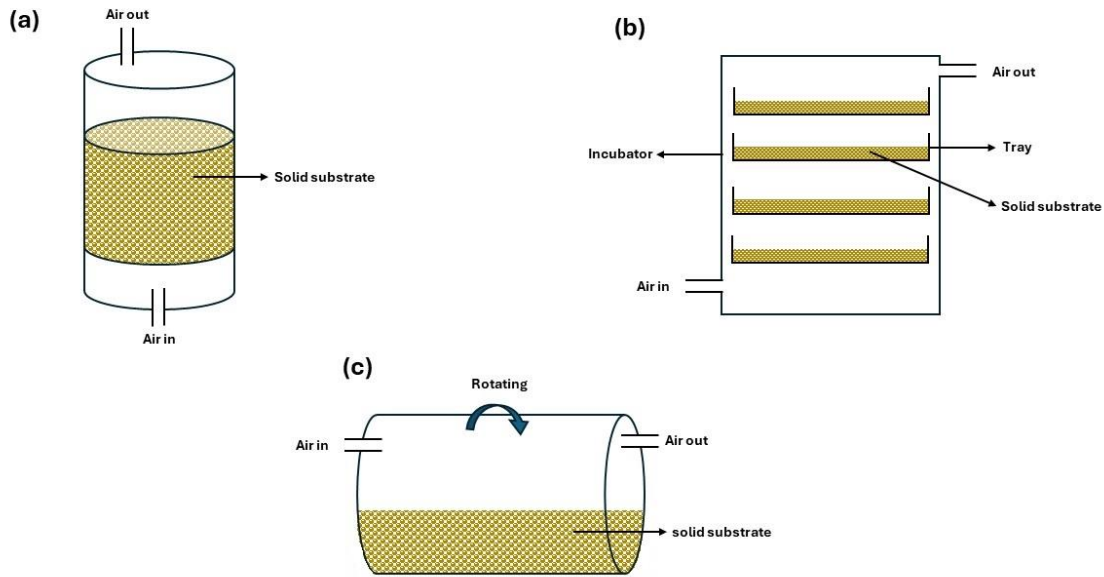


Figure 1.5. Various reactor configurations are usually applied in SSF. (a) packed bed reactor; (b) tray reactor; (c) rotating drum reactor.

Packed bed reactors consist of a cylindrical bed made of metal or glass. In this configuration, the substrate is placed in a column and has continuously forced aeration through the fermentation bed (Sentís-Moré et al., 2023). They are good choices to have more control over parameters like temperature, interstitial oxygen, and moisture, (Molina-Peñate et al., 2023; Rayhane et al., 2019; Sala et al., 2021a).

Stirred drum and rotating drum bioreactors are two different designs of SSF bioreactors that provide agitating without forced aeration. These bioreactors are typically cylindrical drums lying horizontally and partially filled with a solid substrate. Oxygen is supplied by an airflow blowing through the reactor's top part. In a rotating drum reactor, mixing is achieved by rotating the entire

bioreactor while, in stirred drum reactors, the entire reactor is stable and the agitating is provided by mechanical devices such as paddles (Rodríguez-Durá et al., 2023).

A tray bioreactor is generally composed of a chamber with trays put inside this chamber. Here, the substrate is placed in individual trays with layers 1 to 5 cm thick, and there is no forced aeration through the bed, however, in some systems the air is over and under of the trays (Figueroa-Montero et al., 2011; Rodríguez-Durá et al., 2023; Sentís-Moré et al., 2023). Tray reactors are the most used reactor configuration in the industry to do SSF due to their simple and economical structure. Tray bioreactors provide more surface area with better aeration which is an important factor when working with fungi in fermentation (Sala et al., 2022). Compared to other common reactor configurations used in SSF such as packed bed reactors, heat transfer is easier in tray reactors due to better aeration which is an important factor in having a successful SSF. However, heat accumulation may still occur depending on the biodegradability and the porosity of the substrate, the bed thickness (Figueroa-Montero et al., 2011).

It is worth mentioning that, in addition to using a suitable reactor configuration to develop an effective process at industrial scale, it is important to address the potential obstacles and optimize SSF process parameters, considering economic performance. Applying an effective strategy can hinder the drawbacks of the reactor and solve the problems regarding SSF. Several operational strategies have been suggested to keep production in process and facilitate industrialization. One effective approach is the use of sequential batch operation strategy (SBO). The key concept behind SBO is to perform several consecutive batches, where the fermented material from one batch serves as inoculum for the next one, reducing the need for time and the cost of preparing fresh inoculum. This strategy has been reported as a successful operation when performing the process

## Chapter 1

in packed bed reactors using different organic waste to obtain a variety of valuable bioproducts (Cerdeja et al., 2017; Martínez-Avila et al., 2019; Sala et al., 2021a).

Overall, achieving a highly productive, reproducible, and scalable SSF requires extensive research focused on engineering parameters optimized for the process, as well as a thorough understanding of bioreactor designs to enhance operability, facilitate process scale-up and enable the commercialization of SSF products.

# Chapter 2

## Objectives

---

This research has been conducted in Compositing Research Group (GICOM) at UAB. Previously, several studies in the group have focused on the production of bacterial and fungal biopesticides using various agro-industrial wastes. However, this study represents the group's first effort in producing plant biostimulants.

The main objective of this research is to utilize green waste as substrate in solid-state fermentation to produce biopesticide and biostimulant using *Trichoderma harzianum*. To achieve this goal, the following specific objectives were pursued:

- To study the feasibility of using green waste as a substrate for the production of conidial spores as biopesticide and Indole-3-acetic acid (IAA) as plant biostimulant at laboratory scale.
- To identify and analyze the key parameters influencing IAA and conidia production using GW to optimize the simultaneous production of both IAA and spores.
- To investigate the challenges associated with scaling up the process and study the parameters affecting the SSF during scale up.
- To perform the SSF in different reactor configurations at bench scale like packed bed and tray reactors and find a more suitable configuration to produce IAA and spores.
- To evaluate the efficiency of the different operational strategies including the use of a sequential batch operation.

# Chapter 3

## Materials and Methods

---

## 3.1 Materials

### 3.1.1 Substrates

The substrates used in the work were green waste that was mainly composed of lawn grass clippings (G). In the preliminary experiments (Chapter 4 and Chapter 5), pruning waste (PW) from different plants was mixed with G to act as bulking agent. G and PW were collected from the campus of Universitat Autònoma de Barcelona (41.50 °N, 2.10°E, Spain). Depending on the season of collection the freshness of the GW was different (Figure 3.1).

For all the tests, grass was chopped into 1.5 x 1.5 cm pieces using a compost shredder (Figure 3.2 a) and cleaned with tap water. Then, it was air-dried with a constant flow of 5 L min<sup>-1</sup> at room temperature for 10 days (Figure 3.2b, c). During the drying process, the grass was manually mixed once a day.

PW was chopped mechanically before the collection; afterwards, it was cleaned with tap water and dried at 60°C for 6 hours. Both materials (G and PW) were kept at -20°C after drying and until use. For the later experiments (Chapter 5 and Chapter 6), wood chips (WC) was substituted for PW to be used as bulking agent. WC was purchased from Acalora, Palets Pla d'Urgell, (Spain) and was used in SSF as received.

The materials were autoclaved twice 121°C for 30 min prior to the fermentation process. A solution of sterilized sodium phosphate buffer (1M, pH=6.8) was used to prevent significant changes in pH. The concentration of buffer used was 2.6 mL g<sup>-1</sup> DM (dry matter).





Figure 3.1 The different grass clippings and pruning waste collecting in different times of the year. a) fresh grass; b) aged grass; c) a pile of grass clipping; d) fresh pruning waste; e) aged pruning waste



Figure 3.2 a) The compost shredder used to chop the grass clipping; b,c) air drying the grass in a biodrying reactor

### 3.1.2 Fungal strains

*Trichoderma harzianum* (TH) strain CECT 2929 was purchased from the Spanish Type Culture Collection (CECT) (University of Valencia, Valencia, Spain). *Trichoderma viride* (TV) was provided by Biological Control Subdirectorate (SCB) SENASA Laboratory in Peru.

The original strains were kept at  $-80^{\circ}\text{C}$  in sterile cryovials containing 10% glycerol according to the provider's instructions. TH and TV were cultured on malt extract agar and potato extract agar plates, respectively at room temperature for 6-8 days and diluted to approximately  $10^6$  spores  $\text{g}^{-1}$  of dry substrate before inoculating. The spores were extracted and diluted in 0.1% Tween 80 solution before inoculating SSF reactors, to result in a concentration of approximately  $10^7$  spores per gram of dry matter (DM). The appearance of a TH plate culture and the conidial spores of TH is presented in Figure 3.3.

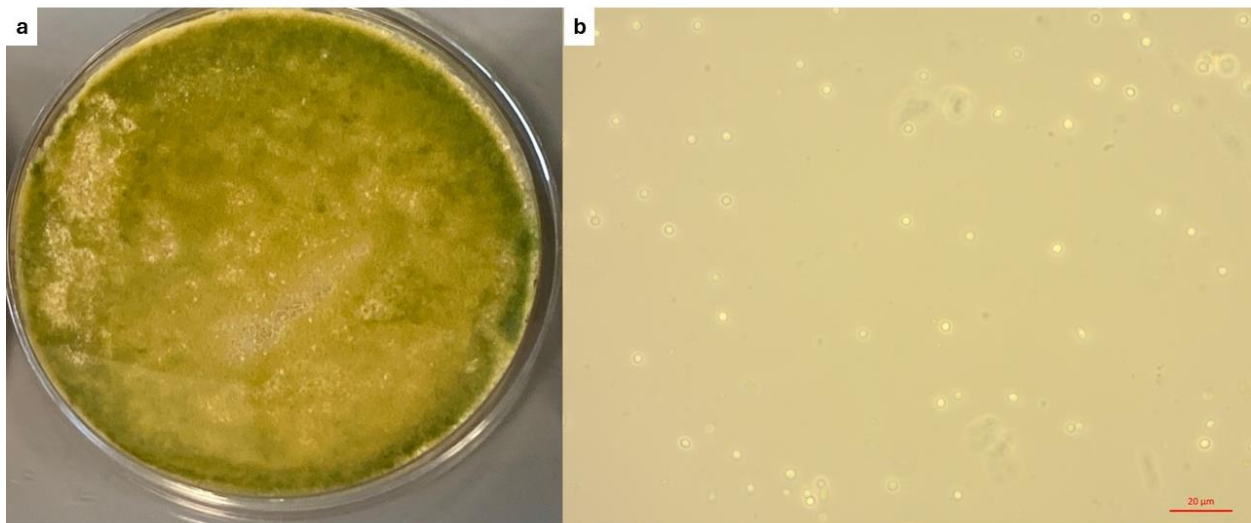


Figure 3.3 *Trichoderma harzianum* a) plate; b) spores.

### 3.2 Solid-State Fermentation (SSF)

In all SSF procedures, the selected air flow was based on the superficial velocity per gram of dry matter ( $\text{m s}^{-1} \text{g}^{-1} \text{DM}$ ), following Equation (3.1):

$$V = \frac{Q}{A} \quad (3.1)$$

Where:

V: superficial velocity ( $\text{m s}^{-1} \text{g}^{-1} \text{DM}$ )

Q: airflow per gram of dry matter ( $\text{m}^3 \text{g}^{-1} \text{DM s}^{-1}$ )

A: reactor area ( $\text{m}^2$ )

#### 3.2.1 0.5 L packed bed reactor setup

The packed bed reactors in this scale were PVC cylinders consisting of an inlet and outlet for the air passing through the reactor. The volume of the reactor was approximately 0.5 L. The inlet of reactors was connected to a mass flowmeter (Mass-Stream D-6311, Bronkhorst, Netherlands) to provide a continuous airflow ( $20 \text{ ml min}^{-1}$ ). A humidifier was used to prevent drying the materials inside the reactor by the input air. The exhausted air was first connected to a water trap to collect possible water from the air. Then the oxygen content of the outlet air was measured by an oxygen sensor (Alphasense, UK). Data was collected and analyzed using self-made software based on Arduino®. To control the temperature inside the reactors, they were placed in water bath with the desired temperature. The system of SSF in 0.5L reactors is shown in Figure 3.4 and Figure 3.5.

### Chapter 3

To prevent contamination, the reactors were soaked in a bleach solution overnight and subsequently disinfected with 70% ethanol prior to fermentation. Material preparation and inoculation were carried out under a laminar flow hood.

To set up the SSF, the reactors were charged with a total 80-100 g of the wet mixture of sterilized grass and pruning waste. The Trp was added as solid powder depending on the target value of the experiment.

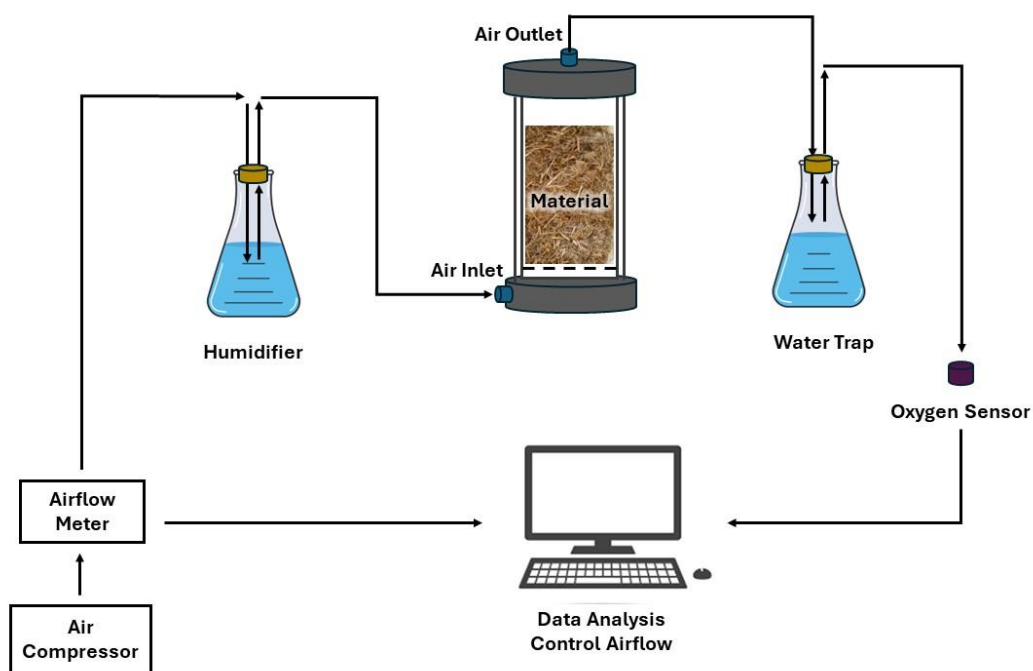


Figure 3.4. The system of SSF with 0.5L packed bed reactors



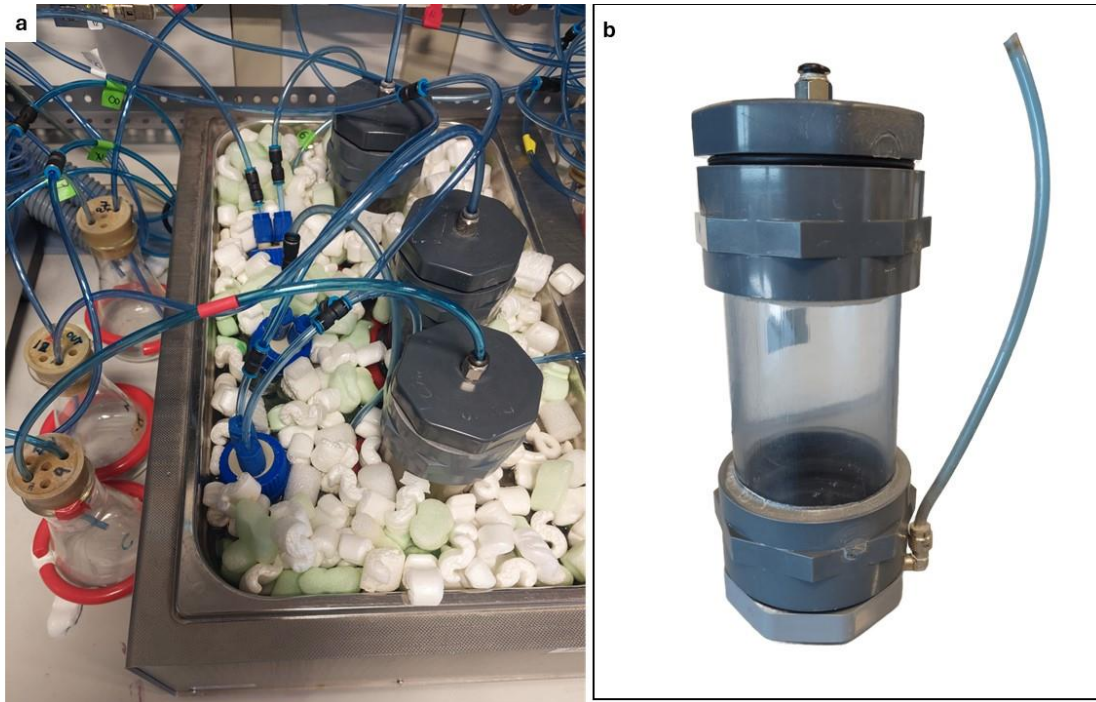


Figure 3.5 The 0.5L reactor a) set up and b) appearance.

### ***3.2.1.1 Design of experiment***

To analyze the effect of different factors on spore and IAA production, a Box-Behnken design was conducted with 15 runs. Three numeric factors with two responses were selected for the design. The factors had three levels including a maximum, a minimum, and a center point. The selected factors were tryptophan concentration, G to PW ratio, and initial moisture while the responses were the number of spores and the IAA concentration. The Experiment was designed and analysed software DesignExpert 11 (Stat-Ease, Inc, United States).

### **3.2.1.2 Time course experiment**

To investigate the different factors during a specific period, a time course experiment was conducted at 0.5L scale. To perform a 10-day time course experiment, all reactors were prepared according to the optimized condition estimated in the experimental design. Every day one reactor was sampled and then discarded. The sample was used for further analysis.

### **3.2.2 22 L packed bed reactor setup**

The fermentations were also conducted in a 22 L stainless-steel cylindrical packed bed reactor equipped with inlet and outlet valves to provide a constant airflow. The reactor included a removable basket with 48 cm height and 24.5 cm diameter, providing a volume of around 22 L (Figure 3.6). The initial matrix properties, such as grass and bulking agent percentages, moisture content, and Trp concentration, were consistent with those optimized in previous experiments using 0.5-L reactors. In these experiments described in Chapter 5, Trp was dissolved in phosphate buffer and mixed with the dry substrate. The airflow rate was set at 1000 mL min<sup>-1</sup>. Temperature button sensors (standard Thermochron iButton device, Maxim Integrated, U.S), were used to monitor the temperature during the fermentation process. As illustrated in Figure 3.7, the sensors were positioned at various points within the reactor.

To minimize the risk of microbial contamination, the reactor was previously cleaned with bleach and water and disinfected with ethanol (70%). The basket of the reactor was autoclaved and filled with sterilized material. The inoculum and phosphate buffer were manually mixed with the sterilized substrate in a disinfected plastic tray under a laminar flow cabin. The fermentation time varied depending on the objective of the experiment and will be detailed for each case.

To have detailed data from different heights of the reactor, the material inside the reactor was divided into three distinct zones, from each of which two samples were collected. We categorized these zones based on the height of the material filling the reactor. Assuming that the height of solid matrix inside the reactor was 25 cm, the top, the center, and the bottom segments of the reactor correspond to approximately 16-25 cm, 8-16 cm, and 0-8 cm, respectively (Figure 3.7).



Figure 3.6. SSF set up in 22 L reactor.

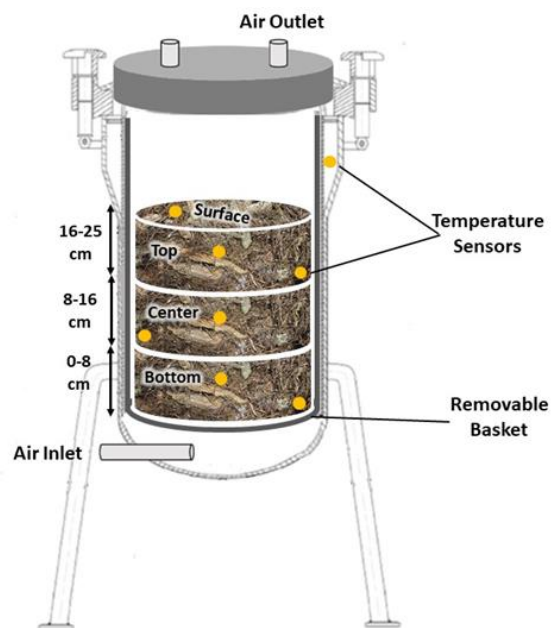


Figure 3.7 Schematics photo of 22 L reactor and the distribution of sampling areas and temperature sensors from different heights.

### 3.2.2.1 Sequential batch operation

The strategy of sequential batch operation (SBO) consists of performing a series of consecutive fermentations using the fermented material of a batch to inoculate the next one. SBO operation was conducted in the 22 L reactor with four consecutive batches. In the first batch, the inoculum was prepared in the same way as that of a single batch as described in 3.2.2. In the following batches, 30% of total wet weight of the fermented material obtained from the previous batch was used as inoculum for the fresh autoclaved material. However, the equal amount of Trp was added in the beginning of all four batches. In SBO experiment, the reactor was sampled as shown in Figure 3.7, where two samples were taken from each part. Here, an additional sample was also collected from the reactor surface.



### 3.2.3 Tray bioreactor setup

The tray bioreactor consists of an incubator (Memmert ® GmbH + Co. Schwabach Bundesrepublik, Germany) and two or three trays. The trays were made of metal mesh sheets with 39.5 cm length, 27.5 cm width and approximately 3 cm of bed height. A constant air was flown into the incubator with a rate of  $500 \text{ ml min}^{-1}$ . To ensure homogeneous air distribution, four air sprinklers were positioned at the bottom of the incubator, facing downwards. There were two exits for air used for gas measurement, one of which (outlet A) was always kept open as air outlet. The system for SSF in the tray reactor is illustrated in Figure 3.8.

To avoid contamination, the autoclaved substrate was inoculated and mixed in a sterilized plastic beaker under the laminar cabin flow. The disinfested metal trays were filled with inoculated substrate in the laboratory. Each tray was loaded with 500 g of the mixture of grass and wood chips with Trp and inoculated with TH. The values for G, WC, Trp, and moisture had been obtained before as optimized values obtained in the optimization process performed in 0.5 L reactors. While all the experiments were conducted inside the incubator, in some experiments, depending on the objective, the process was performed at room temperature, without using the system of temperature control of the incubator. In others, the incubator was on to control the temperature. In both cases, to monitor the temperature profile of the trays, two button sensors (standard Thermochron iButton device, Maxim Integrated, U.S) were put in the tray and compared with one out of the reactor.

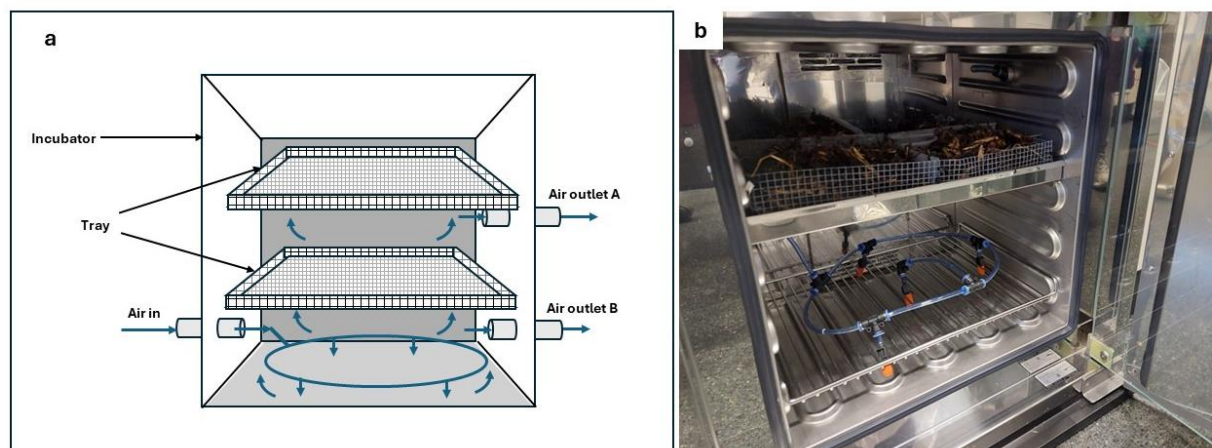


Figure 3.8. The tray reactor. a) a schematic of the system; b) the appearance of set up.

### 3.3 Seed Germination test

This assay aimed to quantify the biostimulant effect of materials fermented with TH on the germination of cucumber (*Cucumis sativus*) seeds. For this purpose, an extract from fermented materials was prepared by mixing 10 g of fermented material to 50 mL of distilled water and stirring for 30 min at room temperature. Then, 1 mL of the extract of three different experiments was added to Petri dishes containing 10 cucumber seeds each. Additionally, two tests were conducted using two different concentrations of pure IAA ( $17.5 \text{ mg L}^{-1}$  and  $1.75 \text{ mg L}^{-1}$ ). For the control, 1 mL of distilled water was added to the seeds. The number of germinated seeds, root length, and shoot length were measured after 2 and 5 days. All tests were performed in triplicate.

The gemination index was calculated using equations (3.2), (3.3), (3.4), and (3.5) obtained from (Y. Luo et al., 2018).

$$SG = \frac{\text{Number of germinated seeds}}{\text{Number of total seeds}} \times 100 \quad (3.2)$$

$$RSG = \frac{\text{Number of germinated seeds of sample}}{\text{Number of germinated seeds of control}} \times 100 \quad (3.3)$$

$$RRG = \frac{\text{Total radicle length of germinated seeds of sample}}{\text{Total radicle length of germinated seeds of control}} \times 100 \quad (3.4)$$

$$GI = RSG \times RRG \times 100\% \quad (3.5)$$

Where:

SG: seed germination

RSG: relative seed germination

RRG: relative radicle growth

GI: seed germination index

### 3.4 Germination of fungal spores

The germination of TH conidial spores obtained under different concentrations of Trp and IAA was monitored real-time using oCelloScope (oCelloScope™, BioSense Solutions ApS, Hirsemærken 1, DK-3520 Farum). To do so, an SDA culture medium was used. SDA was diluted 1:4 and IAA or Trp were added to the medium with various concentrations. The concentrations of IAA in SDA were 0, 0.5, 0.25, and 0.125 g L<sup>-1</sup>, while for Trp the concentrations were 0, 5, and 10 g L<sup>-1</sup>. Aliquots of 50 µL TH conidia were seeded into the wells of a 96-well culture plate with each well containing 50 µL of diluted SDA with different amounts of IAA or Trp. In all tests, the final concentration of TH was 10<sup>5</sup> -10<sup>6</sup> spore mL<sup>-1</sup>. Each test was replicated three times. The

## Chapter 3

germination of TH spores was monitored *in-vitro* at 25, 28, and 30 °C for 24h. The machine took a photo every 2 hours to detect and count the germinated spores. The data was analyzed using UniExplorer software version 12.1.0.249. An image of oCelloScope equipment is presented in Figure 3.9.

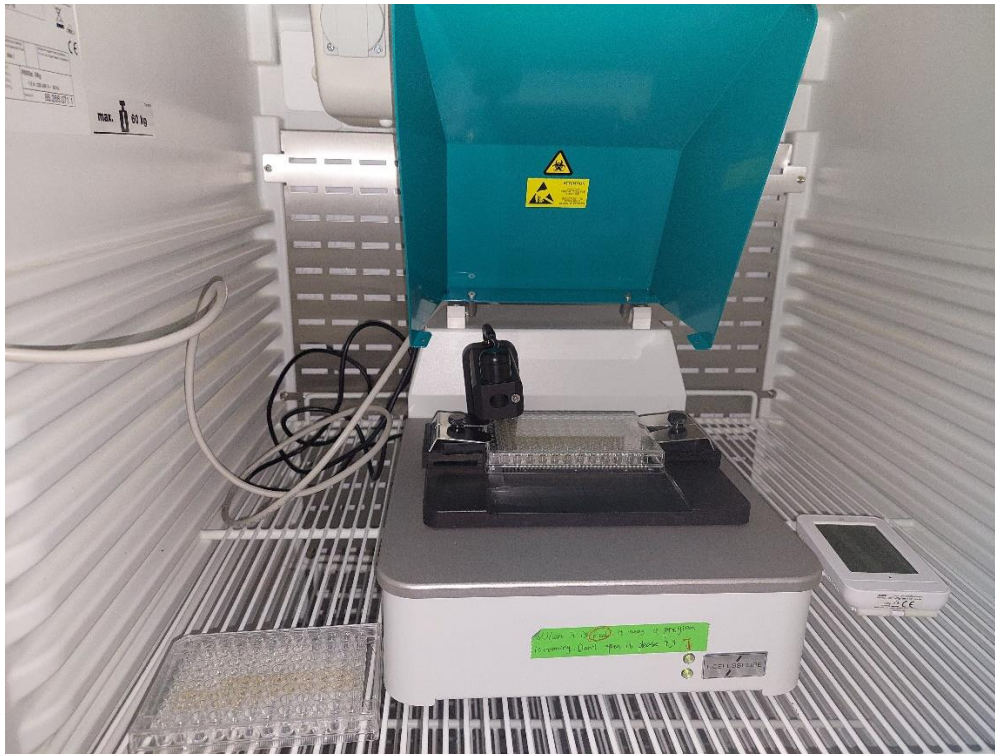


Figure 3.9. oCelloScope system for real-time monitoring of microbial growth

### 3.5 Analytical methods

#### 3.5.1 Analysis of oxygen consumption

To assess microbial activity, the consumption of oxygen was calculated as specific oxygen uptake rate (sOUR) and cumulative oxygen consumption (COC).

sOUR was online monitored during the entire fermentation and as described in section 3.2.1, this involved measuring the oxygen content in the exhaust gases of the reactor using electrochemical sensors and to have a precise value of the air flow a mass flow meter was used. Subsequently, the recorded oxygen consumption data was analyzed using custom software built on an Arduino® platform.

sOUR was calculated using Equation (3.6) (Puyuelo et al., 2010):

$$sOUR = F \times (0.209 - yO_2) \times \frac{P \times 32 \times 60 \times 10^3}{R \times DM \times 10^3} \quad (3.6)$$

Where:

sOUR; the specific oxygen uptake rate (g O<sub>2</sub> kg<sup>-1</sup> DM h<sup>-1</sup>)

F: airflow (mL min<sup>-1</sup>)

yO<sub>2</sub>: the oxygen molar fraction in the exhaust gases (mol O<sub>2</sub> mol<sup>-1</sup>)

P: the pressure of the system assumed constant at 101325 Pa

32: the oxygen molecular weight (g O<sub>2</sub> mol<sup>-1</sup> O<sub>2</sub>)

60: the conversion factor from minute to hour

10<sup>3</sup>: the conversion factor from mL to L

R: the ideal gas constant (8310 Pa L K<sup>-1</sup> mol<sup>-1</sup>)

DM: the initial dry weight of solids in the reactor (g)

10<sup>3</sup>: the conversion factor from g to mg

## Chapter 3

The cumulative oxygen consumption (COC) was also determined for comparison purposes among the experiments. It was measured in g O<sub>2</sub> kg<sup>-1</sup> DM by calculating the area below the oxygen consumption curve (computed through the numerical integration in time) using numerical integration.

### 3.5.2 Spore counting

To determine fungal spore production, a suspension containing fermented material and Tween 80 (0.1%, v/v) was prepared with the ratio of 1 g of fermented solid per 5 mL of Tween solution. This suspension was agitated at 180 rpm for 30 minutes at room temperature and then diluted 1:1000 with Tween solution. In all the tests, the spores were counted in triplicate using a Neubauer chamber (Brand™ 717805) and an optical microscope (Olympus BH2). The number of spores in 1 g of dry matter was calculated with Equation (3.7):

$$\text{Spore Concentration} = \frac{N}{DF \times CV} \times \frac{EV}{DM} \quad (3.7)$$

Where:

Spore concentration: the number of spores per g of dry substrate (spore g<sup>-1</sup> DM)

N: the number of spores counted in the Neubauer chamber

DF: dilution factor of the counting tube

CV: the volume used to count spores in the Neubauer chamber (mL)

EV: extraction volume (mL)

DM: the sample dry matter (g DM).

### 3.5.3 IAA and Trp analysis

A sample of solid material was mixed with a tween 80 solution (0.1% v/v) with a proportion of 1 g of solid: 5 mL of liquid and shaken at 180 rpm for 30 min at room temperature. The mixture then was sieved, and the liquid extract was centrifuged at 10000 rpm for 15 min at 4°C. The supernatant was filtered using a 0.22 µm nylon filter. The filtered extract was preserved at -20°C until analysis and served as a sample for HPLC.

To analyze Trp and IAA, a Dionex Ultimate 3000 HPLC system (Dionex, Idstein, Germany) was used. The system was equipped with an UltiMate 3000 Autosampler, a column compartment, and a photodiode array detector and controlled by Chromeleon™ Chromatography Data System (CDS) version 6.8 (Thermo Scientific).

To analyze IAA, an LC Kinetex® 5µm EVO C18 100 Å column was (250×4.6 mm) . The eluent was isocratic and involved a solution of 2.5% acetic acid in ultrapure water, and acetonitrile in ultrapure water with the proportion of (20:80). The column oven was set at 30 °C and the flow rate was 0.7 ml min<sup>-1</sup>. The fluorometric detector was set at 280 nm. The total run was 15 min, and the peak was observed at 11 min. The chromatographic method was based on the methods used in Kumla et al. (2020) (Kumla et al., 2020) and Apine et al (Apine and Jadhav, 2011) works with some modifications. To prepare the standard curve, pure IAA (98%) (Merck & Co Inc., US) was used with minimum detection limit of 0.5 ppm. To enhance the accuracy of method and decrease the matrix effect, all samples including controls were spiked with an equal aliquot of 5 ppm of IAA.

## Chapter 3

For Trp analysis, the analytical column and the chromatographic method was the same as the one used for IAA detection. Trp and IAA can be detected through one method, however, the peak of Trp was observed at 3 min (Figure 3.10). The curve of standard was prepared for Trp had the minimum detection limit of 50 ppm.

The concentrations of IAA and Trp in the samples were determined by calculating the area of the obtained peak and comparing it to that of the standard curve. For each prepared extract, a triplicate analysis of IAA was performed. The consumption of Trp was calculated by subtracting the initial value of Trp from the final value and presented as percentage.

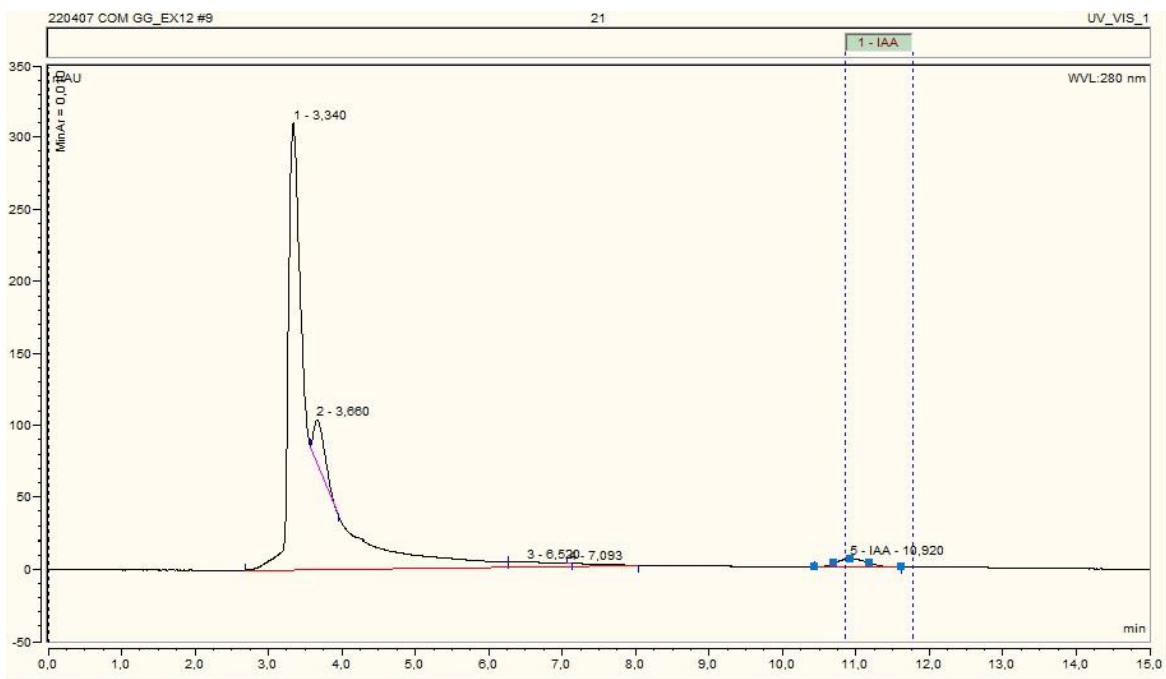


Figure 3.10. The peaks of Trp and IAA in the chromatography that observed in minutes 3 and 11 respectively.



#### **3.5.4 Gas measurements**

To measure the exhaust gases including NH<sub>3</sub>, O<sub>2</sub>, and CO<sub>2</sub> from tray reactor, two different devices were applied. For some experiments, a portable multisensor (POLI Multi-gas detector, mPower Electronics) was used. While for the others, a BIOGAS 5000 gas analyzer (GeoTech, UK) was used. The measurements were conducted during the fermentation from two points of the incubator that demonstrated in Figure 3.8.

#### **3.5.5 Monitoring the contamination**

To check for contamination during the process, an extract from the samples of each batch was prepared as described in section 3.5.2. The extract was diluted with tween 80 (0.1%, v/v) and a serial dilution was prepared ranging from 10<sup>-4</sup> to 10<sup>-6</sup>. Solid microbial cultures were then prepared using these diluted samples on two different culture media: nutrient agar and malt extract agar. The plates were incubated at room temperature, and microbial growth was monitored daily for 7 days.

#### **3.5.6 Microbial identification**

To identify the isolated microorganisms, purified isolates were sent as petri dishes to Instrumental Techniques Laboratory (Nucleic acids analysis area) of Universidad de Leon. The identification was done by performing a qPCR (quantitative polymerase chain reaction) using a thermocycler (GeneAmp PCR 2700 (Applied Biosystems)).

### 3.5.7 Moisture, dry matter and organic matter

To determine moisture content (MC) and dry matter (DM), 10 g of sample was put in a crucible and left in an oven at 105°C for 24 h. The crucible with the dried sample was weighted after cooling, and MC and DM were calculated by following equations (3.8) and (3.9):

$$MC = \frac{W_w - W_d}{W_w - W_t} \times 100 \quad (3.8)$$

$$DM = 100 - MC \quad (3.9)$$

Where:

MC: moisture content

$W_w$ : weight of crucible with wet material (g)

$W_d$ : weight of crucible with dry material (g)

$W_t$ : weight of empty crucible (g)

DM: dry matter

For organic matter (OM) analysis, 1-2 g of the dried sample obtained from dry matter analysis was put in a muffle at 550°C 2 h. The remaining ashes in the crucible were weighted after cooling and OM was calculated following equation (3.10):

$$MC = \frac{W_d - W_a}{W_d - W_t} \times 100 \quad (3.10)$$

Where:

OM: organic matter

$W_d$ : weight of crucible with dried material (g)

$W_a$ : weight of crucible with ash (g)

$W_t$ : weight of empty crucible (g)

### 3.5.8 pH and conductivity

To measure pH and conductivity, a mixture of the sample and distilled water was prepared with the ratio of 1:5 w/v. The suspension was shaken at room temperature for 30 and the supernatant was used for pH and conductivity measurements. pH was measured with an electrometric pH meter (Crison®, micropH2001) and conductivity was measured using an electrical conductivity meter (XS Cond 8).

### 3.5.9 Porosity, water holding capacity and C/N analysis

Air-filled porosity (AFP) is defined as the volume fraction of air (usually reported in a percentage basis) in a porous matrix. It was calculated according to Equation (3.11) as presented by Richard et al. (2004): [40]:

$$AFP = 1 - BD_t \left( \frac{1 - DM}{D_w} \right) + \left( \frac{DM \times OM}{PD_{OM}} \right) + \left( DM \times \frac{1 - OM}{PD_{ash}} \right) \quad (3.11)$$

Where:

AFP: air-filled porosity (%)

$BD_t$ : total bulk density on a wet basis ( $\text{kg m}^{-3}$ )

### Chapter 3

DM: dry matter on a wet basis (%)

OM: organic matter on a dry basis (%)

$D_w$ : water density ( $1000 \text{ kg m}^{-3}$ )

$PD_{OM}$ : the organic fraction particle density ( $1600 \text{ kg m}^{-3}$ )

$PD_{ash}$ : ash particle density ( $2500 \text{ kg m}^{-3}$ )

Water holding capacity (WHC) of the materials was determined by obtaining the difference of the saturated weight and the dried weight of the material. To obtain the saturated weight, the specific amount of the material was soaked in water for 2 hours and then weighted. WHC was calculated according to Equation (3.12):

$$WHC = \frac{(W_s - W_0)}{W_0} \times 100 \quad (3.12)$$

Where:

WHC: water holding capacity (%)

$W_s$ : water saturated weight of the solid sample (g)

$W_0$ : dry weight of the solid sample (g)

C/N analysis was performed by chemical elemental (C, H, N and S) analysis by Servei d'Anàlisi Química (SAQ) in UAB. The analysis was carried out using a CHNS elemental analyzer Flash 2000 (Thermo Scientific).

### **3.5.10 Statistical analysis**

To analyze the results of experimental design including ANOVA and to produce an optimization model, Design Expert 12 (Stat-Ease, Inc, USA) was used. Other statistical analysis including mean comparisons, correlation, regression analysis and PCA were performed using Minitab 17.1.0 (Minitab Inc. State College, Pennsylvania, United States).

## Chapter 4

# Green Waste as a Substrate to Produce Biostimulant and Biopesticide Products through Solid-State Fermentation

---

Part of this chapter has been published in: Ghoreishi, G., Barrena, R., & Font, X. (2023). Using green waste as substrate to produce biostimulant and biopesticide products through solid-state fermentation. *Waste Management*, 159, 84-92.

## 4.1 Overview

In this chapter, the potential of utilizing green waste (grass clippings and pruning waste) as a substrate for solid-state fermentation (SSF) with *Trichoderma harzianum* at a laboratory scale (using 0.5 L packed bed bioreactors) is explored. Various conditioning techniques are studied to enhance the performance of SSF when using green waste. Additionally, the feasibility of simultaneously producing indole-3-acetic acid (IAA) and conidial spores through SSF with *Trichoderma harzianum* is investigated. The key factors influencing IAA and conidia production including tryptophan concentration, moisture, grass content, temperature, and fermentation time are analyzed to optimize their yields. Finally, a test is conducted to evaluate the effectiveness of the SSF-derived material on seed germination.

## 4.2 The materials and conditions of the experiments

To use a homogenous substrate for the experiment and reduce the variation between the results, a large enough amount of grass and pruning waste was collected to be used in all the experiments of this chapter. The characteristics of the grass and pruning waste used in this chapter are presented in Table 4.1. All the fermentations in this chapter were performed in 0.5 L cylindrical packed bed type reactors.

Table 4.1 The characteristics of the grass clipping and pruning waste used in the following experiments

	Grass	Pruning waste
pH	7.18 ± 0.07	5.73 ± 0.13
Conductivity (μS m <sup>-1</sup> )	1520 ± 320	293 ± 47

### 4.3 Experiments

#### 4.3.1 The effect of green waste conditioning procedures on solid state fermentation

In the initial attempt to conduct SSF using grass clippings, TH failed to grow and sporulate. The likely cause for that could be the presence of toxic compounds in the grass due to the use of chemical herbicides. To address this problem, conditioning techniques were applied to reduce the potential toxicity of the grass, likely caused by herbicide use and help to clean the grass more properly. To do so, three different conditioning procedures were applied to the grass to study their effects on TH sporulation. The conditioning methods were as follows: A) Washing the grass and drying it with airflow as described in materials and methods, B) Adding phosphate buffer to the grass before starting fermentation, and C) Combining both conditions A and B.

The results of these conditioning procedures on TH sporulation are shown in Figure 4.1a. As can be seen, after washing and drying the grass, no TH growth was detected. The initial and final pH values were  $6.42 \pm 0.02$  and  $8.23 \pm 0.01$ , respectively. However, when the buffer was used, the final pH was  $7.57 \pm 0.39$  and TH growth reached  $3.7 \times 10^8 \pm 2.4 \times 10^8$  spores  $\text{g}^{-1}$  DM, with. The highest conidia count,  $2.0 \times 10^9 \pm 1.1 \times 10^9$  spores  $\text{g}^{-1}$  DM, was achieved when the grass was washed, dried, and treated with buffer, with a final pH of  $7.46 \pm 0.36$ . These pH measurements suggest that a pH above 8 can negatively impact TH growth, while the buffer helps maintain the pH within a tolerable range for TH. This finding aligns with the optimum pH range of 6-7 for TH growth reported in other studies (Zhang and Yang, 2015).



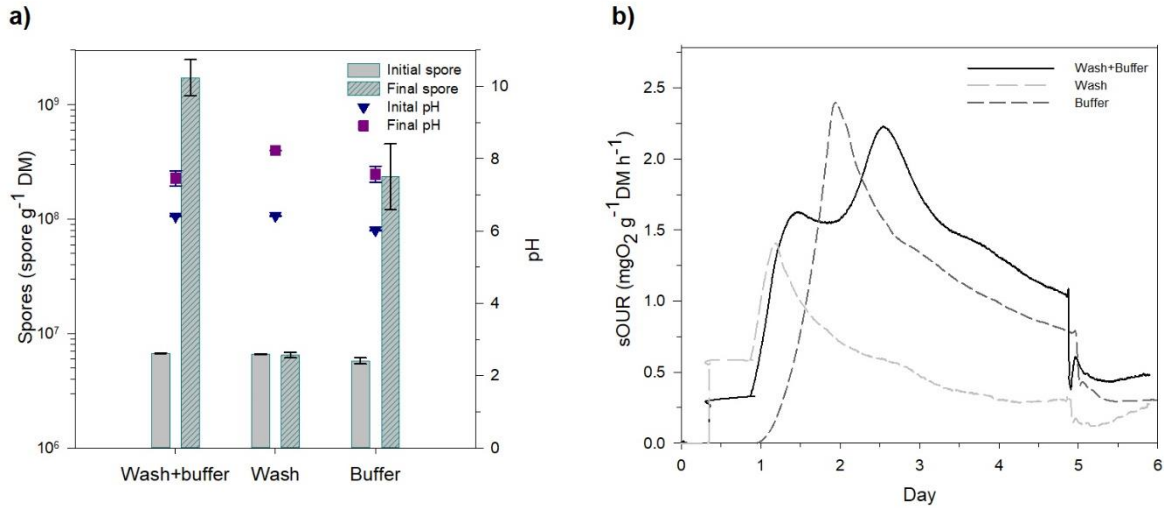


Figure 4.1. Different conditioning procedures for the grass. (a) the effect of conditionings on spore production and pH. (b) The respiration profiles for the conditioning procedures. The experiments were carried out in triplicate and the error bars present standard deviations.

It seems that the conditioning also affected the sOUR profiles of the GW (Figure 4.1b). When it was only washed the maximum sOUR was almost 1.5 g O<sub>2</sub> kg<sup>-1</sup> DM h<sup>-1</sup> with a lag phase of 18h. However, in the two conditionings where the buffer was used the maximum sOUR was between 2 and 2.5 g O<sub>2</sub> kg<sup>-1</sup> DM h<sup>-1</sup> although the lag phases were different. When using just buffer the lag phase was longer (35h) while when washing and buffer were done together the lag phase was 24h. Here the higher sOUR could be related to the higher sporulation of TH.

In summary, these results showed that washing and drying the grass, followed by the addition of buffer, can significantly enhance conidia production. As previously discussed, pretreatment and conditioning of lignocellulosic materials can reduce heterogeneity and increase the degradability of lignocellulosic complexes (Kucharska et al., 2018). For example, enzymatic pretreatment has been used to produce bioethanol from green waste, including a mixture of branches, leaves, tree

prunings, and grass clippings (Sofokleous et al., 2022). Similarly, in another study, iron ion-catalyzed hydrogen peroxide pretreatment was applied to sawdust to produce bio-jet fuels, offering a novel and more environmentally friendly strategy that also improved production (Zhu et al., 2024). While pretreatment is often a complicated and costly step in the valorization of lignocellulosic materials, which can be a limiting factor (Betiku and Ishola, 2023; Zhao et al., 2022), this study showed that fermentation can be improved with a low-cost procedure. This suggests that GW has a high potential as a substrate for valorization through SSF.

### **4.3.2 The feasibility of TH growth and sporulation on grass and pruning waste**

In order to study TH growth on G and PW, fermentation was conducted using G, PW, and the mixture of G and PW (50%:50% (w/w)) for 9 days. Considering the occurrence of maximum spore production observed using the same strain of TH in an SSF process (Sala et al., 2020), a larger span was chosen to be sure the maximum spore production was obtained during the run time.

Figure 4.2a shows the spore production on different percentages of G and PW. On day 5, spore counts were maximum on PW ( $9.03 \times 10^8 \pm 1.01 \times 10^6$  spore  $g^{-1}$  DM). However, after 7 days of fermentation, the number of spores increased on G and the mixture. On day 9, the spore counts were maximum on G and the mixture which were  $1.16 \times 10^9 \pm 1.55 \times 10^8$  and  $1.22 \times 10^9 \pm 1.33 \times 10^8$  spore  $g^{-1}$  DM, respectively.

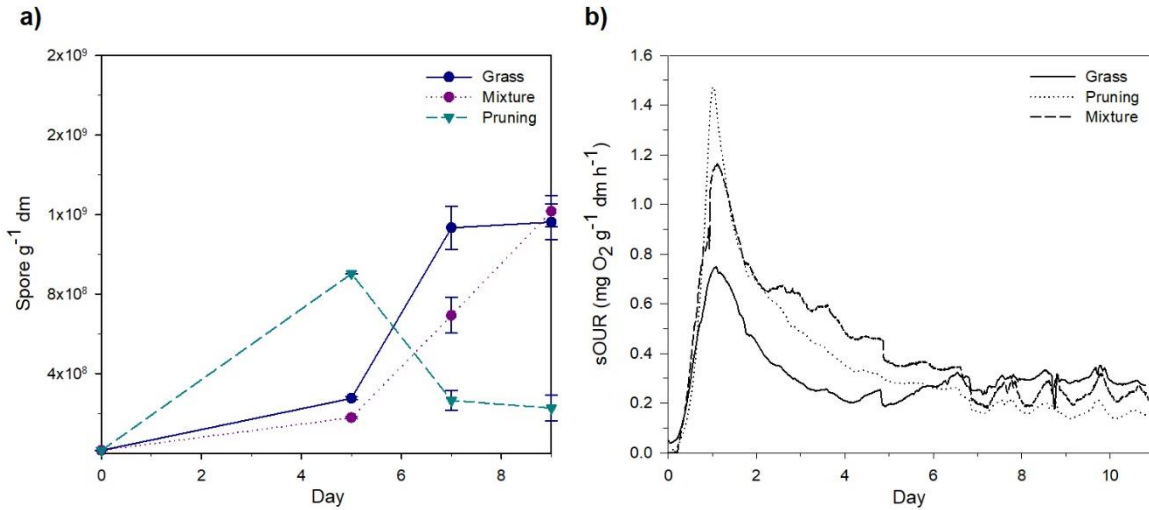


Figure 4.2. (a) Spore counts in different percentages of grass and pruning waste. (b) Respiration profile of different percentages of grass and pruning waste. The experiments were carried out in triplicate and the error bars present standard deviations.

The sOUR profile of the SSF process of G, PW, and the mixture is presented in Figure 4.2b. The maximum sOUR was higher for PW than for G and the mixture meaning that PW contains a small fraction of easily biodegradable organic matter. However, COC for the mixture is  $110.54 \text{ g } O_2 \text{ kg}^{-1} \text{ DM h}^{-1}$  which is higher than the COC of G and PW ( $80.98$  and  $93.09 \text{ g } O_2 \text{ kg}^{-1} \text{ DM h}^{-1}$ , respectively) indicating that the mixture could be more suitable for TH growth. The time to reach the maximum respiration was between 24 to 30 h for all the substrates.

There was no correlation between sporulation and microbial activity. In a similar study, it was reported sporulation of TH with different agro-industrial substrates, and they also did not find a correlation between spore production and the biodegradability of the substrate (Sala et al., 2021b).

Overall, these results suggest that G and PW are promising substrates to be used by TH. Given the low sOUR of grass and the potential for future scale-up, combining these materials likely offers

additional benefits. Moreover, PW can act as a bulking agent and enhance the porosity of the mixture (Sala et al., 2021; Ballardo et al., 2017; Mejias et al., 2018). Therefore, in all the following experiments in this chapter, a mixture of grass and pruning waste was used as the substrate.

### **4.3.3 The effect of tryptophan on spore and IAA production**

A preliminary experiment was carried out to test the feasibility of IAA production using GW and the effect of Trp concentration on spore and IAA production. Tryptophan in three different concentrations of 0.5%, 1 %, and 1.5% (w/w) was added as a powder to the substrate (mixture of G and PW 50%:50%). The number of spores and IAA were checked after 5, 7, and 9 days. As shown in Figure 4.3, TH did not grow with 1% and 1.5% of Trp. It appears that IAA was not produced by the fungi either probably due to the low growth of TH. However, TH growth with 0.5% of Trp was high. The IAA produced by TH were  $9 \pm 2$ ,  $14 \pm 3$ , and  $6 \pm 1 \mu\text{g g}^{-1}$  dry substrate after 5, 7, and 9 days of fermentation, respectively. The number of spores was  $1.6 \times 10^9 \pm 4.5 \times 10^8$ ,  $1.8 \times 10^9 \pm 3.0 \times 10^8$ , and  $1.6 \times 10^9 \pm 4.3 \times 10^8$  spore  $\text{g}^{-1}$  DM on days 5, 7, and 9, respectively. The results show the highest concentration of IAA was obtained on day 7, while the number of spores was the maximum on day 9. However, spore counts on day 9 were not significantly different from the spore counts on day 7 (p-value = 0.52). The oxygen consumption data indicated that the maximum sOUR was  $1.03 \text{ g O}_2 \text{ kg}^{-1} \text{ DM h}^{-1}$ .

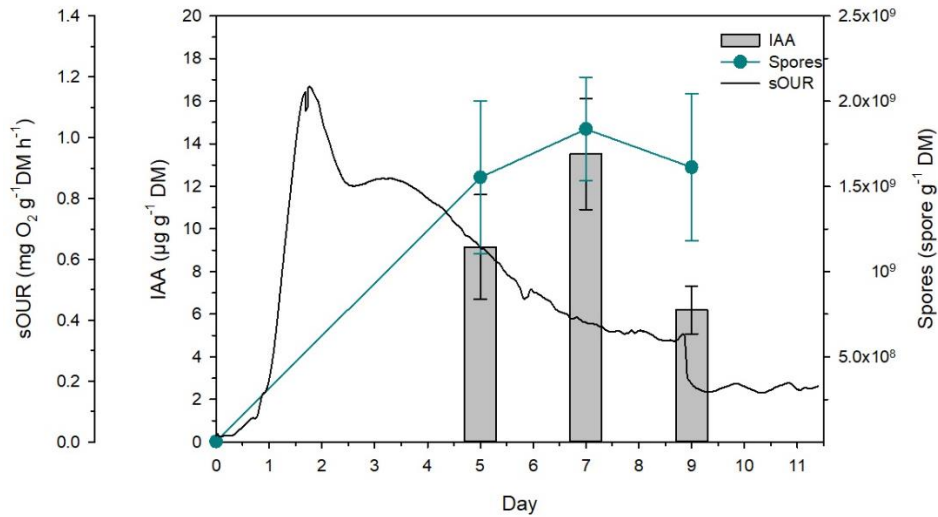


Figure 4.3. The effect of Trp (0.5%) on IAA concentration and spores. The experiments were carried out in triplicate and the error bars are standard deviations. Data from two other Trp treatments were not presented as no IAA and spore production observed.

Based on the results of IAA and spore production, 7 days can be a desirable time for fermentation to produce spores and IAA together. The fermentation time used in the study of (Zanoni do Prado et al., 2019a) was 5 days for IAA production. Sala et al. found that the maximum number of conidial spores produced by TH was obtained in 5-6 days (Sala et al., 2020). This inconsistency in the time of fermentation could be related to the different substrates and different lag phases in the fermentation. More information on this issue will be provided in the following sections.

Based on these results, it is suggested that a mixture of grass and pruning waste is a suitable substrate for producing IAA and conidial spores by TH. However, it appears that higher concentrations of Trp may negatively impact TH growth and sporulation. In a study it was found that in several *Trichoderma* species, growth and sporulation decrease in media containing Trp (Illescas et al., 2021). On the other hand, previous research indicates that Trp can significantly

boost IAA production in microorganisms with a Trp-dependent IAA biosynthesis pathway (Kumla et al., 2020; Mehmood et al., 2019; Reineke et al., 2008). This suggests that the *Trichoderma* strain used in this study likely produces IAA through a Trp-dependent pathway. However, excessive Trp reduces TH growth and sporulation. Therefore, finding an optimized Trp concentration is essential to maximize both spore and IAA production.

### 4.3.4 Optimization of IAA and spore production through SSF (a design of experiment)

The effect of three factors on IAA and spore production was studied by conducting a design of experiment. The selected factors and the tested levels were as follows: tryptophan concentration (0%, 0.25%, and 0.5% (w/w)), grass to pruning waste ratio (20%:80%, 50%:50% and 80%:20% (w/w)), and initial moisture (60%, 70%, and 80%). The parameters and the results of this design of the experiment are presented in Table 4.2. The maximum spore production was  $1.8 \times 10^9 \pm 8.7 \times 10^8$  spore  $g^{-1}$  DM when tryptophan, G to PW ratio, and moisture were 0.25% (w/w), 50%:50% (w/w), and 70%, respectively. However, the highest IAA production was  $75.8 \pm 8.6 \mu g g^{-1}$  DM obtained with tryptophan 0.5%, G: PW (80%:20%), and moisture 70%. In a similar work, an SSF process set up in 250 ml Erlenmeyer flasks containing 10 g of substrate with 1% (w/w) Trp produced 9.83 and 7.15  $\mu g g^{-1}$  DM of IAA by *Bacillus subtilis* and *Trichoderma atroviride*, respectively (Zanoni do Prado, et al., 2019). These data show that in the current work, the amount of IAA produced is higher than that of the work of Zanoni do Prado et al. (2019). For the conidia production, in a submerged liquid fermentation  $1.38 \times 10^8$  spore  $mL^{-1}$  was produced by *Trichoderma* spp (de Rezende et al., 2020). In another study, (Cavalcante et al., 2008) reported that *T. harzianum* produced  $2.28 \times 10^9$  spore  $g^{-1}$  DM through SSF. These data show that the number of conidia obtained in this experiment is in a similar range to other studies.

Table 4.2. The treatments and results of the Box-Behnken experimental design.

<b>Tryptophan</b> (%)	<b>Grass</b> (%)	<b>Moisture</b> (%)	<b>Spore gr<sup>-1</sup> DM</b>	<b>IAA</b> ( $\mu\text{g gr}^{-1}\text{DM}$ )
0.25	20	60	$6.1 \times 10^8 \pm 7.6 \times 10^7$	$16 \pm 5$
0	50	60	$4.5 \times 10^8 \pm 2.0 \times 10^8$	$16 \pm 6$
0.25	80	60	$4.1 \times 10^8 \pm 1.4 \times 10^8$	$27.6 \pm 2.4$
0.5	50	60	$6.9 \times 10^9 \pm 2.1 \times 10^8$	$13.4 \pm 5.4$
0.25	50	70	$1.4 \times 10^9 \pm 1.9 \times 10^8$	$16 \pm 7$
0.25	50	70	$1.8 \times 10^9 \pm 8.7 \times 10^8$	$23 \pm 8$
0.25	50	70	$1.6 \times 10^9 \pm 2.0 \times 10^8$	$18 \pm 8$
0	20	70	$1.6 \times 10^9 \pm 4.5 \times 10^8$	$12 \pm 4.22$
0.5	20	70	$1.6 \times 10^9 \pm 4.5 \times 10^8$	$13.97 \pm 4$
0	80	70	$9.02 \times 10^8 \pm 1.62 \times 10^8$	$17.1 \pm 1.6$
0.5	80	70	$6.5 \times 10^8 \pm 6.5 \times 10^8$	$75.8 \pm 8.6$
0.25	80	80	$6.1 \times 10^8 \pm 3.0 \times 10^8$	$32 \pm 9$
0.25	20	80	$7.94 \times 10^8 \pm 2.02 \times 10^7$	$41.1 \pm 4.4$
0	50	80	$5.9 \times 10^8 \pm 1.5 \times 10^8$	$26 \pm 11$
0.5	50	80	$5.2 \times 10^8 \pm 1.5 \times 10^8$	$36 \pm 11$

To optimize the production of IAA and spores, a prediction model was created using the results of the experimental design. Table 4.3 shows the statistical analysis of the experimental design. For spore production, a modified quadratic model with a data transformation of basic 10 logarithms was used as it was significant. The ANOVA analysis shows that the percentage of grass is the only significant main parameter for the spore response. All the terms of the model were significant

## Chapter 4

except tryptophan and moisture. This means that although tryptophan and moisture content are not significant parameters in the model, their interactions significantly affected the response (spore production). The lack of fit was also not significant, and the model can explain 98.83% of the variability of the response ( $R^2$ ). The model was adjusted to a regression (Equation 4.1) for the response of spore counts:

$$\begin{aligned} \text{Log}^{10}(\text{Spore}) = & 9.21 + 0.0313X_1 - 0.0862X_2 + 0.0016X_3 - 0.0996X_1 X_2 - & 4.1 \\ & 0.0583X_1 X_3 - 0.1268X_1^2 - 0.1005X_2^2 - 0.3394X_3^2 + 0.0723X_2^2 X_3 \end{aligned}$$

Where  $X_1$ ,  $X_2$ , and  $X_3$  are tryptophan%, grass%, and moisture%, respectively. The high intercept of the model suggests that the variables used in the model are not the most significant variables for the response (spore production).

For the analysis of IAA production, the data were best fitted in a linear model with the inverse transformation to predict the optimum condition. The regression equation was as follows:

$$\begin{aligned} \frac{1}{IAA} = & 0.0542 - 0.0174X_1 - 0.0190X_2 - 0.0119X_3 - 0.0118X_3^2 + & 4.2 \\ & 0.0140X_1 X_3^2 + 0.0146X_2 X_3^2 \end{aligned}$$

Where  $X_1$ ,  $X_2$ , and  $X_3$  are tryptophan%, grass%, and moisture%, respectively.

The model was significant in terms of p-value with a non-significant lack of fit.  $R^2$  for this model was 86.01%. All the parameters of the model for IAA were significant meaning the significant effect of Trp, the content of G, and moisture on IAA production.



Table 4.3. The p-value of the model and the parameters for spore and IAA. The created model for spore production is modified quadratic, and for IAA production was a linear model (p-value < 0.05 is significant).

Source	p-value	
	Spore	IAA
<b>Model</b>	0.0003	0.0045
<b>A-Tryptophan</b>	0.0690	0.0064
<b>B-Grass</b>	0.0014	0.0039
<b>C-moisture</b>	0.9371	0.0077
<b>AB</b>	0.0035	
<b>AC</b>	0.0287	
<b>A<sup>2</sup></b>	0.0014	
<b>B<sup>2</sup></b>	0.0040	
<b>C<sup>2</sup></b>	< 0.0001	0.0428
<b>AC<sup>2</sup></b>		0.0710
<b>BC<sup>2</sup></b>		0.0613
<b>B<sup>2</sup>C</b>	0.0444	
<b>Lack of Fit</b>	0.8164	0.5840

The optimized conditions to produce spore and IAA predicted by the model were as follows: tryptophan 0.43%, G: PW (56%:44%), and moisture 74%. Figure 4.4 shows that when moisture is 74%, the number of spores would increase by Trp in the range of 0.2- 0.5%, and lower G content. However, increasing G and Trp improves IAA production (Figure 4.4). The data suggests that a higher grass content in the substrate can enhance IAA production. This agrees with other works reporting that *Trichoderma* spp. produced more IAA when using substrates with low lignin content

## Chapter 4

from various agricultural wastes (Zanoni do Prado et al., 2019a). However, increasing the concentration of Trp resulted in higher IAA production but a decrease in spore numbers. In summary, these results indicate that the optimal conditions for maximizing spore production and IAA yield are not aligned making the optimization process challenging. Therefore, it is recommended to prioritize the optimization of one target over the other while producing both.

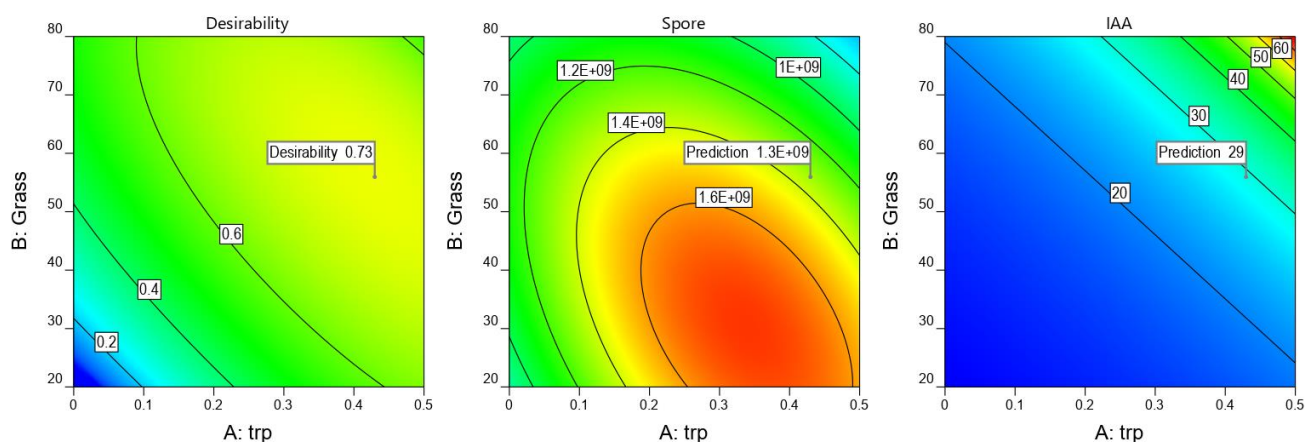


Figure 4.4. The contour profile of the predicted optimized point by the model. The moisture was set at 74%.

### 4.3.5 The effect of temperature on spore and IAA production

To study the effect of temperature on the number of spores and IAA production, three fermentations were set up at different temperatures (25, 27.5, and 30°C). The optimized condition predicted by the model was used for the fermentation. The results indicate that at 30°C, TH produced more IAA ( $25 \pm 9 \mu\text{g g}^{-1} \text{DM}$ ) (Figure 4.5). In contrast, the number of spores was higher at 25°C ( $1.64 \times 10^9 \pm 7.24 \times 10^8 \text{ spore g}^{-1} \text{DM}$ ) while being  $9.4 \times 10^8 \pm 2.5 \times 10^8 \text{ spore g}^{-1} \text{DM}$  at 30°C. sOUR profiles demonstrate much higher activity of TH at 30°C with maximum sOUR of  $2.4 \pm 0.2 \text{ g O}_2 \text{ kg}^{-1} \text{DM h}^{-1}$  compared to maximum sOURs at 25°C and 27.5°C ( $1.1 \pm 0.2$  And  $1.3 \pm 0.6 \text{ g O}_2 \text{ kg}^{-1} \text{DM h}^{-1}$ , respectively).

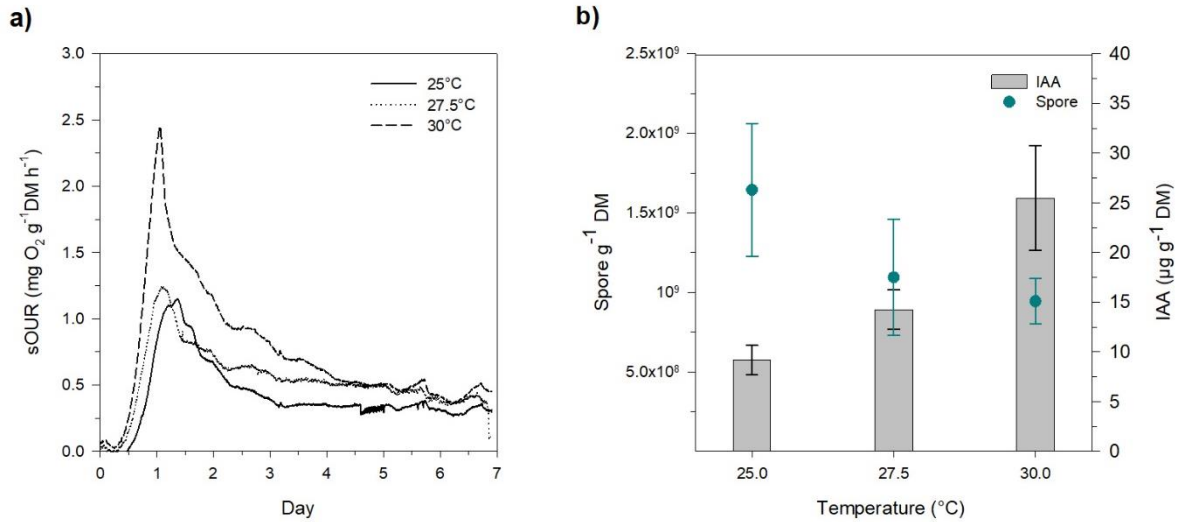


Figure 4.5. The effect of temperature on (a) sOUR and (b) spores and IAA production. The experiments were replicated three times and error bars are standard deviation.

The optimum temperature range for *Trichoderma harzianum* growth was reported to be between 25-30°C (Napitupulu et al., 2019a). However, the fermentation was set up at 30°C for IAA production with *Aspergillus flavipe* (Zanoni do Prado et al., 2019b). Also, a temperature of 28°C was used for *Trichoderma* spp. to grow and produce phytohormones including IAA (Illescas et al., 2021). Based on these findings, 30°C seems to be the preferred temperature for producing IAA using TH and GW. On the other hand, the results suggest that 25°C is more suitable for spore production which is similar to the other studies worked on TH spore production (Sala et al., 2020). The different desirable temperatures for IAA and conidial spore production highlight, again, the challenge of simultaneously maximizing both targets.

### 4.3.6 The effect of fermentation time on IAA and spore production

To obtain more information on the fermentation process a 10-day time course experiment was performed. To do so, 10 reactors with the same conditions were prepared and set up. Each day one reactor was sampled and discarded. The conditions were selected according to the optimized parameters predicted by the model. However, the first time course experiment was conducted without Trp. Here as expected, the production of IAA was much lower due to the absence of Trp in the process (Figure 4.6). The IAA profile shows a higher production of IAA on days 2 and 3 of fermentation. Then, on days 5 and 6 no IAA was detected. However, the maximum value for IAA was observed at day 10 ( $17 \pm 4 \mu\text{g g}^{-1} \text{DM}$ ). The profile of sporulation in this experiment showed an increasing trend until day 9 with the maximum spore counts of  $3.6 \times 10^9 \pm 8.7 \times 10^8$  spore  $\text{g}^{-1} \text{DM}$ . pH increased over time and ranged between 6.95 and 7.72.

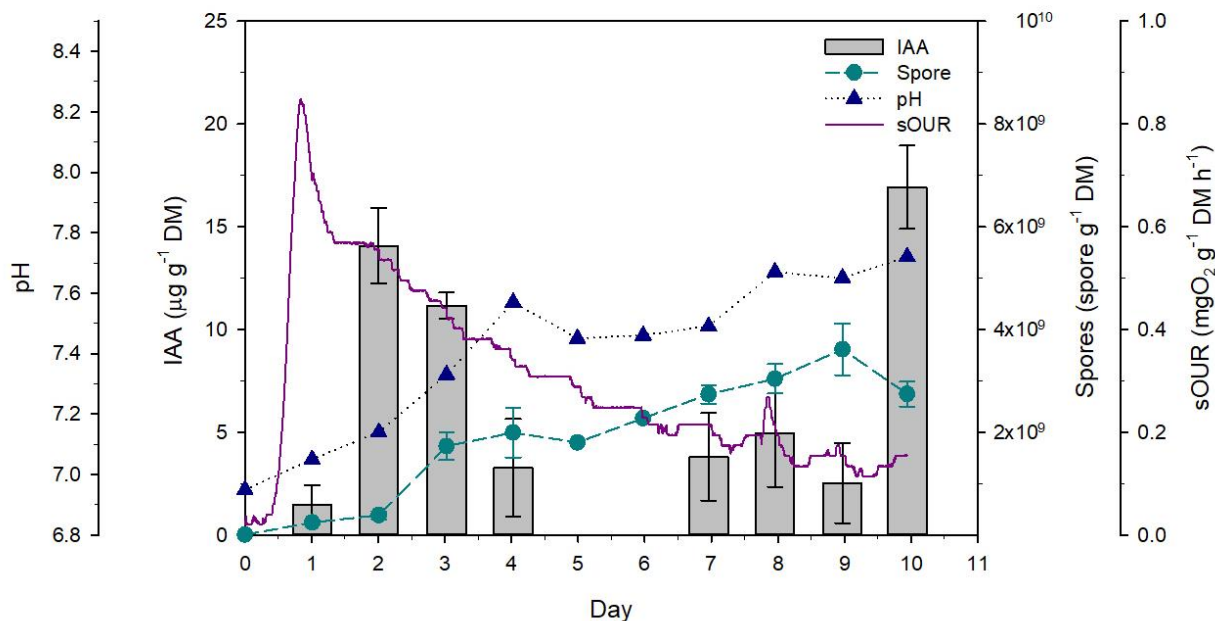


Figure 4.6. The results of a 10-day time course experiment for *T. harzianum* without Trp. The error bars are standard deviations of the triplicated samples taken from a single reactor.

Figure 4.7 presents the results of the second time course experiment that conducted with Trp at a concentration determined by the model. The profiles of spore and IAA production by TH over a 10-day period revealed that the maximum IAA production ( $101.4 \pm 4.1 \mu\text{g g}^{-1} \text{DM}$ ) was obtained after 3 days of fermentation whereas the number of spores was maximum on day 7 ( $3.0 \times 10^9 \pm 8.6 \times 10^8 \text{ spore g}^{-1} \text{DM}$ ). The pH showed an increasing trend until day 4-5 and from an initial value of 7.06 reached 8.22. The pH was 8.05 and 7.84 respectively when the maximum IAA and spores were produced. Then, started declining and on day 10 it was 7.37. The respiration profile showed that the microbial activity was maximum during days 1-2, being the maximum sOUR value of  $1.46 \text{ g O}_2 \text{ kg}^{-1} \text{DM h}^{-1}$ .

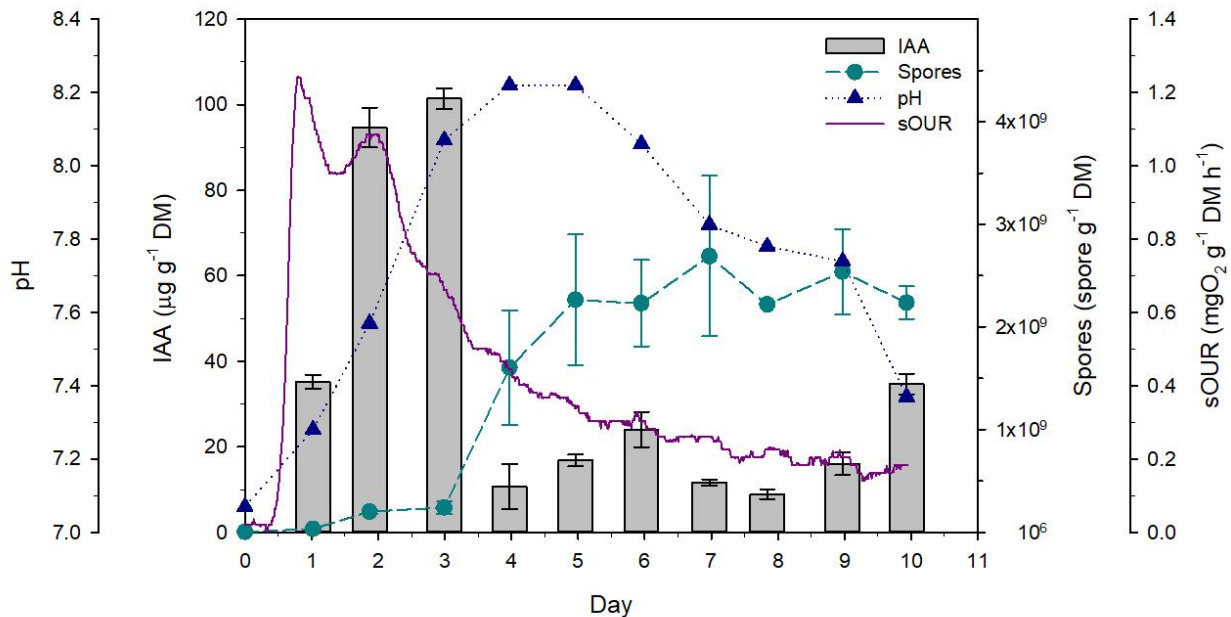


Figure 4.7. The results of a 10-day time course experiment for *T. harzianum*. The error bars are standard deviations of the triplicated samples taken from a single reactor.

The third time course experiment was carried out to see if a different strain of *Trichoderma* produces IAA and conidia similarly to TH using the optimized conditions predicted by the model. In this experiment, *T. viride* (TV) was used as inoculum with the same condition as the TH time course experiment (Figure 4.8). Here, the maximum IAA obtained on day 1 and the maximum spore production obtained on day 4, were  $18 \pm 5 \mu\text{g g}^{-1} \text{DM}$  and  $4.3 \times 10^9 \pm 4.3 \times 10^8 \text{ spore g}^{-1} \text{DM}$  respectively. As can be seen from the data, TV produced more spores and a lower amount of IAA than TH. However, it is worth noting that in both strains, IAA concentration decreased significantly when the number of spores started increasing, even though no contamination was detected. The pH increased over time, when the inoculum was TV, starting from 7.05 on the initial day to 8.15 on day 8. At the time that spores had the biggest number the pH was 7.52 while when IAA was maximum pH was 7.21. The maximum sOUR for TV observed on days 1-2 of fermentation is similar to that of TH ( $1.24 \text{ g O}_2 \text{ kg}^{-1} \text{ DM h}^{-1}$ ).

The results of the time course experiment for TH and TV showed that there was a similar interaction between IAA concentration and the number of spores produced for both strains. This observation could suggest that there is a relationship between IAA and sporulation. The different values of optimized parameters of spores and IAA obtained previously by the model also support the hypothesis. It was mentioned before that IAA acts as a signal for the interaction between plant-fungi and fungi-fungi (Tomberlin et al., 2017). Karina Manzo-Valencia et al. (2016) described that in some of the fungal species, a low concentration of IAA can stimulate sporulation, but high amounts of IAA inhibit the sporulation. A similar interaction was reported to occur between plants and fungi when IAA is the mediator (Keswani et al., 2020). It has also been reported that *Pseudomonas putida* and *T. atroviride* have the ability to degrade excess IAA to reduce the

negative effects on plant growth (Gravel et al., 2007). So, it is possible that TH and TV in the current work also degraded excess IAA to increase their sporulation. However, the information and evidence on this issue are limited and more research is required to elucidate the reasons in more detail.

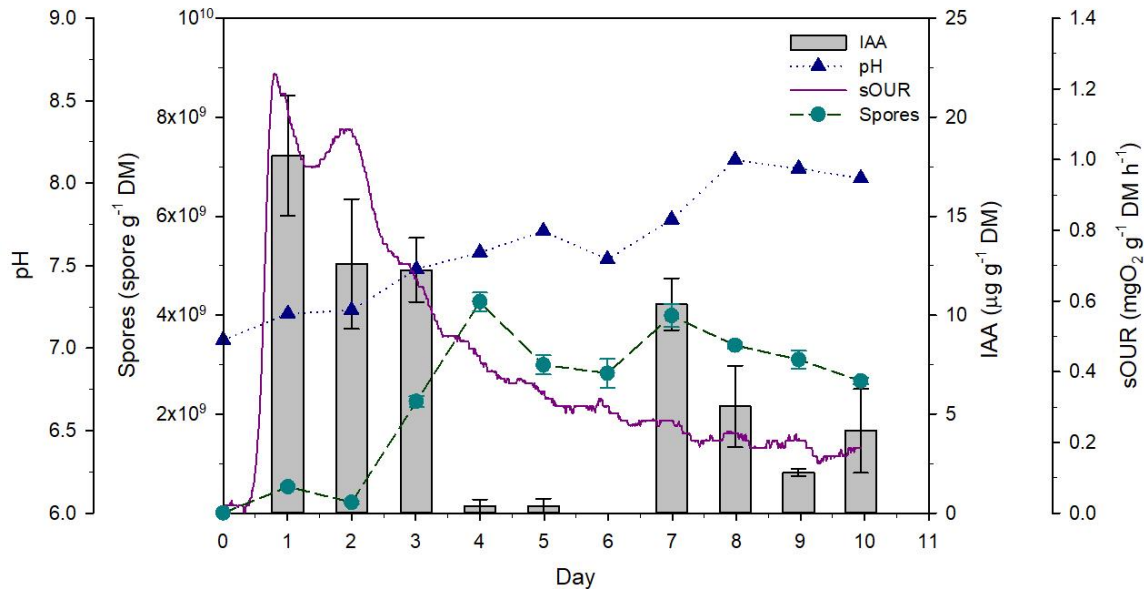


Figure 4.8. The results of a 10-day time course experiment for *T. viride*. The error bars are standard deviations of the triplicated samples taken from a single reactor.

The pH profile for both strains was not similar, however, the pH range was the same (approximately 7-8.3) and agrees with the reports from other studies. In the experiment with no Trp, pH had an increasing trend and was in the desirable pH range for TH. It was mentioned previously that the optimum pH range for *T. harzianum* to produce spores was reported between 6-7 (Sala et al., 2020; Zhang and Yang, 2015). For the IAA also the optimum pH range is neutral (5-8) in most of the microorganisms including *T. harzianum* (Bharucha et al., 2013; Napitupulu et al., 2019b).

The oxygen consumption profiles were similar TH and TV with the approximate sOUR maximum value of  $1.2 \text{ g O}_2 \text{ kg}^{-1} \text{ DM h}^{-1}$  for both experiments. However, when no Trp was used for TH sOUR was lower ( $0.9 \text{ g O}_2 \text{ kg}^{-1} \text{ DM h}^{-1}$ ). This can suggest that adding Trp to the fermentation and the subsequent IAA production increased TH activity.

In summary, these results suggest that for both strains, the fermentation time to obtain the maximum amount of IAA and the number of spores is different. In the conditions studied, for TH, the maximum IAA was produced at days 2-3 of the fermentation while the biggest spore number was obtained at days 7-9. On the other hand, for TV, IAA production reached the maximum on day 1 whereas the number of spores was maximum on day 4 of the fermentation. Considering the obtained results, it is recommended to set the fermentation time at 2-3 days to achieve the maximum IAA level while still obtaining an acceptable spore count, as IAA production appears to be a more promising focus for future research.

### **4.3.7 The fate of added IAA in SSF**

To determine if IAA can be consumed by TH, a 5-day time-course experiment with two sets was performed to monitor the IAA levels during the sporulation and activity of TH in an SSF process. In each set, 5 reactors were prepared, and each day one reactor was opened to analyze and then discarded. In one set  $100 \mu\text{g g}^{-1} \text{ DM}$  of IAA was added to the substrate (mixture of G and PW) while the other set served as a control with no added IAA. As presented in Figure 4.9, the IAA level added to the fermentation decreased from  $81.87 \pm 8.72 \mu\text{g g}^{-1} \text{ DM}$  on the initial day to  $13.89 \pm 1.02 \mu\text{g g}^{-1} \text{ DM}$  on day 2 of the fermentation. Meanwhile, an increase in the number of spores was observed. The number of spores in the fermentation with added IAA ( $3.01 \times 10^9 \pm 4.94 \times 10^8$



spores  $\text{g}^{-1}$  DM) was higher than in the fermentation without added IAA ( $1.96 \times 10^9 \pm 3.24 \times 10^8$  spores  $\text{g}^{-1}$  DM).

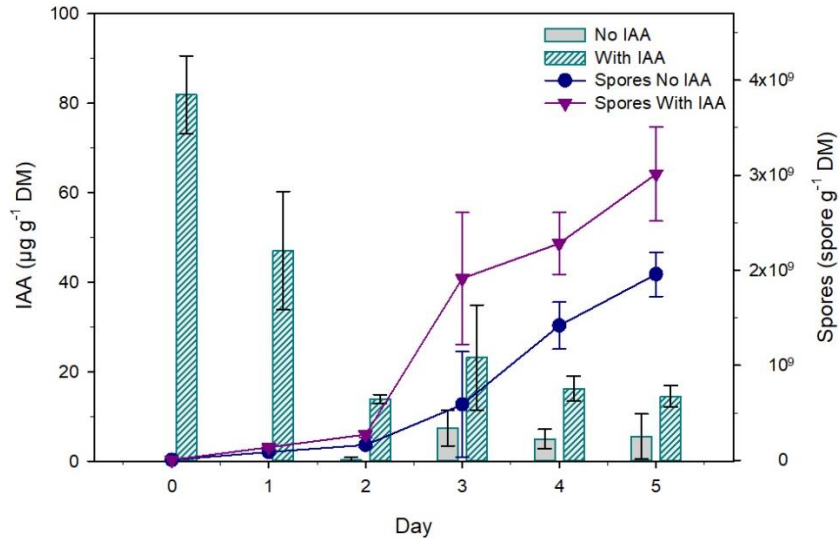


Figure 4.9. The fate of IAA added to the fermentation and its effect on TH sporulation.

The oxygen consumption profiles of the two sets of time courses are presented in Figure 4.10. The profiles showed a similar profile but a slightly higher sOUR when IAA was added with the value of  $1.30 \text{ g O}_2 \text{ kg}^{-1} \text{ DM}$ , while when IAA was not added it was  $1.17 \text{ g O}_2 \text{ kg}^{-1} \text{ DM}$ .

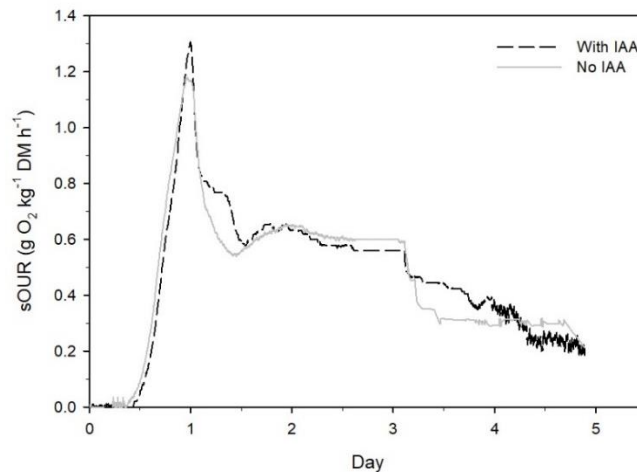


Figure 4.10. sOUR profile in the presence and absence of IAA.

Comparing the recently obtained data to the results presented in 4.3.6, a similar profile can be observed. In all experiments, IAA degradation began before the sporulation reached its maximum. These results support the idea that the consumption of IAA by TH promotes increased sporulation. These results also suggest that about 80% of the IAA added to the fermentation process is recovered. In the present study, the methods used to extract IAA are similar to conventional methods used in other studies on liquid and solid fermentations. These methods are typically suitable for HPLC analysis (Bunsangiam et al., 2021; Nutaratat et al., 2017; Zanoni do Prado et al., 2019b). However, some methods use specific solvents, such as ethyl acetate or ethanol, to partially purify IAA, which are generally applied for TLC analysis (Goswami et al., 2015; Rupal K et al., 2020). IAA recovered from different solid substrates was studied and reported that depending on the substrate and the concentration of IAA added, the recovery could be different (Zanoni do Prado et al., 2019a). It is recommended that more efficient techniques are found to enhance the recovery of IAA from fermented GW such as using special solvents.

### **4.3.8 Germination test**

To test the biostimulant effect of SSF products on seed germination, extracts of three treatments from the design of the experiment were applied to cucumber (*Cucumis sativus*) seeds. The selected treatments were one with the lowest IAA production, one with middle IAA, and one with the highest IAA production. Besides two different concentrations of pure IAA and distillate water were used as controls. The treatments and their corresponding IAA are listed in Table 4.4. Each treatment was performed in triplicate. The results of germinated seeds after 5 days are presented in Table 4.5, Figure 4.11, and Figure 4.12.

Table 4.4. The list of treatments used for cucumber seed germination. Each treatment was tested with three replications

<b>Treatment</b>	<b>IAA (<math>\mu\text{g mL}^{-1}</math>)</b>	<b>Trp (%)</b>	<b>G (%)</b>	<b>Moisture (%)</b>
<b>A</b>	0.77	0	20	70
<b>B</b>	1.22	0.25	80	80
<b>C</b>	4.66	0.5	80	70
<b>IAA 1</b>	17.5			
<b>IAA 2</b>	1.75			
<b>Water</b>	0			

Table 4.5. The results of germination tests. SG%: seed germinated percentage; RSG: relative seed germination; RGG: relative radicle growth; GI: germination index.

	<b>Total radicle length (mm)</b>	<b>SG (%)</b>	<b>RSG (%)</b>	<b>RGG (%)</b>	<b>GI (%)</b>
<b>A</b>	46 $\pm$ 13	80 $\pm$ 10	114.3 $\pm$ 14.2	39.7 $\pm$ 11.2	45.8 $\pm$ 15.5
<b>B</b>	65.67 $\pm$ 26.0	60 $\pm$ 0	85.7 $\pm$ 0.0	56.6 $\pm$ 22.4	48.5 $\pm$ 19.2
<b>C</b>	99 $\pm$ 14.5	70 $\pm$ 10	100 $\pm$ 14.3	85.3 $\pm$ 12.5	86.5 $\pm$ 24.8
<b>IAA1</b>	14.3 $\pm$ 4.0	50 $\pm$ 10	71.4 $\pm$ 14.3	12.3 $\pm$ 3.5	9.1 $\pm$ 4.3
<b>IAA2</b>	33.3 $\pm$ 11.9	53.3 $\pm$ 5.8	76.2 $\pm$ 8.2	28.7 $\pm$ 10.3	21.3 $\pm$ 6.0
<b>Water</b>	116 $\pm$ 5.6	70 $\pm$ 10			

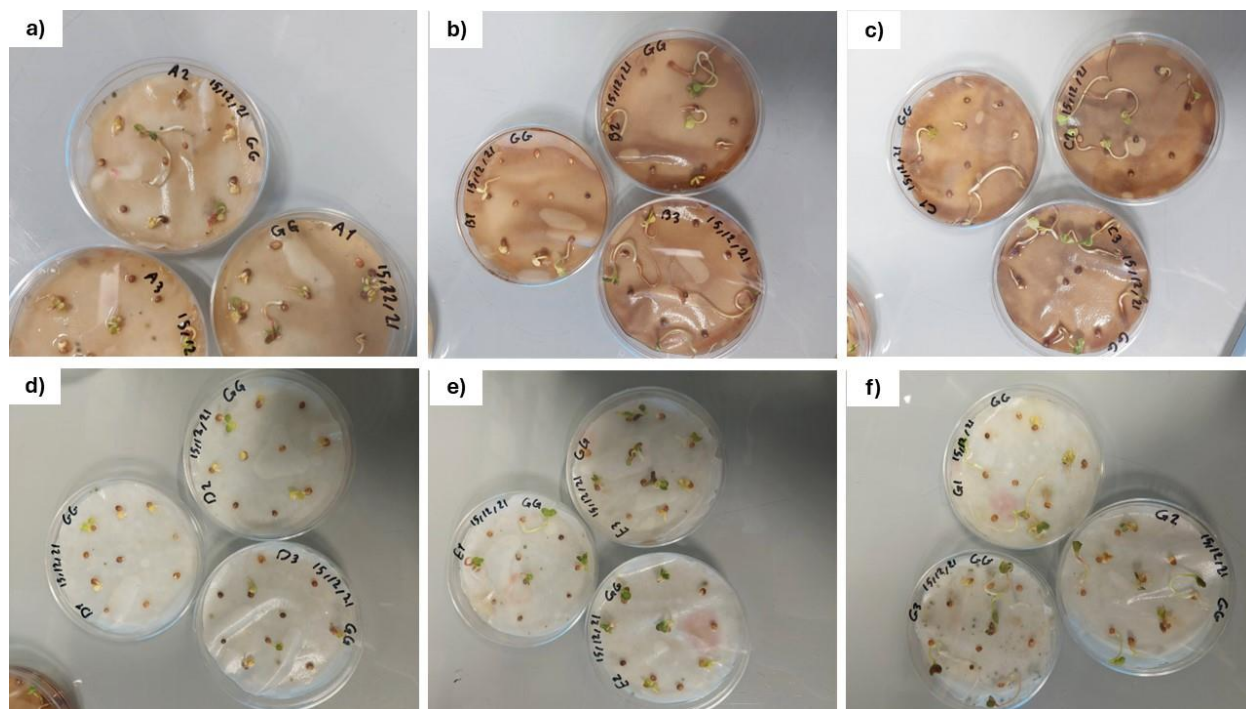


Figure 4.11. the germinated seed with different treatments after 5 days. a) treatment A, b) treatment B, c) treatment C, d) treatment IAA1, e) treatment IAA2, f) distillate water.

According to the results, the highest germination results were observed for treatment C with a GI of 86.5%. The GI for treatments A and B were lower and 45.8% and 48.5% respectively. For treatment A, the number of germinated seeds was more than for treatment C however, the total length of the radicle was much less. These results suggest that using an SSF product with higher IAA content has more positive effects on seed germination. On the other hand, GI was significantly low when using pure IAA, especially for IAA1 which is highly concentrated. However, as observed in Figure 4.12a, the root is too short with a lot of lateral roots. For this reason, the germination indices when IAA1 was applied were too low. The important point is the germination results in IAA2 with GI of 21.3%. This value is much lower than the value of GI for treatment B

which has a similar content of IAA. This is probably due to the other biostimulant effects of the SSF product resulting from the activity of TH.

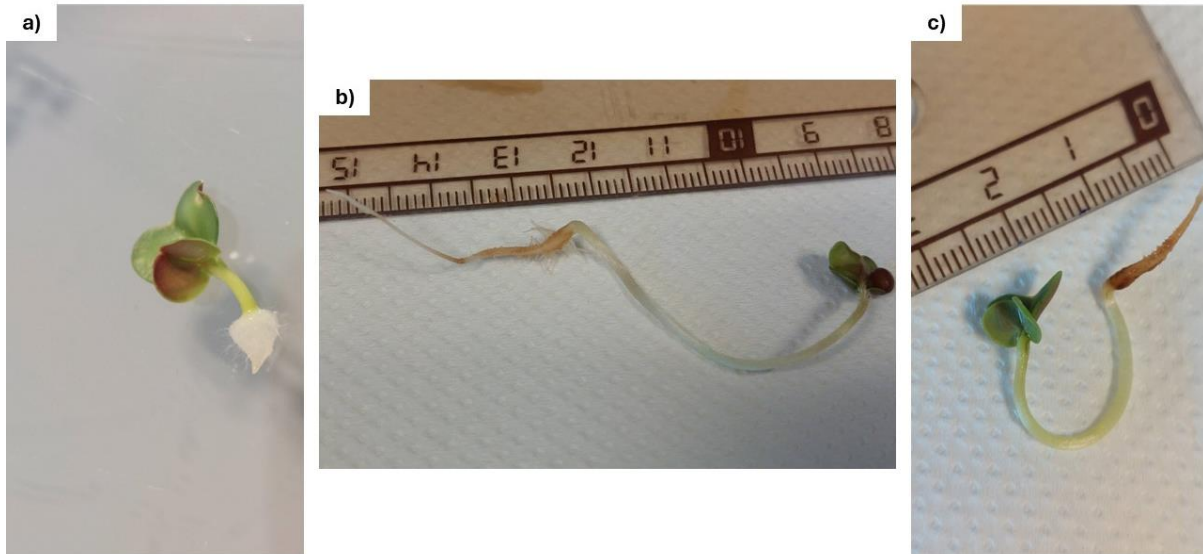


Figure 4.12. a) seed germinated under treatment IAA 1 with short and thick roots. b) seed germinated under treatment C. c) seed germinated with distillate water

The effect of IAA on seed germination varied depending on the plant species and IAA concentration. For example, (Zhao and Zhong, 2013) applied IAA and gibberellic acid to improve the germination of Chinese fir (*Cunninghamia lanceolata*). They showed that IAA in concentrations of  $10^{-4}\text{M}$  ( $17.5 \mu\text{g mL}^{-1}$ ) and  $10^{-5}\text{M}$  ( $1.75 \mu\text{g mL}^{-1}$ ) had the most significant effect on seed germination. However, seed germination and seedling characteristics in sesame increased with  $2 \mu\text{g mL}^{-1}$  of IAA (Subash et al., 2015). Tabatabae et al. reported that IAA application from bacterial production inhibit seed germination of durum wheat depending on the concentration. As IAA at  $5$  and  $10 \mu\text{g mL}^{-1}$  promote the germination while inhibit it at  $20 \mu\text{g mL}^{-1}$  (Tabatabaei et al., 2016).

## Chapter 4

These findings show the positive effect of the SSF extract on seed germination, offering the potential for future applications of the final SSF product derived from green waste. Additionally, they suggest the need for further studies on the application of IAA in seed germination and its impact on other plant growth factors.

### **4.4 Conclusion**

The experiments presented in this chapter suggest that despite the limitations in its heterogenicity, green waste can be an advantageous substrate to produce biostimulant (IAA) and biopesticide (conidial spore) through solid state fermentation. Several key parameters, tryptophan concentration, grass content, and moisture levels, were analyzed to develop a predictive model for simultaneously optimizing the production of IAA and conidial spores. However, the results indicate that the optimal conditions for producing these two products do not align. Further studies suggest that other parameters, such as temperature and fermentation duration, are also different for the production of IAA and spores, as most IAA degrades before sporulation reaches its peak. To better understand the relationship between sporulation and IAA production, an experiment was conducted, revealing that IAA is consumed by TH. However, additional research is recommended to provide further insights and develop strategies to enhance production efficiency.

Furthermore, SSF extracts containing different amounts of IAA were applied to test seed germination, yielding promising results. It is recommended that future research focus on the application of SSF products to plants.

Overall, the findings in this chapter offer new insights into the valorization of green waste through SSF. To provide a basis for scaling up the production, further research is recommended.

## Chapter 5

# Solid-State Fermentation to Produce Biostimulant Agents from Green Waste at Bench-Scale (22 L)

---

Part of this chapter is under review to be published in Chemical Engineering Journal: Ghoreishi, G., Barrena, R., Sánchez, A., & Font, X. (2024). Solid-State Fermentation to Produce Biostimulant Agents from Green Waste: A Circular Approach at Bench-Scale.

The tests regarding spore germination have been conducted during a training mobility (Erasmus+) in University of Copenhagen.

## 5.1 Overview

This chapter explores the feasibility of scaling up the SSF process previously developed to a 22 L volume packed bed for the production of IAA and conidial spores using *Trichoderma harzianum* with green waste as the substrate. First, the effect of key SSF parameters, including the porosity and Trp concentration, at 22 L scale is studied. Additionally, the challenges associated with using GW on a larger scale are investigated. The efficiency of implementing a sequential batch operation as a potential strategy to increase the production of IAA, extend it over time, and spores is also assessed.

Finally, preliminary tests are conducted to study the stability of the final SSF product. This included studying the degradation of IAA in the fermented material at room temperature, as well as evaluating the germination ability of conidial spores after the fermentation. Further tests are performed to examine the effects of IAA, Trp, and temperature on TH spore germination.

## 5.2 The materials and condition of the experiments

For the experiments in this chapter, grass clippings were collected and prepared twice. The first batch, referred to as G1, was used in the initial two experiments. The second batch, G2, was utilized in the sequential batch experiment and the experiments involving different amounts of Trp. Additionally, one sample of pruning waste was collected, and wood chips were also used in some experiments. Table 5.1 presents the basic characteristics of the substrates.



Table 5.1. The characteristics of the substrates used in the current chapter. G1: grass clipping batch 1; G2: grass clipping batch 2; PW: pruning waste; WC: wood chips.

	<b>G1</b>	<b>G2</b>	<b>PW</b>	<b>WC</b>
<b>pH</b>	6.94	7.05	6.85	6.79
<b>Conductivity (<math>\mu\text{S m}^{-1}</math>)</b>	2400	1969	1240	1007
<b>C/N</b>	18.7	18.5	98.5	117.4

All the fermentations in this chapter were conducted in a 22 L packed bed reactor. The ratio of grass to wood chips, as well as the initial moisture content and added Trp, was previously optimized using 0.5 L reactors in Chapter 4. The optimal conditions were 56% grass (G) and 44% pruning waste (PW) (on a dry matter basis), with 0.43% (w/w) Trp and 74% initial moisture.

## 5.3 Experiments

### 5.3.1 Bench-scale SSF performance

#### 5.3.1.1 Preliminary experiment

The preliminary batch experiment in the 22 L bioreactor was conducted using grass and pruning waste over 7 days. Samples were taken from the top of the reactor on days 1, 2, and 3 of fermentation. On the final day (day 7), additional samples were collected from the top, center, and bottom of the reactor. As illustrated in Figure 3.7, top, center and bottom parts are the zones that are located between 16-25 cm, 8-16 cm, and 0-8 cm of the bed height respectively. The results are presented in Figure 5.1. The concentration of IAA on day 3 reached  $347 \pm 69 \mu\text{g g}^{-1}$  DM, and by day 7, it was  $327 \pm 44 \mu\text{g g}^{-1}$  DM, that interestingly were much higher than those obtained at 0.5 L

scale. The number of spores was  $9.1 \times 10^8 \pm 2.2 \times 10^8$  spores  $\text{g}^{-1}$  DM at day 3. However, on day 7 the spores could not be counted due to the contamination shown in Figure 5.2.

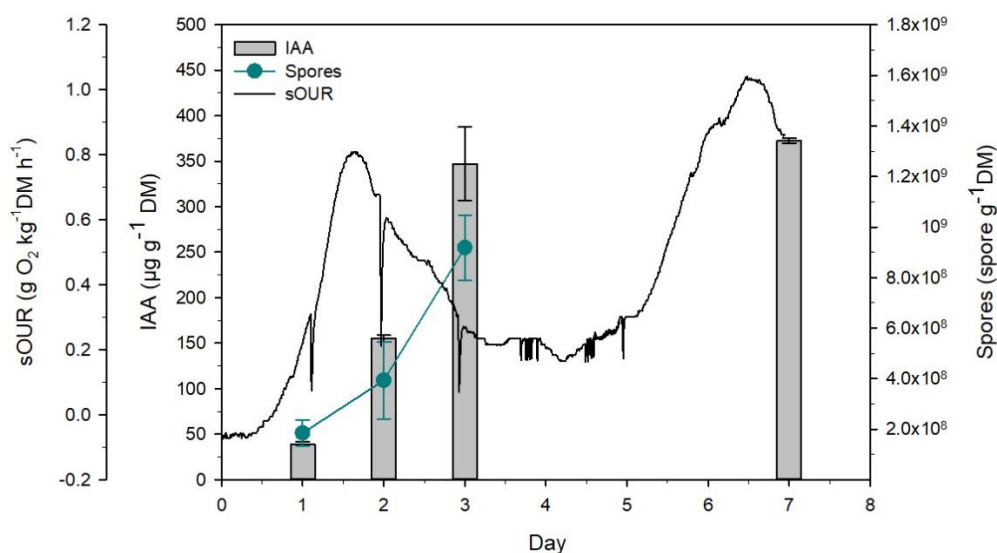


Figure 5.1. The results of the preliminary experiment in the 22 L reactor with pruning waste as bulking agent. The error bars are the standard deviation of the samples taken from different zones of the reactor.

At the end of fermentation, the oxygen consumption profile (Figure 5.1) revealed the contamination by showing a sOUR peak. The first and the second peak of sOUR were 0.81 and 1.04  $\text{g O}_2 \text{ kg DM}^{-1} \text{ h}^{-1}$  respectively. Figure 5.3 shows the temperature profiles in different zones of the reactor. The maximum temperature, 31°C (day 2), was recorded at the reactor's center, while the temperature in the lateral parts of the reactor was lower. Two temperature peaks can also be observed, coinciding with the peaks of sOUR, indicating the periods of maximum biological activity.

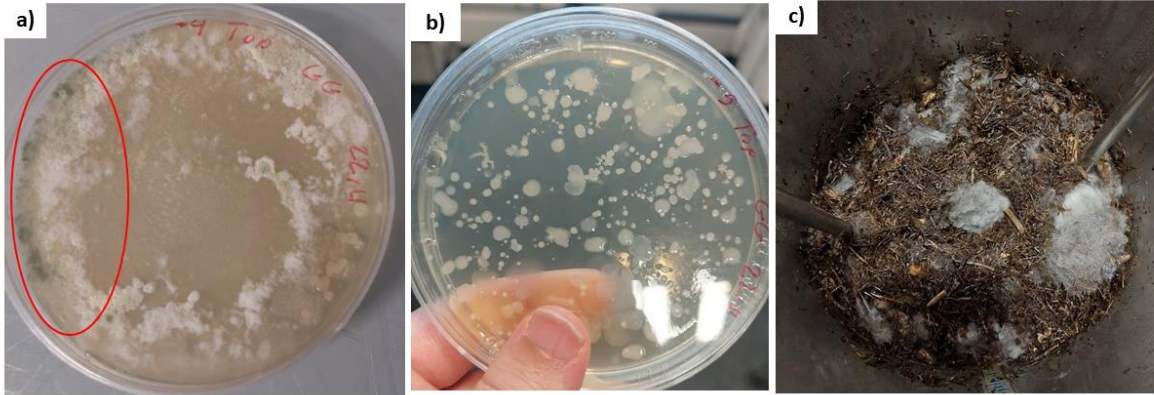


Figure 5.2. The contamination observed in the reactor. a) The plate prepared from the samples on day 3 of fermentation, b) The plate prepared from the samples on day 7 of fermentation, c) The SSF at day 7.

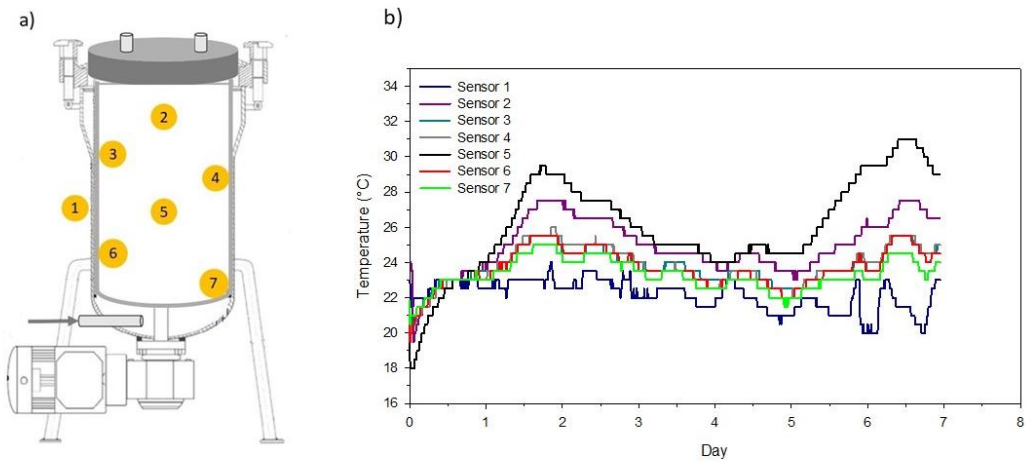


Figure 5.3. a) The location of the sensors, b) The temperature profiles of the fermentation in different zones of the reactor.

## Chapter 5

The contamination was also detected after preparing microbial cultures from samples taken on days 3 and 7 (Figure 5.2). At day 3, TH growth was observed as well as contamination (Figure 5.2a), while at day 7, the contamination completely dominated, and no TH growth was observed (Figure 5.2b). This suggests that the unexpectedly high production of IAA at days 3 and 7 of the fermentation was likely due to the contamination. To identify the contaminating microorganisms, cultured plates were observed and three single colonies with different morphological characteristics were detected. These colonies were isolated and sent for molecular identification, with the results presented in Table 5.2 and Figure 5.4.

Table 5.2. The identification of the three isolated colonies.

Isolate	Identification (Blast/NCBI)	Similarity
1	<i>Pantoea eucrina</i>	> 99%
2	<i>Pantoea brenneri</i>	> 99%
3	<i>Enterobacter ludwigii</i>	> 99%

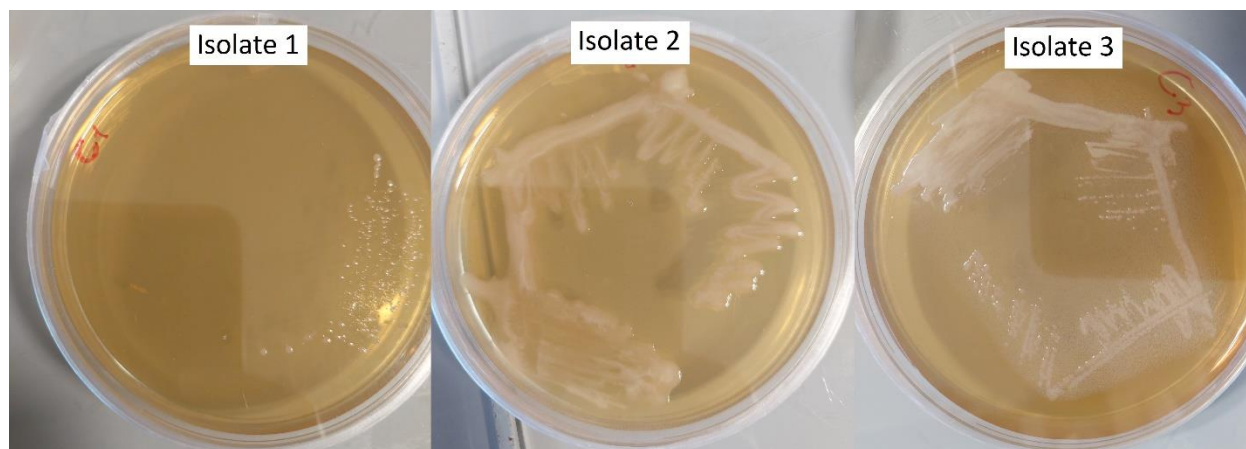


Figure 5.4. The culture of the isolated colonies.

The three isolates were gram negative bacteria from the Enterobacteriaceae family. *Pantoea* spp. is a newly established genus that is isolated from water and soil in a wide range of environmental conditions. This group of bacteria can be used in various industrial and agricultural applications. Some species are known for biological control and biostimulant activities while others are found to be used for bioremediation (Walterson and Stavrinides, 2015). Recent studies have highlighted the potential of IAA production in various *Pantoea* species. For example, *P. agglomerans* was found to have Trp- dependent metabolic pathway to produce IAA (Luziatelli et al., 2020). In the same study, a 5 L stirred tank bioreactor was applied to produce IAA, and it was found IAA produced up to 263 mg L<sup>-1</sup> using a saline medium containing yeast extract, saccharose, and Trp in the exponential growth phase. The growth conditions such as temperature, Trp concentration, and aeration was studied for *P. agglomerans* to optimize IAA production (Melini et al., 2023). Another study reported the IAA production and plant growth promoting of *P. dispersa* by analysis of bacterial metabolites (Kulkarni et al., 2013).

The biostimulant activity of *P. eucrina* has been also reported to produce useful metabolites for plants including ammonia production, IAA synthesis, and phosphate solubilization (Malleswari. D and Bagyanarayana. G, 2013). Similarly, *P. brenneri* showed the ability to enhance potato growth in green house by effectively solubilizing various inorganic phosphates and producing organic acids and phosphatases (Suleimanova et al., 2023). However, no studies have been found for IAA production by *P. brenneri*.

*Enterobacter ludwigii* is another bacterium that has been reported to have a plant growth-promoting effect. It has been reported that this bacterium has the capability to solubilize calcium triphosphate and to antagonize *Fusarium solani* mycelial growth and spore germination (Shoebitz

et al., 2009). *E. ludwigii* was found to produce IAA and affect significantly on the improvement of rice growth and production (Ningsih Susilowati et al., 2002).

Based on the current data, it can be inferred that some of the isolated microorganisms could have the ability to produce IAA and cause the high levels of IAA observed in the fermentation. Even that, this work is focused on the production of IAA and spore by TH. Thus, from a contamination point of view, the cleaning techniques should be improved to prevent contamination that could affect the reproducibility of the process. Nevertheless, the finding of microorganisms that appeared to produce high levels of IAA is noteworthy and requires further tests in the future to confirm their IAA production capabilities and assess their safety. Subsequently, to apply these bacteria in SSF, more detailed studies are necessary to optimize the production and conduct a successful process.

### ***5.3.1.2 The effect of bulking agent***

Due to the contamination observed in the previous fermentation, another batch was conducted under the same conditions including the use of PW as bulking agent, but with stricter cleaning protocols. This time, inoculation was performed inside a laminar flow cabin. Samples were taken on days 2 and 3 from the top of the reactor and on day 7 from the top, the center, and the bottom of the reactor. As presented in Figure 5.5, the production of IAA peaked on day 3, with a value of  $62 \pm 8 \mu\text{g g}^{-1} \text{DM}$  and then the levels dropped to:  $25 \pm 3 \mu\text{g g}^{-1} \text{DM}$ , on day 7. Furthermore, the spore counts on day 7 were higher than those of day 3, with values of  $9.5 \times 10^8 \pm 3.9 \times 10^8$  and  $7.2 \times 10^8 \pm 1.1 \times 10^8$  spores  $\text{g}^{-1} \text{DM}$ , respectively. The maximum values for sOUR and temperature were  $0.9 \text{ g O}_2 \text{ kg}^{-1} \text{ DM h}^{-1}$  and  $31^\circ\text{C}$  respectively. In order to interpret the performance of the 22 L reactor, Table 5.3 compares the results of previously reported 0.5 L fermentation and 22 L reactors using in both cases G and PW as bulking agent.

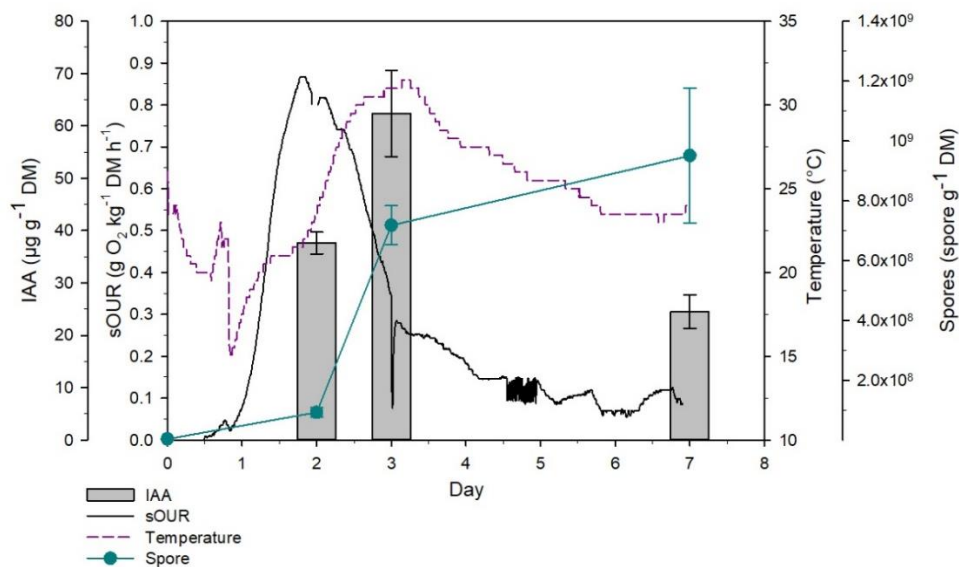


Figure 5.5. 22 L reactor SSF performance using pruning waste. The error bars are the standard deviation of the samples taken from different zones of the reactor.

## Chapter 5

Table 5.3. Different parameters were measured for the fermentation in 0.5 L and 22 L reactors PW and WC as bulking agent. IAA, Indole-3-acetic acid; sOUR, specific oxygen uptake rate; COC, cumulative oxygen consumption. <sup>a</sup> The presented values of IAA and spore productions were the maximum observed (day 3 for IAA and day 7 for spores).

	0.5 L (PW)	0.5-L(WC)	22 L (PW)	22 L (WC)
<b>IAA production (<math>\mu\text{g g}^{-1}</math> DM)<sup>a</sup></b>	102 $\pm$ 4	107 $\pm$ 10	62 $\pm$ 8	120 $\pm$ 17
<b>Spore production (spores <math>\text{g}^{-1}</math> DM)<sup>a</sup></b>	3.0 $\times$ 10 <sup>9</sup> $\pm$ 8.6 $\times$ 10 <sup>8</sup>	8.1 $\times$ 10 <sup>8</sup> $\pm$ 4.9 $\times$ 10 <sup>8</sup>	9.5 $\times$ 10 <sup>8</sup> $\pm$ 3.9 $\times$ 10 <sup>8</sup>	1.3 $\times$ 10 <sup>9</sup> $\pm$ 2.6 $\times$ 10 <sup>8</sup>
<b>Maximum sOUR (g O<sub>2</sub> kg<sup>-1</sup>DM h<sup>-1</sup>)</b>	1.6	0.6	0.9	1.1
<b>COC on day 3(g O<sub>2</sub> kg<sup>-1</sup>DM)</b>	41.7	28.3	28.7	48.1
<b>Lag phase (h)</b>	11.3	16.4	28.2	13.6
<b>Initial pH</b>	7.1	6.8	7.0	6.8
<b>pH on day 3</b>	8.1	7.3	8.0	7.7
<b>Final pH</b>	7.8	8.2	8.6	-
<b>Porosity (%)</b>	> 70	>70	62.1	69.3
<b>Bulk Density (kg m<sup>-3</sup>)</b>	25.0 $\pm$ 1.3	23.6 $\pm$ 0.8	418.9	318.3
<b>Initial temperature (°C)</b>	25	30	24	25
<b>Maximum temperature (°C)</b>	25	30	31	31
<b>Initial C/N</b>	-	-	19.1	18.7
<b>Final moisture (%)</b>	73.2 $\pm$ 0.9	27.9 $\pm$ 1.5	75.8 $\pm$ 0.2	78.7 $\pm$ 0.9
<b>Airflow (mL min<sup>-1</sup>)</b>	20	20	1000	1000
<b>Specific airflow (mL min<sup>-1</sup> g<sup>-1</sup> DM)</b>	0.67-0.93	0.67-0.93	0.99	1.12



According to Table 5.3 and the results obtained in the previous chapter, the IAA production over a 7-day period showed a similar pattern in both scales. It reached its peak on the third day of fermentation and then declined later. The decrease in IAA levels after three days is due to its consumption by *T. harzianum* for sporulation that has been described in Chapter 4. Nevertheless, it is observed that the maximum levels of IAA and spores produced in the 22 L reactor using PW were lower than those observed in the 0.5 L reactor according to Table 5.3. This pattern is similar to that of the maximum sOUR and COC with the values of 1.6 g O<sub>2</sub> kg<sup>-1</sup>DM h<sup>-1</sup> and 80.1 g O<sub>2</sub> kg<sup>-1</sup>DM, respectively in the 0.5 L fermentation and 0.9 g O<sub>2</sub> kg<sup>-1</sup>DM h<sup>-1</sup> and 42.0 g O<sub>2</sub> kg<sup>-1</sup>DM, respectively in the 22 L fermentation. Besides, a shorter lag phase (11.3 h) was observed in 0.5 L volume reactor fermentations.

The difference observed in the results obtained in the two different scale reactors could be due to the effect of scale up that is associated with a group of factors including lack of porosity-agglomeration, higher temperature, and differences in inlet airflow distribution or pH and moisture heterogeneity (Pallín et al., 2022). However, as presented in Table 5.3, there were no issues with heat accumulation in the process and the pH remained within a similar range in both scales. Besides, the level of airflow used in this experiment was 0.99 min<sup>-1</sup> g<sup>-1</sup> DM was similar to the airflow of applied to 0.5 L scale. However, the porosity of the material is 62.1% that appeared to be low compared to similar studies. Sala et al. (Sala et al., 2021b) showed that the production of aerial conidia of *T. harzianum* in the 22-L packed bed reactor using beer draff with a low porosity (around 60%) has been enhanced when increase the porosity up to 80% with the help of bulking agent (wood chips). However, in composting, which is a similar process to SSF, the recommended porosity value is around 30% (Ruggieri et al., 2009), therefore it can be concluded that the current process as a fungal SSF need higher porosity to provide a proper aeration. Indeed, previous studies

have highlighted the significance of porosity as a critical factor in the scale-up process (Molina-Peñate et al., 2023; Ruggieri et al., 2009; Zhang et al., 2017), especially for the production of aerial conidia (Sala et al., 2021a). The lower porosity could hinder proper aeration and oxygen distribution inside the organic matrix resulting in a different maximum sOUR of 1.6 and 0.9 g O<sub>2</sub> kg<sup>-1</sup>DM h<sup>-1</sup> in 0.5 L and 22 L reactors, respectively. However, the higher sOUR could also be attributed to a higher biodegradable organic matter content. The compaction of the substrate could have been also influenced by factors such as mass quantity and mass quantity and mass settlement (Casciadori et al., 2014; Ruggieri et al., 2009), which are common challenges when scaling up SSF processes (Oiza et al., 2022).

In an attempt to overcome the lack of porosity, wood chips (WC), was substituted for PW which had been successfully used in previous works using the same reactor configuration. This bulking agent is cleaner, more easily available, and more homogenous. Additionally, the biological activity of wood chips as sOUR is very low (0.6 g O<sub>2</sub> kg<sup>-1</sup> DM h<sup>-1</sup>, Table 5.3) suggesting a minimum impact on the process in the terms of biodegradability of organic matter (Sala et al., 2021a). The amount of WC used in the fermentation was 44% of dry material, equal to the amount of PW, reaching a porosity of 69.3%. Samples were taken from the top, the center, and the bottom of the reactor after a 3-day fermentation, which is the time when IAA concentration peaks (Figure 5.6).

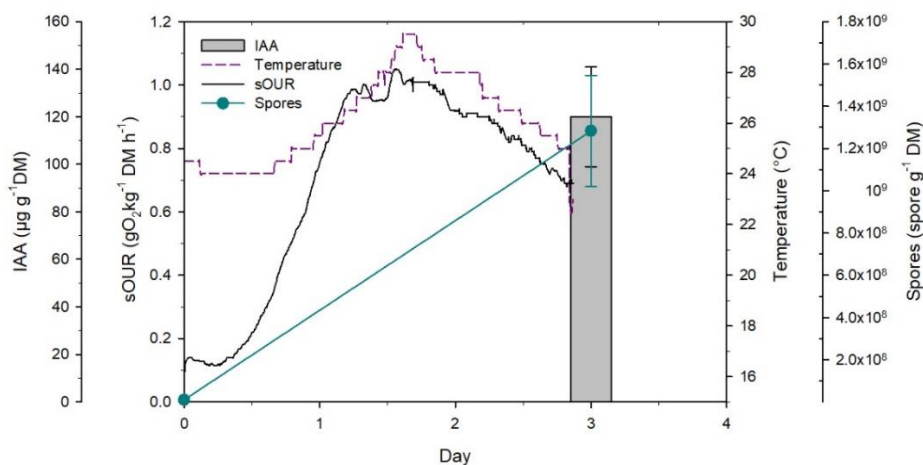


Figure 5.6. 22 L reactor SSF performance using wood chips. The error bars are the standard deviation of the samples taken from different zones of the reactor.

As observed in Figure 5.6, the overall average production of IAA in the reactor reached  $120 \pm 17 \mu\text{g g}^{-1} \text{DM}$ , with an average spore count of  $1.3 \times 10^9 \pm 2.6 \times 10^8 \text{ spores g}^{-1} \text{DM}$ . These results indicate that the production of IAA and spores in the 22 L reactor with a mixture of G and WC, showed a substantial increase when compared to the values observed in the fermentation with a mixture of G and PW ( $62 \mu\text{g g}^{-1} \text{DM}$ ). In fact, the concentrations of IAA and spores achieved in this experiment were slightly higher than those of the 0.5 L reactors with PW as a bulking agent. Therefore, it can be inferred that WC acts as a more effective bulking agent when compared to PW in the 22 L reactor, which can be due to several factors. As mentioned before, porosity could be a limiting factor impacting the performance of SSF, with a particular influence on sOUR, especially in larger scale operations (Ruggieri et al., 2009), and as observed in Table 5.4 which is discussed later. Increased porosity facilitates improved aeration inside the reactor, which is crucial for the growth and sporulation of *Trichoderma* (Hamrouni et al., 2020). The porosity of the mixture of G+PW and G+WC on the 22 L reactor was 62.1% and 69.3% respectively, whereas the material

inside the 0.5 L reactor (G+PW) exceeded 70% porosity. The reason behind the lower porosity in the 22 L compared to 0.5 L is the compaction of G as a result of increased substrate height that was used in the reactor. As can be seen in Table 5.3, the bulk density of materials inside the reactors of 0.5-L with both PW and WC are respectively 25.0 and 23.6 kg m<sup>-3</sup> suggesting low compaction. While the bulk density of material inside at 22-L scale was much higher being 418.9 and 318.3 kg m<sup>-3</sup> respectively when the bulking agent was PW and WC. However, after using WC, the bulk density decreased which is a sign of decreasing compaction. Besides, several physical parameters, including water holding capacity, moisture, and particle size influence the porosity of the substrate in the reactor (Casciatori et al., 2014; Karimi et al., 2014). Concerning particle size, both PW and WC particles were larger than 1 cm, with PW showing less homogeneity. The final moisture content in fermentations involving PW and WC showed marginal differences, while a considerable difference appeared in water holding capacity which was 39.5% for PW and 83.9% for WC. Hence, it appears that WC's more uniform particle size and higher water holding capacity contributed to an increase in porosity (Table 5.4).

Table 5.4. Characterization and the specific oxygen uptake rate (sOUR) of the substrates used in fermentation.

	<b>Grass</b>	<b>Pruning Waste</b>	<b>Wood Chips</b>
<b>Size</b>	1-3 cm	1-7 cm	1-5 cm
<b>Initial moisture (%)</b>	23.7	13.0	9.8
<b>Water holding capacity (%)</b>	95.3	39.5	83.9

It was observed that the maximum sOUR of the 22 L reactor was higher when WC was used, in contrast to the sOUR of the fermentation with PW. Additionally, the lag phase of respiration activity was shorter in the fermentation with WC (Table 5.3). It is also referred to that these

parameters can be influenced by various factors such as porosity or enhanced degradability (Barrena et al., 2011), which results in the improvement of fermentation productivity (Sala et al., 2021b).

The initial temperature of the material inside the reactor was 25°C and the maximum temperature in the center of the reactor reached 31°C at day 3. In contrast to the temperature changes observed during the fermentation with PW, it is likely that sufficient aeration and porosity effectively maintained the temperature below 31°C, despite the heightened biological activity. The C/N ratios of the substrate at the beginning of the fermentation were similar. Previous works show that materials with a C/N ratio of around 20 are adequate for sporulation and IAA production (Sala et al., 2021b; Wang et al., 2019).

In comparing the production of IAA in the current study with the findings from the 0.5 L reactor, a wide range of production can be observed. This range can be attributed to factors such as the scale of the experiment, the fermentation method employed, and the specific microorganism utilized as the producer. The production of IAA through liquid and submerged fermentation has been extensively studied at different scales. Because liquid-phase conditions often yielding higher IAA concentrations due to their superior homogeneity and ease of control (López-Gómez and Venus, 2021). For instance, recent research has reported the successful production of 3600 mg L<sup>-1</sup> of IAA at a pilot scale (100 L) utilizing *Rhodospiridiobolus fluvialis* (Bunsangiam et al., 2021). In a separate laboratory-scale study, *Pichia fermentans* was used to produce IAA under submerged conditions with pretreated wheat straw, achieving a production yield of 150 mg L<sup>-1</sup> (Giri and Sharma, 2020). Nutaratat et al (Nutaratat et al., 2016) also obtained 1627 and 2744 mg L<sup>-1</sup> IAA

through batch and fed batch fermentations, respectively using *Rhodosporidium paludigenum* in a 2 L stirred tank fermenter with a working volume of 1 L.

In contrast, as discussed in the previous chapter, there are only a few studies that worked on producing IAA through SSF despite its potential economic and environmental advantages including lower water consumption, no wastewater generation and easier downstream process. This fact is probably because achieving a successful high yield process is more complicated due to the substrate heterogeneity and to the performance challenges of SSF (López-Gómez and Venus, 2021). For instance, in a lab-scale SSF study, *Bacillus subtilis* and *Trichoderma atroviride* produced around 10 and 8  $\mu\text{g g}^{-1}$  dry matter (DM) (equivalent to approximately 1.1 and 0.8  $\text{mg L}^{-1}$ ), respectively (Zanoni do Prado et al., 2019a). In another work conducted in 250 mL flasks with 10 g of solid substrate, Zanoni de Prado et al (Zanoni do Prado et al., 2019b) reported the maximum production of IAA and analogues was produced by *Aspergillus flavipes* around 1800  $\mu\text{g g}^{-1}$  DM (183  $\text{mg L}^{-1}$ ) using soybean bran as substrate. In the same paper, it was observed that IAA production by *T. harzianum* was 2.3  $\mu\text{g g}^{-1}$  DM (23  $\text{mg L}^{-1}$ ). These data determine that considering the working scale (22 L) and the substrate (GW) used in the present study under more realistic conditions, the amount of IAA produced by *T. harzianum* is a significant achievement. Although IAA production is lower in SSF compared to submerged and liquid fermentation due to the complexity of the process, SSF still offers benefits such as reduced water consumption and simpler downstream processing, making it an attractive alternative. In the current study, the SSF products can be directly used as compost for plants, removing the need for time and energy consuming purification steps. In a study conducted in another thesis of our group, The final fermented solid material of the current study was applied to lettuce (*Lactuca sativa L*) and the results showed a significant improvement in the growth factors such as fresh weight, plant height, and leaf quantity,

as well as in chemical parameters including total phenol content, chlorophylls, carotenoids, and antioxidant activity (C. Solano, G. Ghoreishi, A. Sanchez, R. Barrena, X. Font, C. Ballardo, 2024).

In conclusion, keeping proper porosity is key to successfully scaling up SSF processes while maintaining fermentation biological activity and achieving similar productivity. This idea has already been observed in similar processes like composting (Ruggieri et al., 2009, 2008). According to the current results and the results of previous studies, porosity, measured as AFP, is a scale-up criterion for fungal SSF (Sala et al., 2021a).

### ***5.3.1.3 The effect of the amount of tryptophan in bench-scale batch SSF***

With the aim of reducing the amount of Trp used at bench-scale, two additional fermentations were conducted in the 22 L reactor with 0.2% (w/w) and no Trp and compared to the fermentation with 0.43% (w/w). It has been described in Chapter 4 that a prediction model for optimizing the production of IAA and spores was developed and suggested a Trp concentration of 0.43% (w/w) as an optimized level used in the fermentation.

In all the fermentations WC was used as a bulking agent because it was better in terms of yield as explained. Figure 5.7a and Figure 5.7b show the results from these two fermentations in comparison to the one with 0.43% Trp. The analysis of IAA production revealed that the average IAA levels in samples collected from various parts of the reactor were  $26 \pm 8 \mu\text{g g}^{-1} \text{DM}$  and  $12 \pm 7 \mu\text{g g}^{-1} \text{DM}$  for the 0.2% Trp and no Trp fermentations, respectively. These values were considerably lower than those obtained in the fermentation with 0.43% Trp at the same scale. In terms of spore production, the fermentation using 0.2% Trp yielded  $1.2 \times 10^9 \pm 2.1 \times 10^8$  spores  $\text{g}^{-1} \text{DM}$ . When no Trp was added, spore production decreased to  $6.7 \times 10^8 \pm 2.5 \times 10^8$  spores  $\text{g}^{-1} \text{DM}$ .

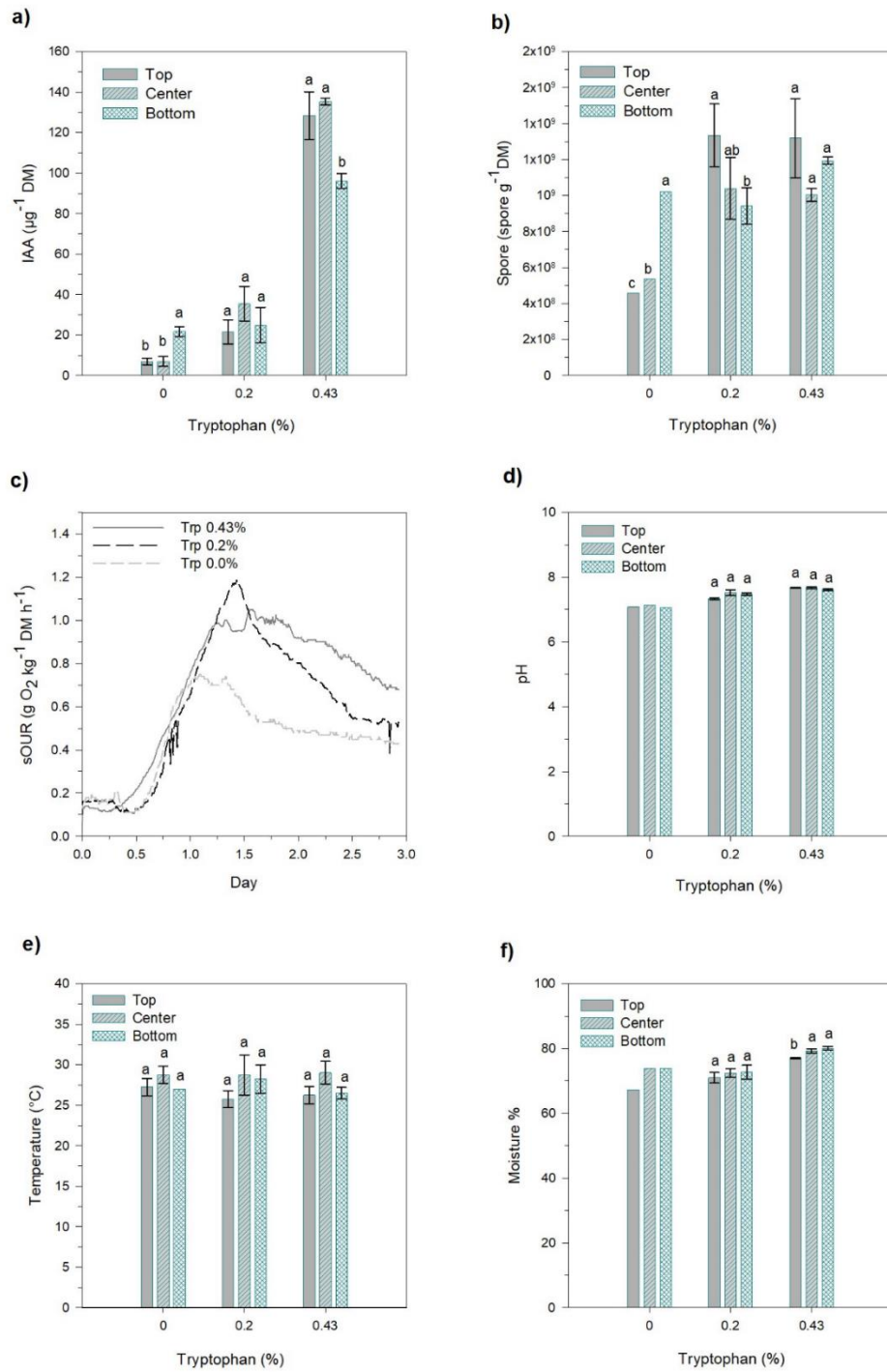


Figure 5.7. Performance of 22 L reactor SSF using different concentrations of Trp. a) Production of IAA, b) Sporulation, c) Specific oxygen uptake rate (sOUR), d) pH, e) Maximum temperature, and f) Final moisture. Different letters indicate significant differences between the zones of the reactor sampled ( $p < 0.05$ ) based on Tukey analysis.



Figure 5.7c compares the respiration profiles of the fermentations with different concentrations of Trp. The lag phase was similar for the three fermentations. However, regarding the maximum sOUR, when Trp in the fermentation was 0.43% and 0.2%, it was 1.2 and 1.1 g O<sub>2</sub> kg<sup>-1</sup> DM h<sup>-1</sup>, respectively. Instead, when no Trp was added, the maximum sOUR was 0.7 g O<sub>2</sub> kg<sup>-1</sup> DM h<sup>-1</sup>. Nevertheless, when Trp concentrations exceeded 0.2%, there was no significant effect on sporulation (Figure 5.7b). These results indicate that Trp in low concentrations is a contributing factor for enhancing the growth and sporulation of *T. harzianum* under SSF conditions. However, IAA production (Figure 5.7a) seems to be affected by the amount of Trp used as a precursor. An improvement in IAA production was observed with Trp amounts higher than 0.2%. Consequently, these findings suggest that a Trp concentration of 0.43% is a desirable level for producing IAA on a 22-L scale. These results agree with the results obtained in 0.5L lab-scale reactors suggesting that increasing the concentration of Trp in the reactor up to 0.5% (w/w) can increase the IAA production. Other studies confirm that adding Trp to the fermentation increases IAA production in the processes that utilize microorganisms possessing Trp-dependent IAA metabolic pathway. For instance, Zanoni de Prado (Zanoni do Prado et al., 2019b) found a 500-fold increase in IAA production when 1.5% (w/w) of Trp was added to an SSF process using *Aspergillus flavipes*.

These findings also support the idea that high sOUR and a larger number of fungal spores may also be positively correlated (Sala et al., 2021b). In this sense, sOUR appears as another critical parameter to be considered a successful SSF. In other words, when scaling up sOUR must be maintained as a result of a scale-up strategy based on other criteria.

Figure 5.7 provides additional information about the spatial distribution of both IAA and spore production inside the reactor. No considerable differences were observed in the production of IAA

and the sporulation of TH in all parts of the reactor in the experiments with different concentrations of Trp. Despite this, in the fermentation with 0.43% Trp, IAA production was significantly lower in the bottom of the reactor. Figure 5.7e and Figure 5.7f shows that the temperature in the center of the reactor is higher than in the other parts of the reactor. Furthermore, the moisture content was higher in the bottom and lower in the top of the reactor. Anyway, these observations highlight one of the main problems when scaling up SSF: organic matrices heterogeneity and the presence of gradients in non-stirred reactors (Oiza et al., 2022). In this regard, mathematical models have been developed to predict the behavior of the SSF process in packed bed reactors despite that the heterogeneity making the modeling complicated. A model was developed to estimate the heat and mass transfer in different sections of a pilot-scale packed bed reactor. They showed that the variation in the temperature and moisture was because the airflow was not uniform in the bed sections. (Terezinha Jung Finkler et al., 2021b). Lopes Perez et al. also designed a model to predict the fungal growth kinetics through SSF in a bench-scale packed bed reactor. They described the bed height and the maximum temperature as the parameters in the model that can be changed by the variation of superficial air velocity (Lopes Perez et al., 2018). The behavior of axial heat transfer also modeled in a packed bed reactor to scale up the production of fungal pectinase through SSF (Terezinha Jung Finkler et al., 2021a). These studies showed that the non-uniform distribution of airflow in the reactor can affect the final production by changing the temperature and moisture profile. However, an estimation model is required in the present study to give a deeper understanding of the variation observed in the different parts of the reactor.

On the other hand, the design of the bioreactor is also a principal factor in overcoming the heterogeneity of SSF. In fact, it is one of the reasons that using packed bed reactors for SSF at an industrial scale is not preferred. Tray bioreactors are the most used bioreactor design on the

industrial scale due to their simple operation and construction (López-Gómez and Venus, 2021). Because of the more superficial area of the tray reactors, there is less issue with the heat accumulation, and it is a more adopted reactor configuration to use filamentous fungi in SSF (Sentís-Moré et al., 2023).

### 5.3.2 SSF in sequential batch bench-scale strategy

Once the type of bulking agent and Trp concentration were selected, SBO-based SSF was implemented as a process strategy to maintain IAA production sustained in time. Figure 5.8 shows the SSF performance of the sequential batch operation strategy. This experiment consisted of four consecutive batch fermentations. In each batch, the reactor was sampled in four parts: surface, top, center, and bottom as explained in the materials and methods section. Two samples were taken from each part. To obtain a comprehensive representation of both the entire reactor and the different areas of the reactor, average values were independently calculated for each part and the entire volume reactor. As shown in Figure 5.8a and Figure 5.8b, the highest concentration of IAA was achieved in batch 1, with an average value of  $119 \pm 16 \mu\text{g g}^{-1} \text{DM}$ . Afterward, in batches 2 and 3, the average IAA production declined to  $96 \pm 17 \mu\text{g g}^{-1} \text{DM}$  and  $26 \pm 17 \mu\text{g g}^{-1} \text{DM}$ , respectively. In batch 4, this value averaged  $53 \pm 6 \mu\text{g g}^{-1} \text{DM}$ . In terms of spore counts, batch 1 also showed the highest value ( $1.1 \times 10^9 \pm 3.6 \times 10^8$  spores  $\text{g}^{-1} \text{DM}$ ), as presented in Figure 5.8c. In the subsequent batches, there was a gradual decrease in spore counts:  $8.4 \times 10^8 \pm 3.1 \times 10^8$ ,  $4.1 \times 10^8 \pm 1.7 \times 10^8$  and  $3.6 \times 10^8 \pm 7.8 \times 10^7$  in batches 2, 3, and 4, respectively. Regarding the distribution of the production in the reactor, Figure 5.8c exhibited that the number of spores counted in the different parts of the reactor in each batch were not significantly different. However, this was not the same for IAA in Batch 1 and 3 (Figure 5.8a).

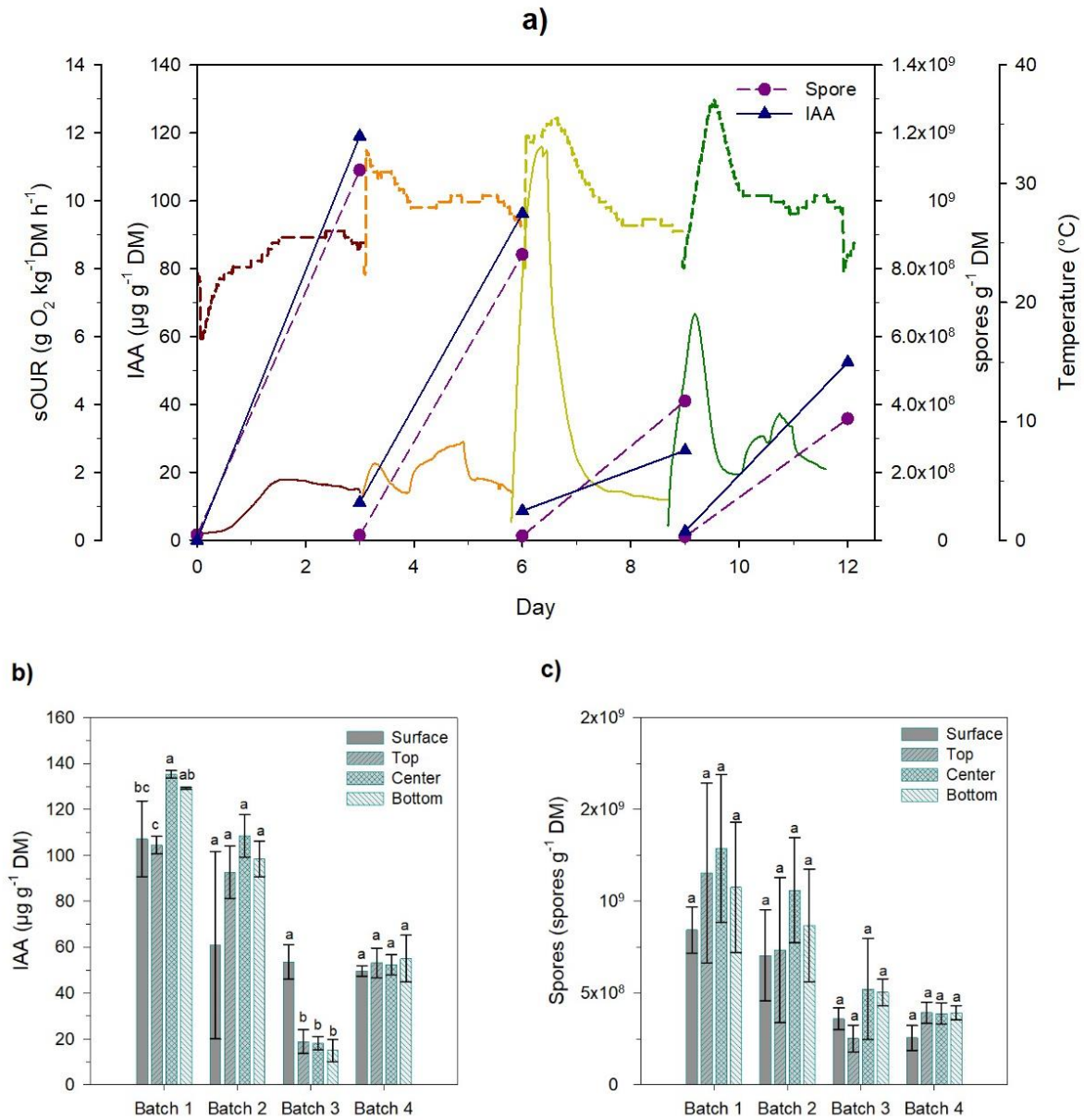


Figure 5.8. Performance of SBO SSF strategy: (a) The profiles of IAA production, number of spores, specific oxygen uptake rate (sOUR), and temperature. The red, orange, yellow, and green dashed curves respectively correspond to the temperature profile of batch 1, batch 2, batch 3, and batch 4, while the red, orange, yellow, and green solid curves correspond to sOUR profile of batch 1, batch 2, batch 3, and batch 4, respectively. (b) Production of IAA and (c) Spores count in distinct parts of the reactor. Different letters indicate significant differences between the zones of the reactor sampled ( $p < 0.05$ ) based on Tukey analysis.

Figure 5.8a also presents the profiles of respiration, temperature, IAA concentration and spore production of four batches together. Respiration profiles indicated a typical pattern of microbial activity in batch 1 with maximum sOUR of  $1.8 \text{ g O}_2 \text{ kg}^{-1} \text{ DM h}^{-1}$ . In contrast, the second batch displayed two distinct peaks in sOUR, showing  $2.2$  and  $2.9 \text{ g O}_2 \text{ kg}^{-1} \text{ DM h}^{-1}$ , respectively, suggesting microbial contamination. However, this fact did not seem to affect IAA and spores' production by TH. The unexpected high sOUR in batches 3 and 4 clearly indicated microbial contamination. The microbial culture of the SSF samples also revealed the contamination providing a possible explanation for the low production of both spores and IAA (Figure 5.9). As can be seen in Figure 5.9a2, a normal culture of TH has a green color, while in Figure 5.9b2 that from batch 2 just some green spots of TH growth were observed and in the plates from batches 3, and 4 (Figure 5.9c2 and Figure 5.9d2) TH did not grow.

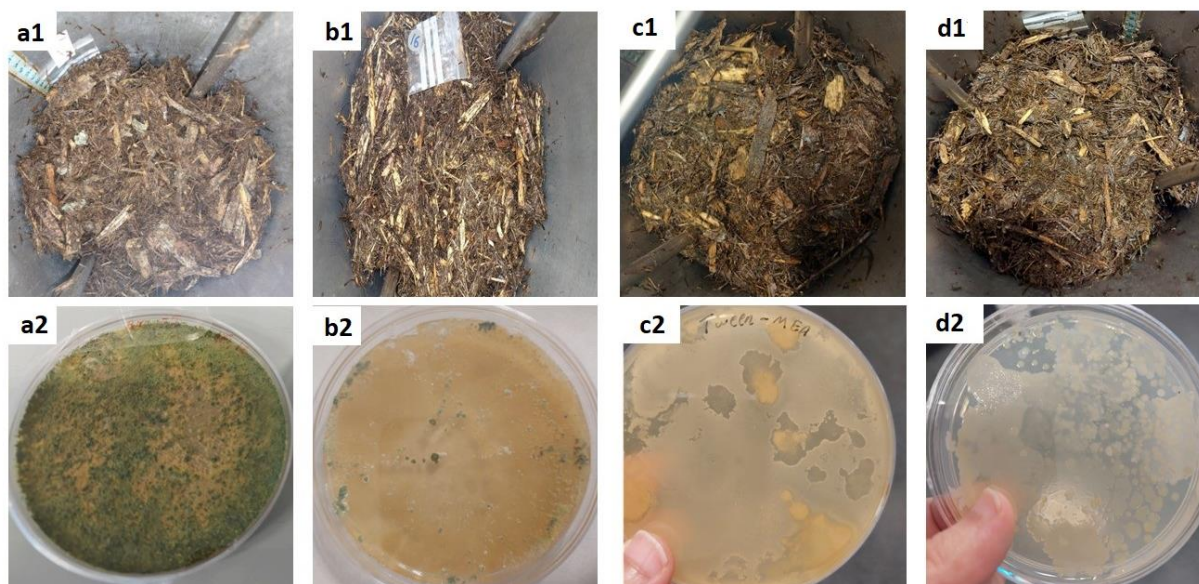


Figure 5.9. The photos of sequential batch experiment at the end of each batch and the microbial culture prepared from each batch. A1) Batch 1, A2) A normal culture of *Trichoderma harzianum* with no contamination, B1) Batch 2, B2) Plate cultured from batch 2, C1) Batch 3, C2) Plate cultured from batch 3, D1) Batch 4, D2) Plate cultured from batch 4.

Additionally, the increasing temperature inside the reactor was a sign of the potential existence of unexpected microorganisms. The maximum temperature observed in the center of reactor during SBO was 37°C, higher than that observed in batch experiments (Table 5.3). Although it has been found that TH can tolerate a wide range of temperatures, when temperatures exceed 30°C some growth factors, including sporulation, are diminished (Napitupulu et al., 2019b; Zhang et al., 2021). This can favor other microorganisms to take advantage of and grow in organic material. As previously mentioned, avoiding high temperatures in packed bed reactors is an important factor to have a successful fermentations, especially dealing with higher mass in higher scales and sequential batch configurations (Cerda et al., 2017; Martínez-Avila et al., 2019).

All these observations, as well as the contamination observed in the initial experiment with the 22 L reactor, suggest that green waste, particularly lawn grass clippings, is a challenging substrate for fermentation processes in packed bed reactors using sequential batch operation strategies. Despite its acceptable porosity and biodegradability (as indicated by sOUR), scaling up SSF can be a complex and non-straightforward process. (Oiza et al., 2022). One of the reasons for this phenomenon is caused by the difficulty of sterilizing the grass despite running two cycles of sterilization because in general the sterilization of a solid matrix is not easy. Besides, this might be due to the unavoidable inclusion of soil particles during grass collection, where some resistant microorganisms can be present. It seems that these microorganisms started growing as the fermentation temperature increased and take advantage of TH in the reactor. In fact, keeping the process sterilized to avoid other microorganisms growing is a big challenge in SSF, especially in larger scales (Chilakamarry et al., 2022). Improving cleaning techniques for the substrate or changing the SBO strategy will probably help to manage the problem.

Summarizing, the outcome of IAA and spore production in batch 1 was similar to that of the single batch with the same condition indicating the reproducibility of the fermentation being this one of the main problems of SSF (Abraham J et al., 2017). In this study, we demonstrate that with an accurate conditioning of the starting material, these problems can be overcome. In batch 2, the obtained IAA was slightly lower but still within an acceptable range. Meanwhile, spore production in the initial two batches exhibited a similar range. Therefore, this strategy showed success in two sequential batches. However, due to the complexity of contamination when performing sequential batch operation strategy utilizing GW, it is recommended to conduct further experiments to find more effective cleaning techniques and SBO strategies to manage the contamination.

### 5.3.3 Analysis of the SSF products: IAA degradation

To investigate the stability of IAA after finishing SSF, two SSF samples from the experiment containing 0.2% Trp were left at room temperature in plastic bags for 13 days. During this period, the IAA levels in the fermented material were measured. The samples of fermented material were wet solids, consisting of a mixture from different parts of the reactor. Before starting the test, the IAA concentration of the samples had been measured and then stored at  $-20^{\circ}\text{C}$  for one month. The amount of IAA before freezing was respectively  $44.10 \pm 4.91$  and  $35.4 \pm 8.7 \mu\text{g g}^{-1}$  DM for samples A and B.

As shown in Figure 5.10, both samples exhibited similar degradation profiles. In Sample A, the IAA level decreased from  $42.77 \pm 3.19 \mu\text{g g}^{-1}$  DM to nearly zero after 7 days, followed by an increase up to  $11.75 \pm 1.09 \mu\text{g g}^{-1}$  DM at day 13. Similarly, the IAA concentration in Sample B dropped from  $36.04 \pm 0.52 \mu\text{g g}^{-1}$  DM on the first day to  $3.26 \pm 0.49 \mu\text{g g}^{-1}$  DM by day 7, and then increased. After 13 days, the IAA levels in B reached  $16.02 \pm 3.83 \mu\text{g g}^{-1}$  DM. Comparing the amount of IAA before and after freezing suggests the stability of IAA in SSF products at  $-20^{\circ}\text{C}$ . However, most of the IAA was degraded at room temperature for 7 days. The IAA degradation at room temperature might be due to increased TH activity after defrosting the SSF product. Another possibility is that light exposure caused the IAA degradation, as IAA is known to be sensitive to photodegradation (Leasure et al., 2013). However, recent research has shown that the IAA produced by *Micrococcus luteus* remained stable in the supernatant of cell culture and crude extract after autoclaving ( $121^{\circ}\text{C}$ , 15 min) and light exposure for 30 days. When stored at  $4^{\circ}\text{C}$ , its stability increased to 2 months (Boonmahome and Mongkoltharuk, 2023). As previously mentioned, IAA is a key signaling molecule for interactions between plants and microbes, as well as between



microorganisms themselves. This signaling typically involves the production and degradation of IAA in response to various environmental factors such as temperature, pH, and light, which occur through complex metabolic pathways (Tang et al., 2023). It is also possible that IAA degradation was influenced by the signaling processes of surviving TH cells. Further tests is required to determine the stability of IAA under different conditions.

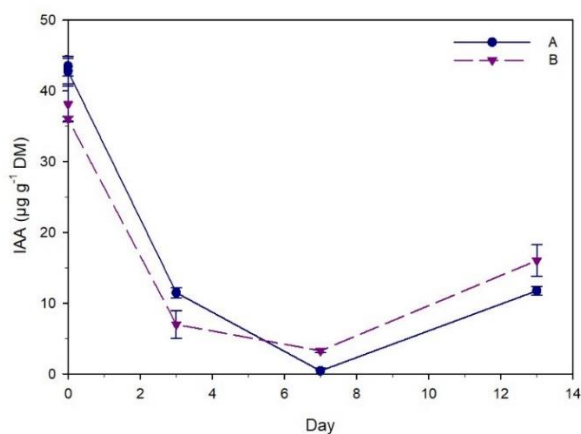


Figure 5.10. IAA degradation in SSF product at room temperature. The error bars are the standard deviation of the samples taken for HPLC.

#### 5.3.4 The effect of temperature, IAA, and Trp on spore germination of *T. harzianum*

To confirm the previous findings indicating that Trp and IAA have distinct effects on TH sporulation at different concentrations, a complementary experiment was conducted. In this test, TH spore germination was measured under different Trp and IAA concentrations. The germination of spores was monitored using an oCelloscope at temperatures 25, 28, and 30°C over 24 hours. To do the test, Different concentrations of Trp (5 and 10 g L<sup>-1</sup>) and IAA (0.125, 0.25, 0.5, and 1 g L<sup>-1</sup>) were added to 50% SDA, and a liquid TH suspension. The TH suspension was extracted from a culture plate and diluted so that the final TH concentration was 10<sup>5</sup> -10<sup>6</sup> spore mL<sup>-1</sup>.

## Chapter 5

At all temperatures, when the IAA concentration was  $1 \text{ g L}^{-1}$ , spores failed to germinate, instead accumulated in one spot and then disappeared as shown in Figure 5.11a. At an IAA concentration of  $0.5 \text{ g L}^{-1}$ , most spores disappeared, with only a few begin to germinate (Figure 5.11b). To compare the germination in higher concentrations of IAA with a normal spore germination, Figure 5.12 has been presented where shows TH spore germination in SDA without treatment (control). As can be seen, the spores slowly start to form germ tubes and germinate over time and after 24 hours, almost all of them germinated. Nevertheless, due to the low or zero survival rate and subsequent germination, in higher concentrations of IAA, it was not possible to calculate the germination percentage.

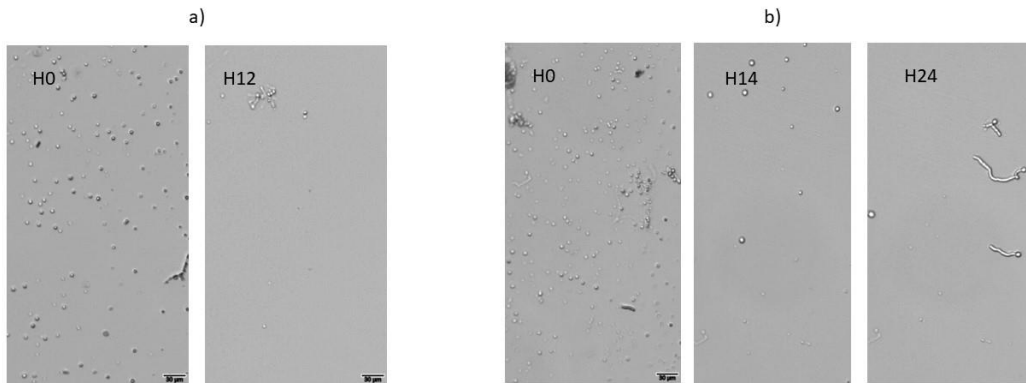


Figure 5.11. (a) Photos of *T.harzianum* spores germinating in the presence of  $1 \text{ g L}^{-1}$  IAA. After 12 hours, most of the spores disappeared and the rest accumulated in one spot. (b) Photos of *T.harzianum* spores germinating in the presence of  $0.5 \text{ g L}^{-1}$  IAA. Most of the spores disappeared after 14 hours and a few germinated after 24 hours.

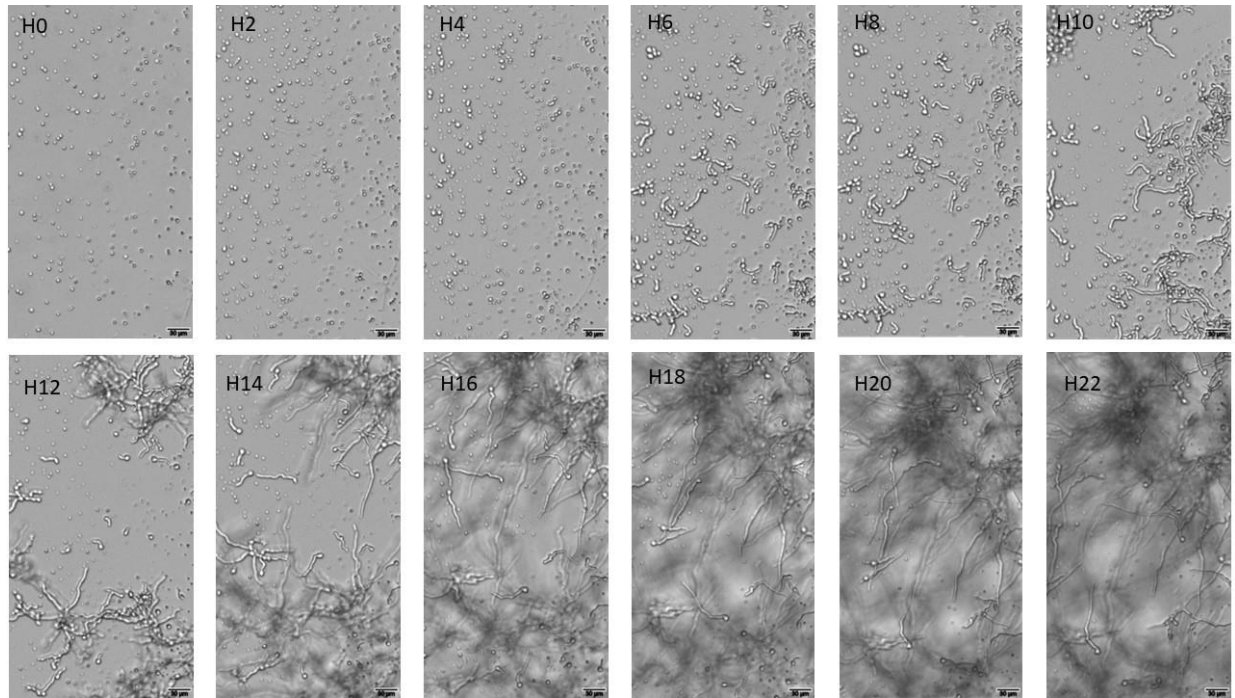


Figure 5.12. Photos of *T.harzianum* spores germinating during 22 hours.

Figure 5.13 shows the results of germinating spores at 25°C. The germination percentage after 24 hours varied from 84.8% to 90.4% while the minimum and the maximum values were observed at the concentrations of 0.125 g L<sup>-1</sup> of IAA and 5 g L<sup>-1</sup> of Trp respectively. The profiles were also similar; however, the rate of germination was slightly higher when 0.25 g L<sup>-1</sup> of IAA was used.

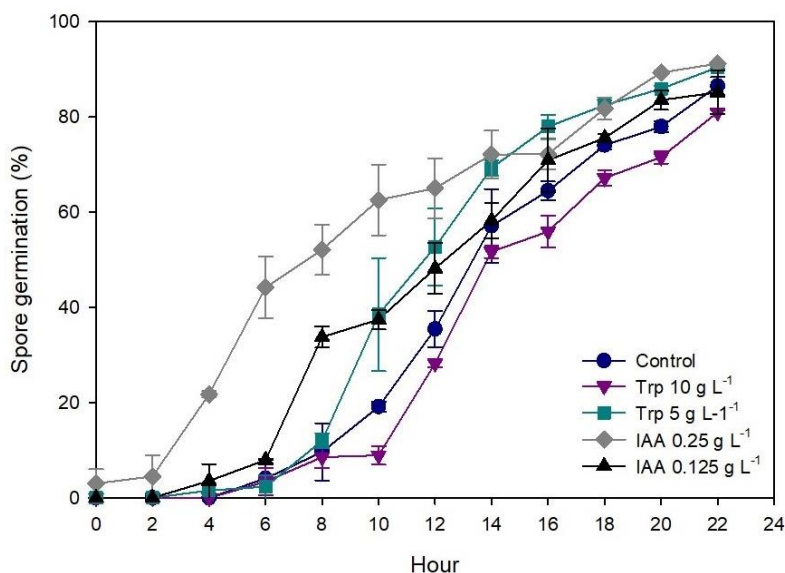


Figure 5.13. The germination percentage of *T.harzianum* spores in the presence of different concentrations of Trp and IAA at 25°C. The error bars are the standard deviation of the triplicate germination data.

At 28°C, the percentage of germination after 24 hours was in a similar range for all the treatments (between 92.3% and 98.1%). The germination rate began similarly for all treatments, except at the concentration of 0.25 g L<sup>-1</sup> of IAA, where it was significantly higher than in the other treatments during the initial hours. The percentage of germination with 10 g L<sup>-1</sup> of Trp decreased slightly compared to control (Figure 5.14).

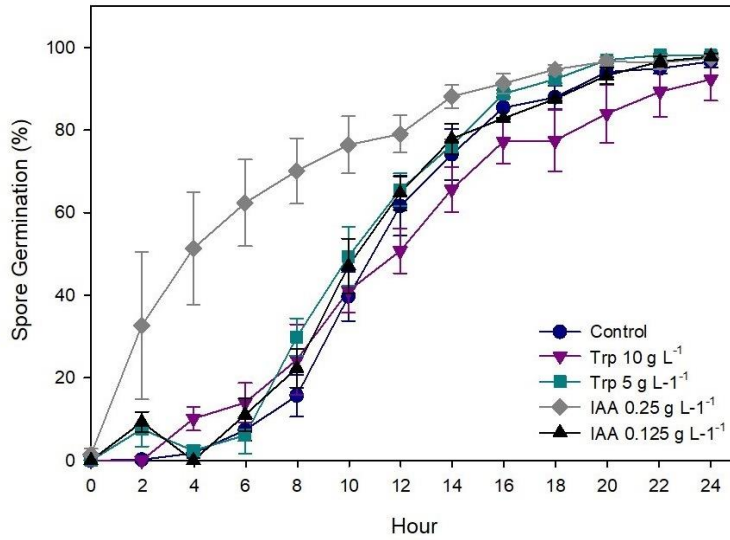


Figure 5.14. The germination percentage of *T.harzianum* spores in the presence of different concentrations of Trp and IAA at 28°C. The error bars are the standard deviation of the triplicate germination data.

At 30°C, the number of germinated spores was too low to be calculated at an IAA concentration of 0.25 g L<sup>-1</sup>, but it could be measured at 0.125 g L<sup>-1</sup>. After 24 hours, the percentage of spore germination at both levels of Trp was similar to the control. However, during the first 12 hours, the germination rate was higher when 5 g L<sup>-1</sup> of Trp and 0.125 g L<sup>-1</sup> of IAA were used compared to the control (Figure 5.15).

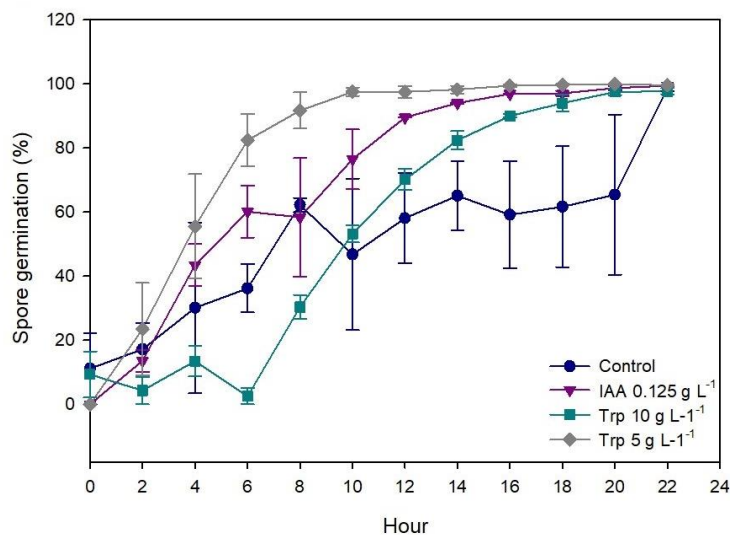


Figure 5.15. The germination percentage of *T.harzianum* spores in the presence of different concentrations of Trp and IAA at 30°C. The error bars are the standard deviation of the triplicate germination data.

The results suggest that higher concentrations of IAA (0.5 and 1 g L<sup>-1</sup>) negatively affect spore germination, while lower concentrations (0.25 and 0.125 g L<sup>-1</sup>) enhance the germination rate. Additionally, a lower concentration of Trp (5 g L<sup>-1</sup>) slightly improved germination, whereas a higher concentration reduced it.

Temperature also appears to influence the effects of IAA and Trp on spore germination. The same concentration of IAA (0.25 g L<sup>-1</sup>) increased the germination rate at 28°C but nearly stopped it at 30°C. Conversely, Trp at both concentrations improved the germination rate and percentage at 30°C compared to 25°C and 28°C.

As described in the previous chapter, low levels of Trp (below 0.5% w/w) enhance TH growth and sporulation, while higher levels reduced both. The current results suggest that IAA also affects TH growth differently depending on its concentration. Research has shown that IAA can act as either

an inducer or an inhibitor of microbial growth. For instance, it has been found that IAA at lower concentrations (0.1 and 1  $\mu\text{g mL}^{-1}$ ) induced the growth of *Pantoea dispersa*. While, at higher concentrations (10 and 100  $\mu\text{g mL}^{-1}$ ) the bacterial growth decreased (Kulkarni et al., 2013). Similarly, Low concentrations of IAA (0.5, 5, and 50  $\mu\text{M}$ ) promote the growth of *Fusarium delphinoides*, while high concentrations (500 and 5000  $\mu\text{M}$ ) inhibit it. In contrast, in *Fusarium graminearum* a growth inhibition showed growth inhibition at all concentrations of IAA (Tang et al., 2023).

The results obtained in this experiment provide a good example of the inhibitory and stimulatory role of IAA on TH spore germination based on the concentration. Furthermore, these data can be further evidence that TH consumes IAA and supports the results of the previous chapter.

## 5.4 Conclusion

In this chapter, the first steps towards the scale-up process of the production of IAA and conidial spores of TH were addressed using GW as the substrate in packed bed bioreactors. A reproducible process was achieved for producing IAA and spores in a 22 L reactor single batch experiment despite the challenges of using a heterogeneous substrate like GW. Porosity appeared as a key factor to implement a successful bench-scale SSF in a packed bed bioreactor. The outcome of the experiment of sequential batch operation suggested the need for new strategies to address potential contamination issues arising from the complex composition of GW. Furthermore, preliminary tests on the stability of IAA indicate that more targeted research is needed to enhance the usability of the final SSF product in agriculture. Finally, studying the impact of different Trp and IAA

## Chapter 5

concentrations on spore germination of TH showed that both IAA and Trp can affect differently on spore germination based on their concentrations.



## Chapter 6

# Enhancing the Production of Biostimulant through SSF in Tray Bioreactors

---

Part of this chapter is under preparation to be published in a scientific journal.

## 6.1 Overview

In this chapter, the SSF process was performed in a tray bioreactor design to produce IAA and conidial spores using GW as substrate and TH as inoculum. Different experiments were conducted to study the reactor configuration in a larger scale on the productivity of the process to provide an insight into a robust scaling up. Furthermore, new strategies are suggested to improve the yield of SSF. Finally, the outcome of the experiments in the tray reactor was compared to that of the 22 L reactor.

## 6.2 The materials and conditions of the experiments

In all the following experiments the same sample of grass clipping was used. The bulking agent was the same wood chips used in the previous chapters. The characteristics of the grass used in this chapter are presented in Table 4.1.

Table 6.1 The characteristics of the grass clipping used in the tray experiments.

pH	$6.20 \pm 0.27$
Conductivity ( $\mu\text{S m}^{-1}$ )	$1247 \pm 169$
C/N	18.5
Water holding capacity	96.5%

For all experiments, the ratio of grass and wood chips, the initial moisture, and the added Trp were according to the optimization results obtained in Chapter 1. These conditions are as follows: grass 56% (on a dry basis); wood chips 44% (on a dry basis); initial moisture 74%, and Trp 0.43% (w/w). The total wet weight for each tray was 500 g.

## 6.3 Experiments

### 6.3.1 Experimental setups in tray bioreactor

#### 6.3.1.1 First experimental setup (Experiment A)

To determine the production of IAA and conidial spores through SSF in tray bioreactor, three experiments were conducted. Figure 6.1 shows the profiles of IAA production, spore count, Trp consumption, and temperature in the first tray bioreactor experiment. This experiment was a 7-day time course, with samples taken on days 2, 3, and 7 of the process and conducted in one tray. Results indicated an increasing trend in IAA production, peaking at  $201 \pm 23 \mu\text{g g}^{-1} \text{DM}$  on day 7. Similarly, the highest spore count,  $9.1 \times 10^7 \pm 1.2 \times 10^7$  spores  $\text{g}^{-1} \text{DM}$ , was observed on day 7. Trp concentration decreased from an initial value of  $13.5 \text{ mg g}^{-1} \text{DM}$  to  $4.7 \pm 0.1 \text{ mg g}^{-1} \text{DM}$  by day 7.

Temperature was monitored using sensors, with values ranging from a minimum of  $17.0 \text{ }^\circ\text{C}$  to a maximum of  $22.0 \text{ }^\circ\text{C}$ . Due to low pressure inside the incubator, the conventional system used in our laboratory failed to measure oxygen consumption, resulting in no oxygen profile for this experiment. Photos of fermentation in the tray bioreactor are presented in Figure 6.2.

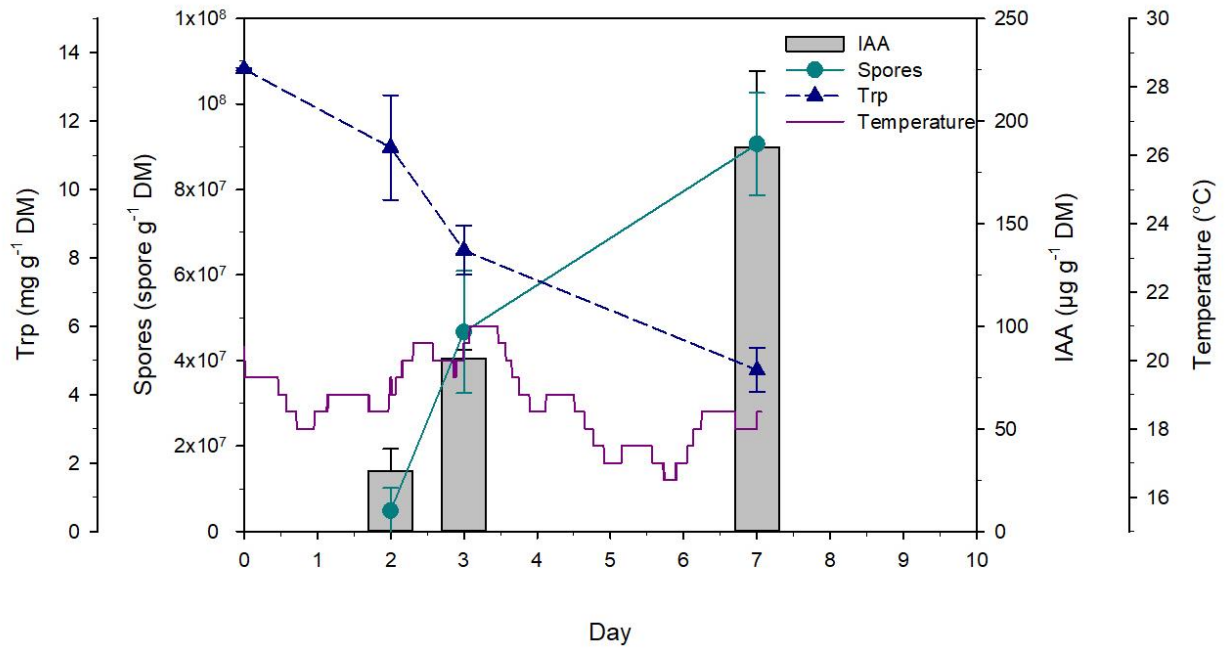


Figure 6.1. The profiles of IAA, spores, Trp, and temperature of Experiment A. The error bars correspond to the standard deviation of sample replications taken from a single tray.



Figure 6.2 SSF in tray bioreactor. a) Initial material of the fermentation, b) Fermented material after 10 days of process, c) Fermented material from a closer view to observe *Trichoderma*.

### 6.3.1.2 Second experimental setup (Experiment B and C)

The second time-course experiment was conducted with two trays inside the incubator. This experiment lasted 10 days, with samples taken on days 3, 5, 7, and 10. Here, the emission of  $\text{NH}_3$  was measured with a portable multisensor (POLI Multi-gas detector, mPower Electronics) for both trays. The results are presented in Figure 6.3 and Figure 6.4.

For tray 1 (the upper tray) which is called Experiment B, the maximum IAA production was observed on day 5 ( $128 \pm 29 \mu\text{g g}^{-1} \text{DM}$ ), after which it decreased to  $0.0 \mu\text{g g}^{-1} \text{DM}$  on day 10. Sporulation peaked on day 7 at a concentration of  $1.1 \times 10^9 \pm 3.5 \times 10^8$  spores  $\text{g}^{-1} \text{DM}$ . The initial concentration of Trp dropped from  $14.9 \pm 0.6 \text{ mg g}^{-1} \text{DM}$  to  $3.8 \text{ mg g}^{-1} \text{DM}$  on day 3 and continued to decrease slightly until day 5. The amount of Trp on days 7 and 10 was so low that ( $<0.5 \text{ mg g}^{-1} \text{DM}$ ) could not be detected through the current HPLC methodology. The temperature ranged from a minimum of  $18.0^\circ\text{C}$  to a maximum of  $23.0^\circ\text{C}$ . The  $\text{NH}_3$  profile showed a peak on day 2 at 24 ppm, a decrease by day 5, and a second peak on day 7 at 32 ppm. The level of  $\text{NH}_3$  emitted from the process is too low compared to other studies. For example,  $\text{NH}_3$  emission of organic fraction of municipal solid wastes from a 50 L reactor was reported around 1000 ppm (Maulini-Duran et al., 2014). The maximum  $\text{NH}_3$  emission of the mixture of hair waste with sludge while winterization residue with sludge during SSF were 500 and 100 ppm respectively (Maulini-Duran et al., 2015).

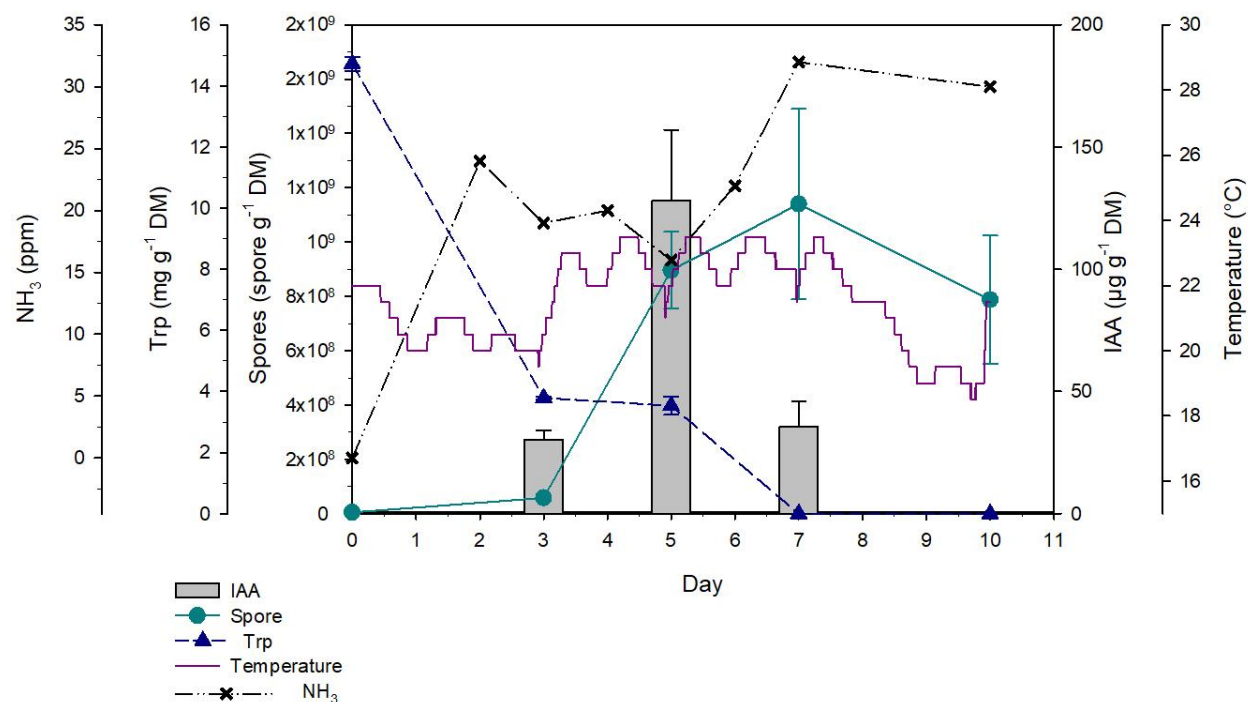


Figure 6.3. The profiles of IAA, spores, Trp,  $\text{NH}_3$ , and temperature of Experiment B. The error bars are the standard deviation of sample replications taken from a single tray. The Trp values lower than  $0.5 \text{ mg g}^{-1} \text{ DM}$  presented as zero in the graph.

For tray 2 (Experiment C), the IAA profile was similar to Experiment B, peaking on day 5 at  $148.8 \pm 38.6 \mu\text{g g}^{-1} \text{ DM}$ . However, the IAA level remained stable on day 7 and decreased to  $25. \pm 10 \mu\text{g g}^{-1} \text{ DM}$  by day 10. The highest spore count,  $1.1 \times 10^9 \pm 3.4 \times 10^8 \text{ spores g}^{-1} \text{ DM}$ , was observed on day 5. Trp consumption was rapid, decreasing from  $14.7 \pm 0.2 \text{ mg g}^{-1} \text{ DM}$  on day 1 to  $3.6 \pm 0.2 \text{ mg g}^{-1} \text{ DM}$  on day 5, and remained almost unchanged until day 7. The amount of Trp at day 10 was less than  $0.5 \text{ mg g}^{-1} \text{ DM}$  that was not detected by the HPLC method used in this work. The temperature ranged between  $18.0^{\circ}\text{C}$  and  $23.5^{\circ}\text{C}$ . The  $\text{NH}_3$  profile was the same as tray 1. As in

this experiment, the  $\text{NH}_3$  was measured from one point (point A, see 3.2.3), its values were the same for both trays.

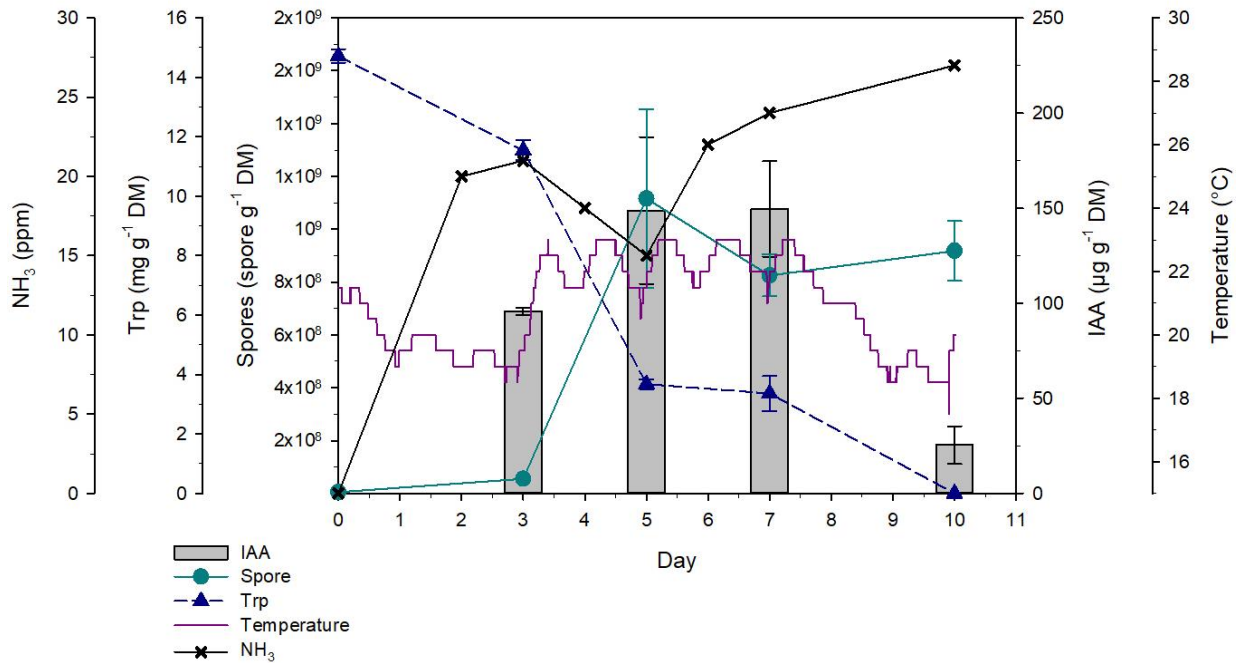


Figure 6.4. The profiles of IAA, spores, Trp,  $\text{NH}_3$ , and temperature of Experiment C. The error bars are the standard deviation of sample replications taken from a single tray. The Trp values lower than  $0.5 \text{ mg g}^{-1} \text{ DM}$  presented as zero in the graph.

### 6.3.1.3 Third experimental setup (Experiment D and control)

The third experiment was also carried out with two trays however, one tray was prepared without adding Trp as a control. Here, a new device (BIOGAS 5000 gas analyzer (GeoTech, UK)) was applied to measure  $\text{O}_2$  as well as  $\text{NH}_3$  from two points of the incubator presented in Chapter 3., Because, as commented before, the experimental system normally used to measure  $\text{O}_2$  cannot be used in this type of incubator. Figure 6.5 shows the results of the tray with Trp (the lower tray)

which is named Experiment D. conducted similarly to experiments B and C. The maximum IAA concentration was  $110.3 \pm 11.3 \mu\text{g g}^{-1} \text{DM}$  on day 5, decreasing to  $83.8 \pm 17.2 \mu\text{g g}^{-1} \text{DM}$  on day 7, and remaining steady at  $83.1 \pm 10.4 \mu\text{g g}^{-1} \text{DM}$  on day 10. Sporulation peaked on day 7 ( $9.1 \times 10^8 \pm 2.6 \times 10^8$  spores  $\text{g}^{-1} \text{DM}$ ) and remained constant on day 10 ( $9.0 \times 10^8 \pm 3.0 \times 10^8$  spores  $\text{g}^{-1} \text{DM}$ ). Trp levels decreased from  $13.5 \pm 0.8 \text{ mg g}^{-1} \text{DM}$  on the initial day to  $3.9 \text{ mg g}^{-1} \text{DM}$  at day 5. The level of Trp at days 7 and 10 was non-detectable through the current HPLC method ( $<0.5 \text{ mg g}^{-1} \text{DM}$ ). The highest and lowest temperatures in the tray were respectively  $22.5^\circ\text{C}$  and  $17.0^\circ\text{C}$ . The level of  $\text{NH}_3$  measured from point A was between 5 and 14 ppm while, at point B it was lower ranged between 5 to 10 ppm. The oxygen level profiles obtained from points A and B were similar. The oxygen level reduced to 20.7% of the air in both points (Figure 6.6) meaning the airflow was enough) to maintain aerobic conditions.



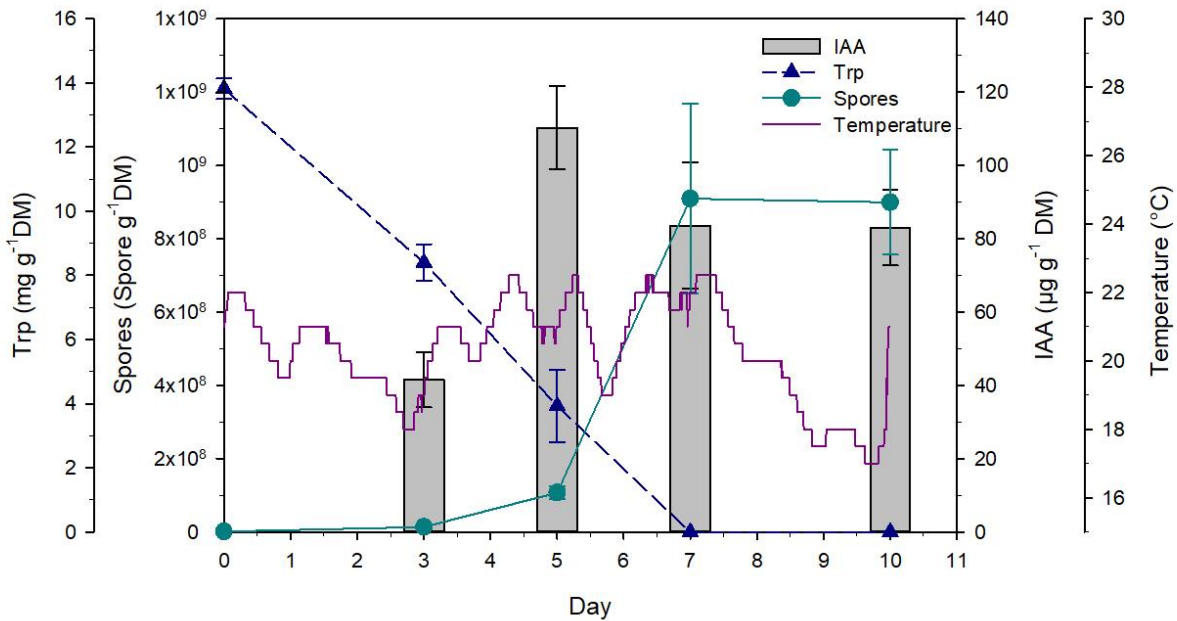


Figure 6.5. The profiles of IAA, spores, Trp, and temperature of Experiment D. The error bars are the standard deviation of sample replications taken from a single tray. The Trp values lower than  $0.5 \text{ mg g}^{-1} \text{ DM}$  presented as zero in the graph.

In the other tray (the upper one), the fermentation was performed without adding Trp which was a 7-day time course (a control) (Figure 6.7). As can be seen, the production of IAA was very low in this experiment. The maximum production was  $9 \pm 3 \text{ µg g}^{-1} \text{ DM}$  at day 7. The spore count was also at the highest level on day 7 of the fermentation ( $1.5 \times 10^9 \pm 4.7 \times 10^8 \text{ spores g}^{-1} \text{ DM}$ ). While the temperature ranged between  $18.0$  and  $22.0^\circ\text{C}$ . The profile of  $\text{NH}_3$  and  $\text{O}_2$  were similar to experiment D.

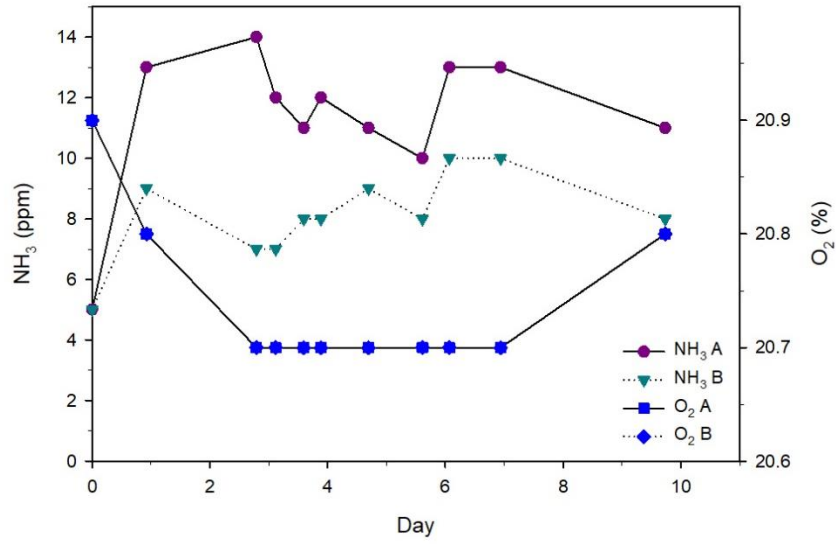


Figure 6.6. The profiles of NH<sub>3</sub>, and oxygen from points A and B of the incubator for experiment with no Trp and experiment D.

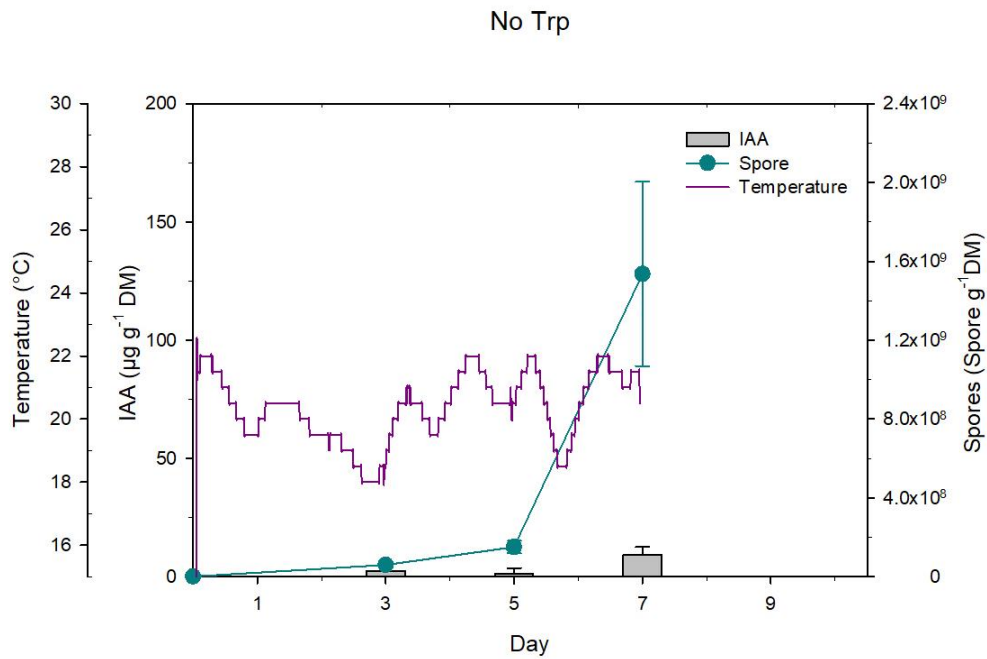


Figure 6.7. The profiles of IAA, spores, and temperature of experiment with no Trp. The error bars are the standard deviation of sample replications taken from a single tray.

Although experiments A, B, C, and D were conducted under the same conditions, the results show variations in the profiles, particularly for IAA. As mentioned in Chapter 5, one of the advantages of tray reactors over other configurations, such as packed bed reactors, is their reduced result heterogeneity. However, studies on tray bioreactors for SSF have also noted variability in parameters throughout the process (Samadi et al., 2016; Sentís-Moré et al., 2023).

By looking more deeply into the current results, some logical patterns can be observed. These patterns are illustrated in the profiles of each parameter for all experiments, as presented in Figure 6.8. As can be seen in Figure 6.8a, in all experiments, IAA production increased until day 5. On day 5, the minimum variability of IAA production was seen between experiments. However, on day 7 and 10, the IAA production continued much differently for each experiment. On day 7, in experiment A, IAA increased. For experiments B and D, IAA decreased on day 7 of fermentation. However, in experiment C, the amount of IAA did not change on day 7. On day 10, IAA decreased in experiments C and D while, it did not change in experiment B. (No data for experiment A on day 10). The maximum IAA production was observed in experiment A on day 7 which was  $201 \pm 23 \mu\text{g g}^{-1} \text{DM}$ .

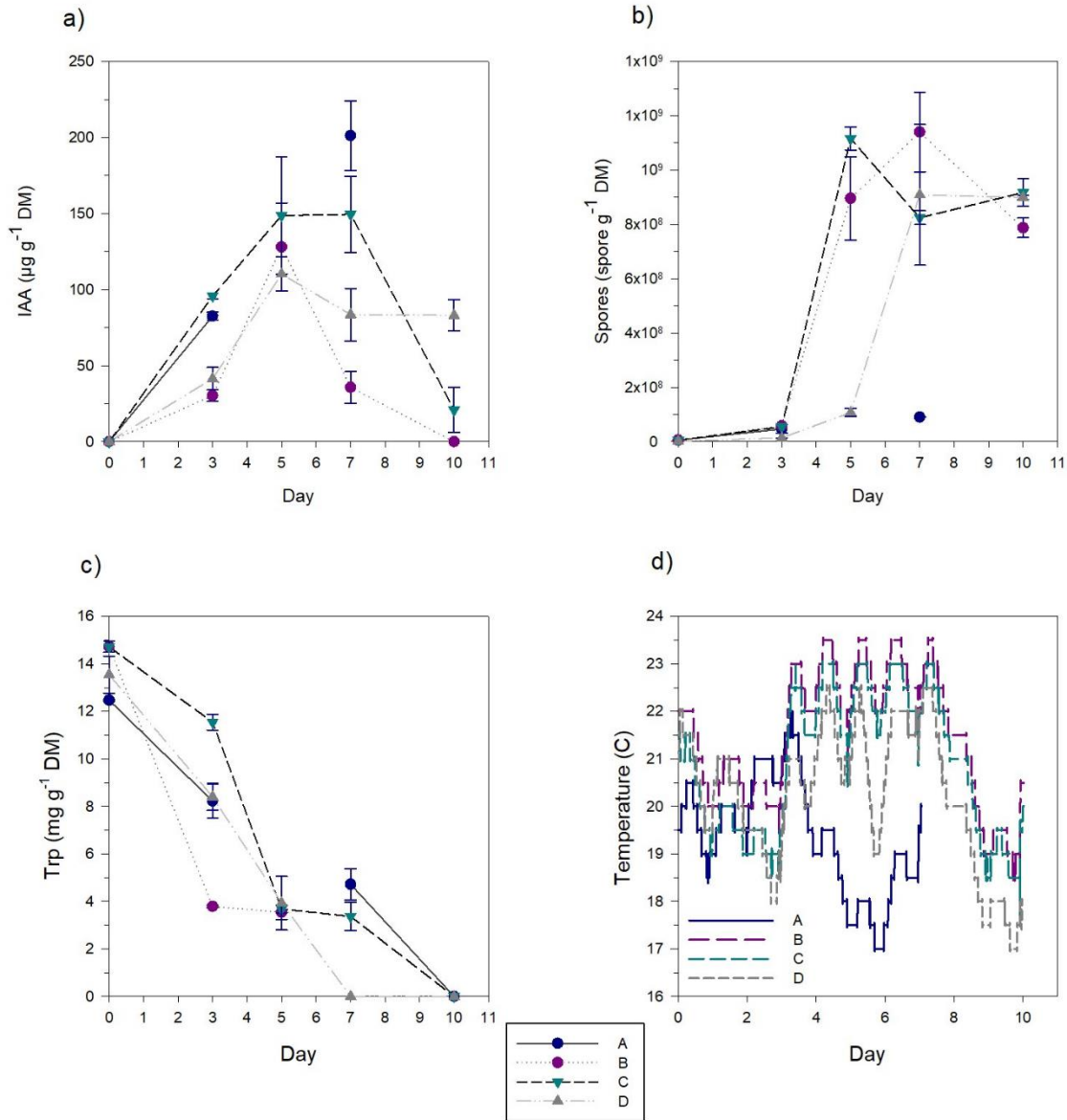


Figure 6.8. All profiles of IAA, number of spores, Trp, and temperature for experiments A, B, C, and D. a) IAA, b) Number of spores, c) Trp, d) Temperature. The error bars are the standard deviation of sample replications taken from a single tray. The Trp values lower than  $0.5 \text{ mg g}^{-1} \text{ DM}$  presented as zero in the graph.

For the spore production (Figure 6.8b), the profiles indicated that the maximum spore production was  $1.1 \times 10^9 \pm 3.2 \times 10^8 \text{ spore g}^{-1} \text{ DM}$  which was obtained in experiment B on day 7. The number

of spores was in a similar range ( $8.0 \times 10^8$ -  $1.0 \times 10^9$  spore  $\text{g}^{-1}$  DM) in all experiments except for experiment A where the sporulation was much lower than the others (around  $10^7$  spore  $\text{g}^{-1}$  DM). The sporulation increased until day 7 except for experiment B. On day 10, the number of spores was similar to all the experiments, but the profiles did not show the same trend.

As presented in Figure 6.8c, the initial level of Trp was measured in a range of 13.5-14.9  $\text{mg g}^{-1}$  DM for the experiments. It was found that Trp was consumed rapidly until day 5 and the level of Trp was in a similar range in all the experiments. After day 5, the consumption of Trp continues with a slower rate resulting in more varied values of Trp at day 7. However, the final concentrations of Trp at day 10 for all the experiments were so low that could not be detected.

It was explained in Chapter 33.2.3 that, although the trays were placed inside the incubator, the system for controlling the temperature was turned off and the temperature of the process was affected by the room temperature. To monitor the alteration of temperature, two temperature sensors were placed in each tray and the results are presented in Figure 6.8d. The temperature profiles were similar in experiments B, C and D. The declining trend of the temperature was observed after day 7 of the fermentation. The temperature ranged between 23.5 and 17.0 °C. However, in experiment A, the temperature decreased to 17.0 °C after 3 days and the maximum temperature did not go above 22.0 °C.

#### **6.3.1.4 Principal components analysis (PCA)**

To better understand the relationship between IAA and other parameters in the different experiments, a PCA and a regression analysis were conducted. The values used for these analyses are IAA, number of conidial spores, the amount of Trp consumed in percentage from the final of

## Chapter 6

fermentation, as listed in Table 6.2. The results of the PCA are presented in Table 6.3 and Figure 6.9.

Table 6.2 The values of IAA, number of spores, Trp, and temperature obtained from experiments A, B, C, and D. All the values have one replication. All the values of Trp consumed that are more than 90% considered 100% for PCA and regression analysis.

Experiment	IAA ( $\mu\text{g g}^{-1}$ DM)	Spore (spores $\text{g}^{-1}$ DM)	Trp Consumed (%)	Temperature Max ( $^{\circ}\text{C}$ )
A	181.57	$8.96 \times 10^7$	69.23	22
A	221.11	$9.16 \times 10^7$	61.02	22
B	0	$8.13 \times 10^8$	> 90	23
B	0	$7.62 \times 10^8$	> 90	23.5
C	33.47	$8.82 \times 10^8$	> 90	23.5
C	8.13	$9.54 \times 10^8$	> 90	23
D	90.90	$8.93 \times 10^8$	> 90	22.5
D	75.23	$9.06 \times 10^8$	> 90	22.5

Table 6.3 The eigenvalues and variance percentage of each component in PCA

PCA component	Eigenvalue	Variance (%)	Cumulative variance (%)
PC1	3.5733	89.3	89.3
PC2	0.3506	8.8	98.1
PC3	0.0612	1.5	99.6
PC4	0.0148	0.04	100

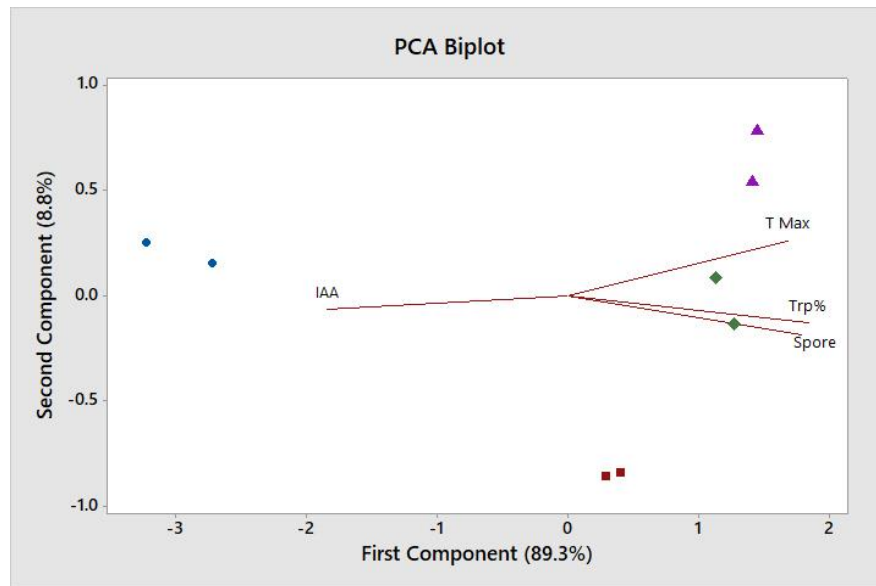


Figure 6.9 The biplot of the first two components of PCA. The data have been separated based on maximum temperature: blue circles, maximum temperature of 22°C; red squares, 22.5°C; green diamonds, 23°C; and purple triangles, 23.5°C.

According to Table 4.1Table 6.3, almost 98% of the data variance is explained by two principal components (PC1 and PC2). The biplot of PC1 and PC2 (Figure 6.9) reveals that sporulation, temperature, and the consumed Trp are relevant factors on the final IAA levels. The data indicate that higher final IAA corresponds with lower spore counts and lower levels of Trp consumption. Additionally, elevated IAA levels are related to a lower maximum temperature. On the other hand, spore production appeared to be highly dependent on the Trp consumed and relatively associated with the maximum temperature.

To obtain more data, linear regressions of IAA, Trp consumed, number of spores and maximum temperature were performed and are presented in Figure 6.10. Table 6.4 also presents the  $R^2$  and the p-values of the regression analysis. As it can be seen, IAA with Trp consumed, spores, and

## Chapter 6

maximum temperature were negatively related. While the number of spores is positively related to the consumption of Trp. The relationships of the number of spores with maximum temperature, and that of between Trp consumed and maximum temperature appeared not highly dependent together with the  $R^2$  values of 51.0 % and 58.9 %, respectively. However, the relations are statistically significant ( $p < 0.05$ ). Altogether, the results of the regressions and PCA showed a similar outcome.

When the optimization model was developed in Chapter 4, it was also observed that the relationship between IAA production and sporulation are negatively correlated. However, initial Trp was found to affect positively IAA production. This discrepancy can be attributed to the fact that in Chapter 4 only the initial Trp levels were considered, whereas the current analysis considers final Trp levels as they fluctuate during fermentation, influenced by other parameters. Both here and in Chapter 1, it is evident that the spore counts are affected by the level of Trp.

The outcomes of the four tray fermentations, analyzed using PCA and linear regression, indicate that the variation in IAA levels after day 5 of fermentation is linked to the activity of TH, as showed by fungal sporulation. The findings suggest that TH utilizes Trp for sporulation, and when Trp levels become insufficient, the fungus begins degrading IAA, probably to be used for sporulation. This consumption of IAA by TH has been also observed in Chapter 4. As previously noted, Trp is a rare amino acid that requires significant energy for biosynthesis by microorganisms (Tang et al., 2023). It serves as a crucial precursor for many physiological processes, both in its original form and as a degraded indole form (Engin et al., 2015). Additionally, Trp has been reported to be involved in the pathogenesis of *Aspergillus fumigatus* (Templeton et al., 2018).



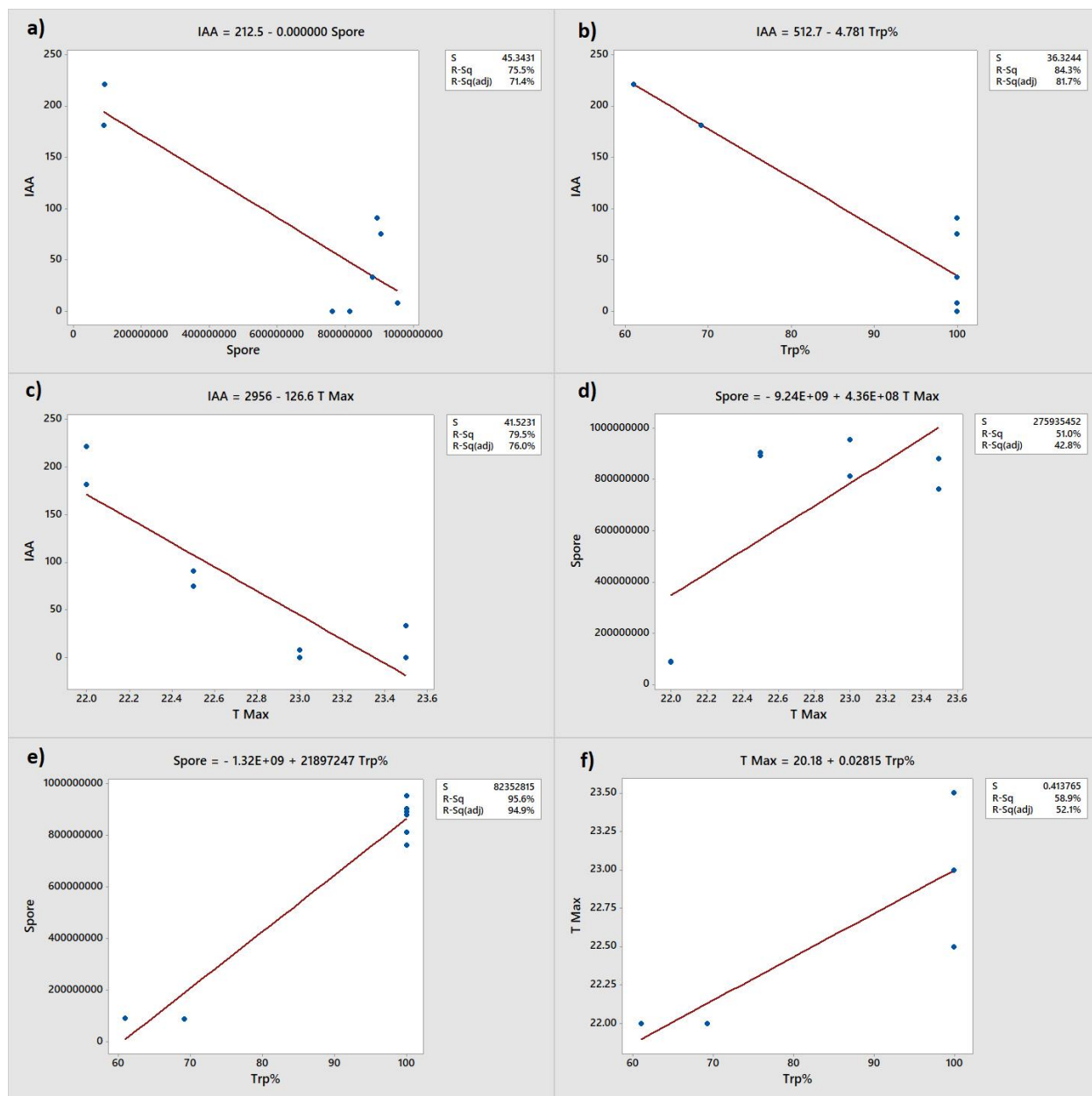


Figure 6.10. The linear regressions of a) IAA and spores, b) IAA and consumed Trp, c) IAA and maximum temperature, d) spores and maximum temperature, e) spores and consumed Trp, and f) maximum temperature and consumed Trp.

Table 6.4. The R<sup>2</sup> and P value of the different regressions performed with the data from tray reactors.

Parameters	R <sup>2</sup> (%)	P value
<b>IAA vs Trp consumed</b>	75.5	0.001
<b>IAA vs Spores</b>	84.3	0.005
<b>IAA vs Temperature max</b>	79.5	0.003
<b>Spores vs Trp consumed</b>	95.6	0.000
<b>Spores vs Temperature max</b>	51.0	0.015
<b>Trp consumed vs Temperature max</b>	58.9	0.026

Furthermore, evidence shows that IAA in microorganisms is not only a secondary metabolite secreted from the cell but also a molecule that regulates various microbial processes related to growth, stress adaptation, and communication with other microorganisms (Duca and Glick, 2020). Studies show that different concentrations of IAA have both promoting and inhibitory effects on microbial growth. For instance, *Saccharomyces cerevisiae* was showed as highly sensitive to high concentrations (5000  $\mu\text{M}$ ) of IAA, while the same concentration did not affect *Ustilago esculenta* (Sun et al., 2014). Low concentrations (0.5, 5, and 50  $\mu\text{M}$ ) of IAA promoted the growth of *Fusarium delphinoides*, but high concentrations (500 and 5000  $\mu\text{M}$ ) inhibited its growth. In contrast, in *Fusarium graminearum* a growth inhibition was observed at any concentration of exogenous IAA (Tang et al., 2023).

On the other hand, the obtained data suggested that when the temperature was below 18°C, IAA degradation stopped or decreased because of the lower activity of TH. PCA and linear regression analysis also confirm a negative relationship between maximum temperature and final IAA level.

It has been observed that certain genes involved in the metabolism of IAA are expressed under stress conditions. In *Azospirillum brasilense*, IAA production has been found to increase under carbon limitation, reduced growth rate, and acidic pH conditions (Spaepen et al., 2007). Conversely, another study on *Azospirillum brasilense* indicated that IAA production decreases under various stress conditions such as high temperatures (45°C) and the presence of chemicals like NaCl and H<sub>2</sub>O<sub>2</sub> (Molina et al., 2018). These studies indicate that the behavior of microorganisms related to IAA production varies significantly under different environmental conditions. Therefore, controlling IAA biosynthesis in a heterogeneous and more realistic process like SSF, which naturally has more unknown contributing factors, is complicated. It requires more detailed work focusing on the effects of environmental stresses on IAA production.

### **6.3.2 SSF in tray experiments with low temperature**

As described in 6.3.1 and 6.3.1.4, the varying degradation IAA post-production appears to be influenced by the activity of TH, which is related to temperature. It is assumed that the IAA degradation after it is produced can be stopped or decreased at low temperature as a result of low activity of TH. To examine the effect of low temperature on IAA profile, two experiments were conducted over 10 days under different temperature regimens. In these two regimens, the initial temperature was kept at minimum range that TH could start growing, then decreased after three days to reduce the activity of the fungus. All experimental conditions were consistent with those described in section 6.3.1, except for the controlled temperature.

### 6.3.2.1 Temperature regimen 1

In the first regimen, the temperature was maintained at 22.5 °C for the initial three days, then decreased to 20.0 °C for the remainder of the experiment. The experiment was carried out with one tray. But two conditions were applied in a single tray as follows: the tray was divided into two equal parts using metal mesh sheets, as showed in Figure 6.11. In one part, SSF was performed with the same conditions as the experiments A to D. In the other part, an SSF was performed with 0.2% (w/w) of Trp while, the other parameters were similar to the previous experiments. As explained in 6.3.2, it seems that by decreasing the temperature, the rate of Trp consumption as well as IAA degradation decreased. To test if it is possible to reduce the amount of Trp to reduce the costs of the process and keep the production high at low temperature, a fermentation was performed using 0.2% (w/w) of Trp.



Figure 6.11 Performing SSF in one tray with conditions. a) SSF with 0.2% Trp, b) SSF with 0.2% (left) and 0.43 (right) % Trp, c) Final appearance of SSF tray reactor.

Figure 6.12 showed the results of fermentation with 0.43% of Trp. Here, IAA production peaked at  $171.4 \pm 7.2 \mu\text{g g}^{-1}$  dry matter (DM) on day 5, followed by degradation starting on day 7, with a final value of  $129.23 \pm 0.90 \mu\text{g g}^{-1}$  DM by day 10. Maximum sporulation was observed on day 10, with  $2.0 \times 10^8 \pm 1.5 \times 10^7$  spores  $\text{g}^{-1}$  DM. The consumption of Trp showed a decreasing trend until

day 7. Then, the value remained almost unchanged at day 10 with the final concentration of  $3.9 \pm 0.2 \text{ mg g}^{-1} \text{ DM}$ . These results suggest that while IAA degradation continued after day 5, the rate of both IAA degradation and Trp consumption slowed due to the lower temperature after day 3.

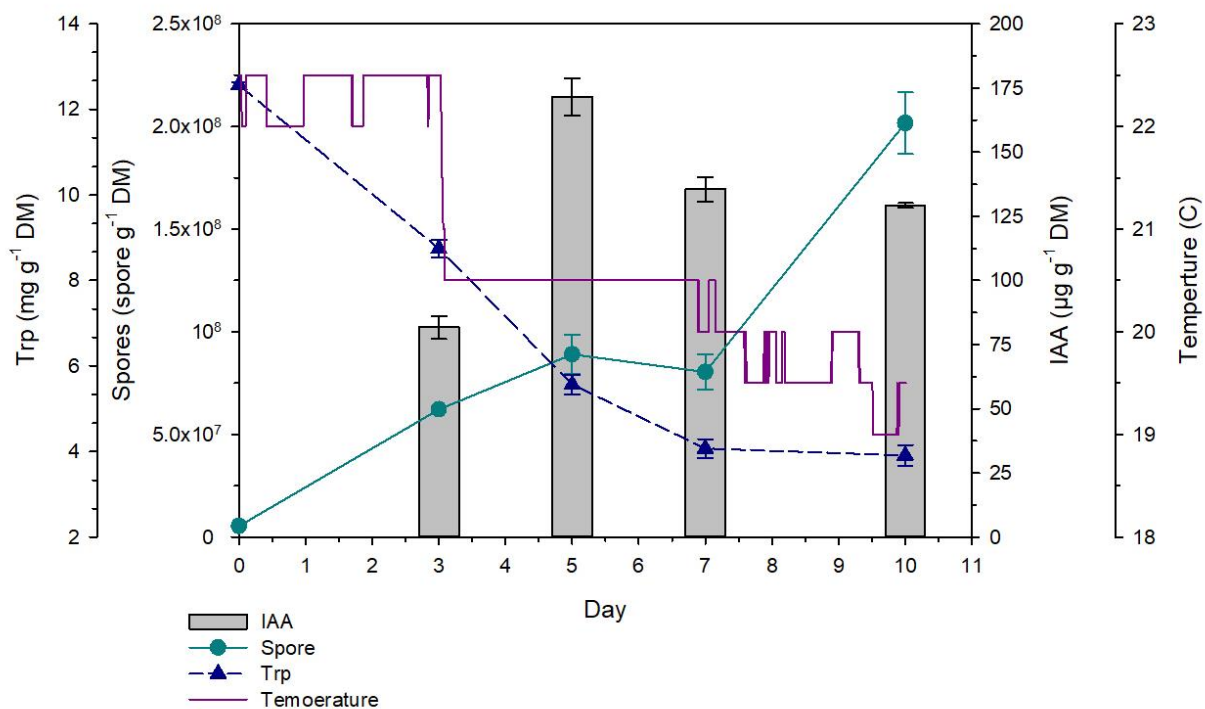


Figure 6.12. The profiles of IAA, spores, Trp, and temperature of experiment with 0.43% (w/w) Trp under temperature regimen 1. The error bars are the standard deviation of sample replications taken from distinct parts of the tray for an individual experiment.

The results of fermentation with 0.2% Trp is illustrated in Figure 6.13. As can be seen, the level of IAA produced is lower than the produced with Trp 0.43%. IAA production peaked at day 7 of fermentation with a value of  $53 \pm 9 \mu\text{g g}^{-1} \text{ DM}$ . While the maximum spore count observed at day 10 of fermentation ( $1.2 \times 10^8 \pm 7.5 \times 10^6 \text{ spores g}^{-1} \text{ DM}$ ). The initial concentration of Trp was  $6.3 \pm 0.2 \text{ mg g}^{-1} \text{ DM}$  most of which was consumed before day 7.

These results suggest that reducing the amount of Trp directly affects the IAA production. It seems the priority of fungus to use Trp is not for IAA production. This supports the results obtained from the 22 L packed bed reactor which has been described in Chapter 5.

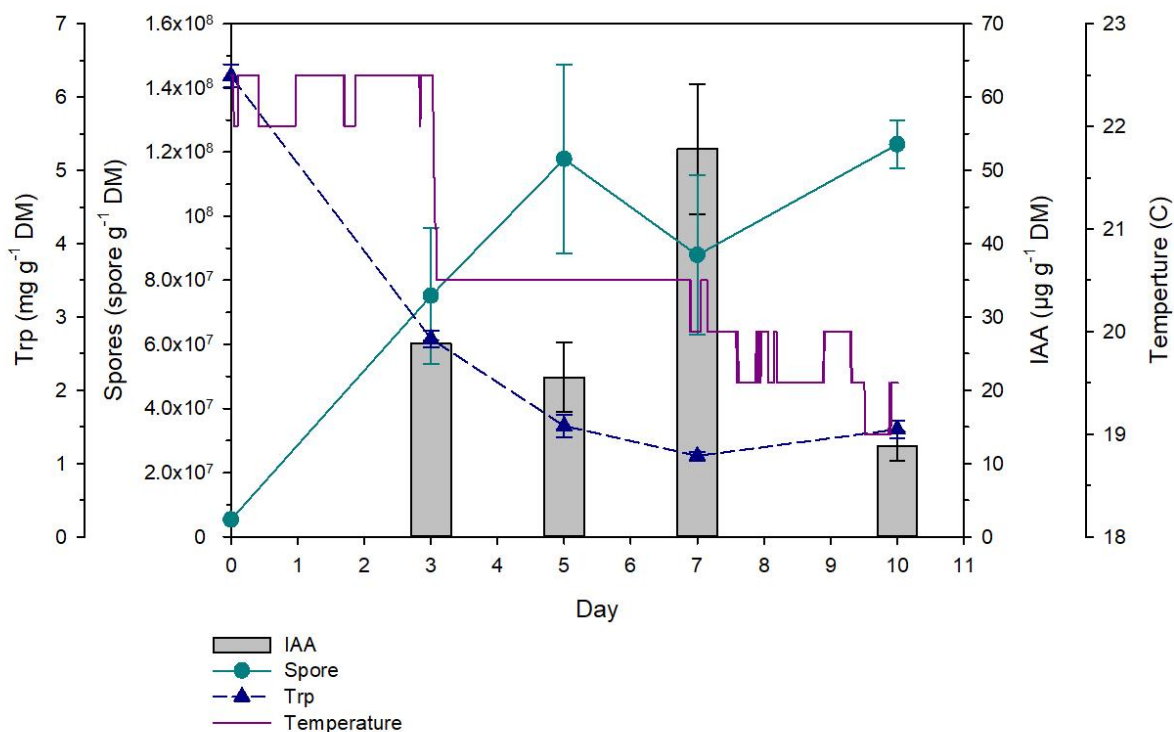


Figure 6.13. The profiles of IAA, spores, Trp, and temperature of experiment with 0.2% (w/w) Trp under temperature regimen 1. The error bars are the standard deviation of sample replications taken from distinct parts of the tray for an individual experiment.

The profiles of exhausted  $\text{NH}_3$  and  $\text{O}_2$  for the fermentations with 0.2% and 0.43% of Trp were the same and are presented in Figure 6.14. The oxygen level measured at point A decreased from 20.9% to 20.6% after nearly 2 days, while at point B, the minimum oxygen level was 20.7%. Because the difference between the two points is negligible, this suggests that the air distribution inside the incubator is almost the same as what was observed in the last experiment.

The  $\text{NH}_3$  concentrations exhausted from the incubator were low. The values ranged from 0 to 5 ppm at point A and from 0 to 3 ppm at point B.

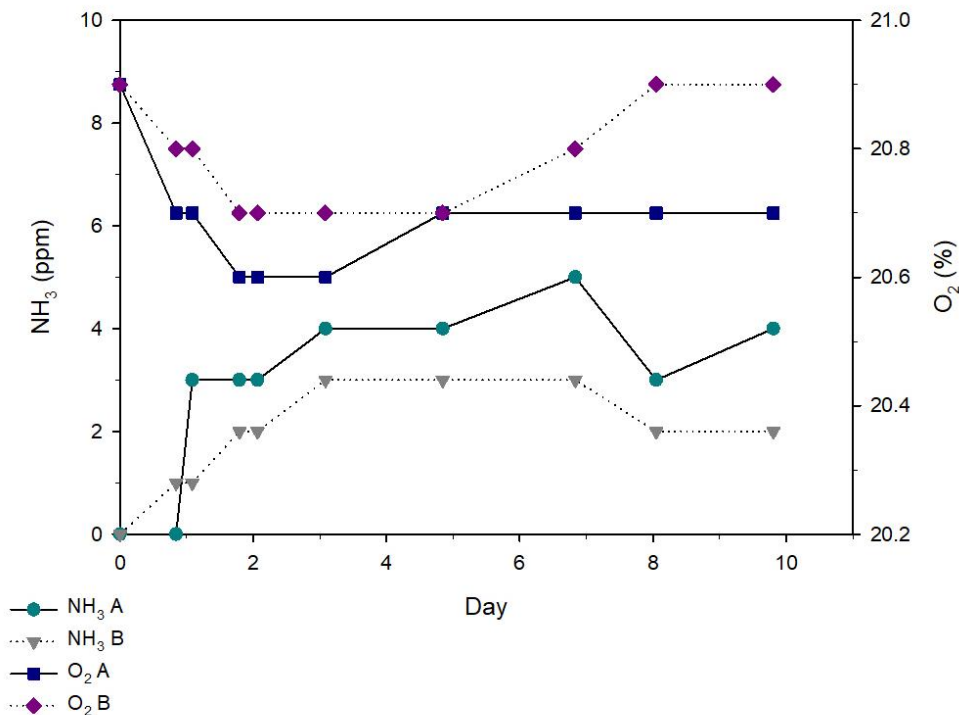


Figure 6.14. The profiles of  $\text{NH}_3$  and oxygen from points A and B of the incubator of the experiment under temperature regimen 1.

### 6.3.2.2 Temperature Regimen 2

As observed, IAA degraded slightly at the given temperature during the first regimen. Therefore, in the second regimen, the temperature was decreased to more closely match the profile of Experiment A, which showed high IAA production. The temperature was set at 21.5 °C which is the average of the initial temperatures observed in Experiment A for the first three days. It was then reduced to 18.0 °C, the minimum temperature that the incubator could maintain. As shown in Figure 6.15a, IAA levels increased over the ten days, reaching a maximum of  $199.9 \pm 15.7 \mu\text{g g}^{-1}$

## Chapter 6

DM on day 10. Sporulation also increased, with the highest spore count recorded on day 10 ( $1.6 \times 10^8 \pm 2.7 \times 10^7$  spores  $\text{g}^{-1}$  DM). The profile of Trp levels was similar to the profile observed in the first regimen for the initial five days, but from day 5 to day 10, Trp levels remained relatively constant. The final Trp concentration on day 10 was  $4.99 \pm 0.04$  mg  $\text{g}^{-1}$  DM, higher than in the previous experiment.

The oxygen level measured at point A was slightly lower than at point B (Figure 6.15b). The lowest levels were observed after 2 days, with 20.5% at point A and 20.6% at point B. Subsequently, the oxygen levels at both points increased and remained almost unchanged until the end of the fermentation. For  $\text{NH}_3$ , similar profiles were observed at points A and B, although the  $\text{NH}_3$  level at point B was slightly lower. The values ranged from 0 to 6 ppm at point A and from 0 to 5 ppm at point B. The exhausted  $\text{NH}_3$  levels were relatively low in all experiments. However,  $\text{NH}_3$  values were higher when measured with the POLI Multi-gas detector, likely due to the use of a different device. When using the BIOGAS 5000 gas analyzer,  $\text{NH}_3$  levels were higher for experiments D and without Trp because these values were derived from two trays for both experiments, whereas for the other experiments, the values were from a single tray. Nevertheless, as mentioned earlier, the level of  $\text{NH}_3$  in these experiments is very low compared to the  $\text{NH}_3$  levels measured in other studies from different kinds of organic wastes. The  $\text{NH}_3$  emissions of the organic fraction of municipal solid waste was processed in a 50 L reactor reported around 1000 ppm (Maulini-Duran et al., 2014). Similarly, the level of  $\text{NH}_3$  was between 1000 to 2000 ppm for the from a school food waste (Madrini et al., 2016).

These findings indicate that maintaining a lower temperature ( $18^\circ\text{C}$ ) not only prevented IAA degradation but also promoted continuous production. Thus, this regimen yielded more favorable results compared to the higher temperature regimen.



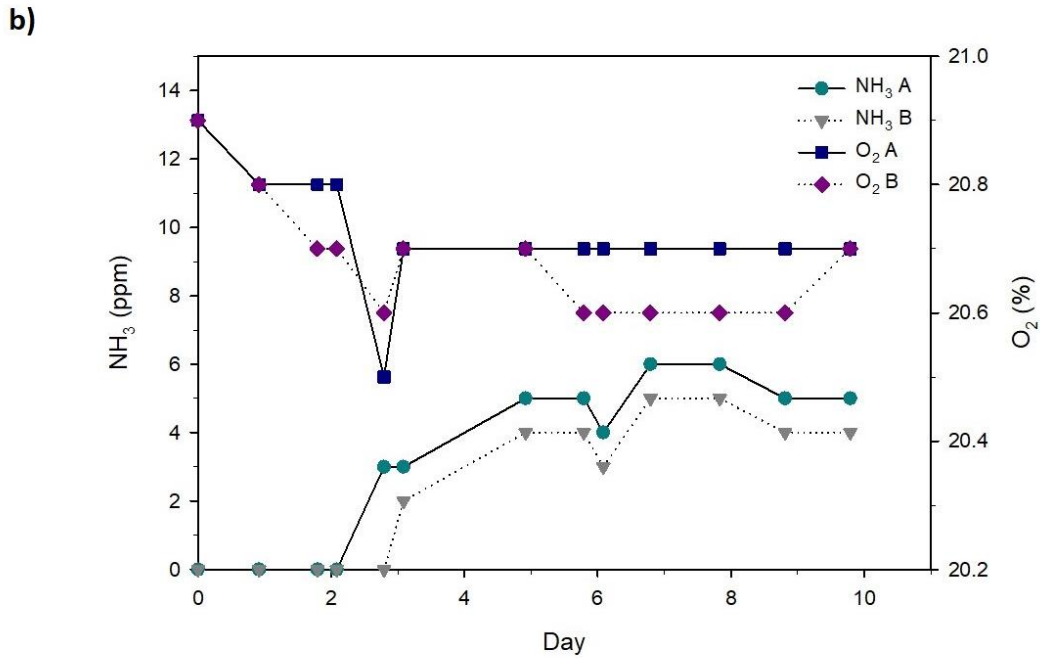
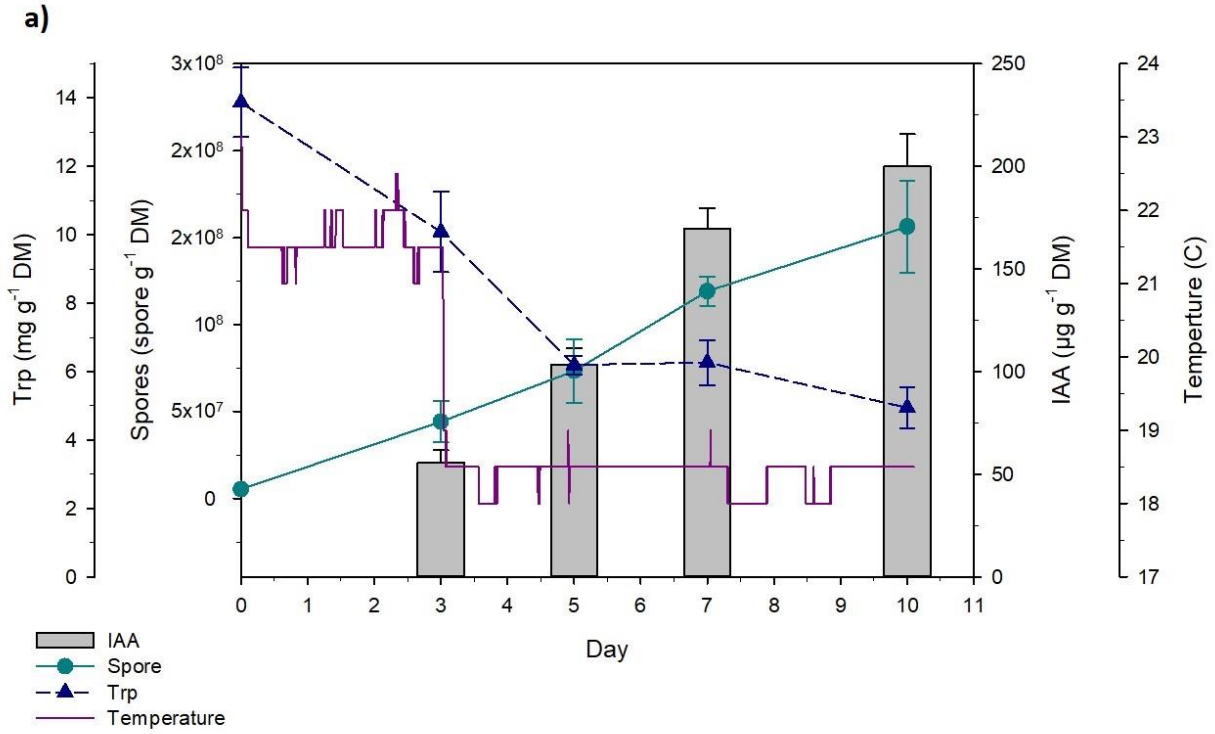


Figure 6.15. The results of SSF under temperature regimen 2. a) The profiles of IAA, spores, Trp, and temperature.

b) The profiles of NH<sub>3</sub> and oxygen from point A and B of the incubator. The error bars are the standard deviation of sample replications taken from a single tray.

Recent studies have explored the optimization of tray bioreactors for SSF. Sentís-Moré et al. (Sentís-Moré et al., 2023) investigated the effects of temperature and relative humidity on protein modification in oilseed meals, revealing stratification within the bioreactor trays. Dallastra et al. (Daize et al., 2023) developed a novel pilot-scale tray bioreactor with integrated upstream operations, showing improved fungus and lipase production. Samadi et al. (Samadi et al., 2016) optimized SSF conditions for single-cell protein production using sugarcane bagasse as substrate. They identified optimal parameters for moisture content, fermentation time, and temperature. Gujarathi et al. (Gujarathi et al., 2015) applied multi-objective optimization to SSF processes, considering enzyme activity, fermentation time, and product yield. These studies highlight the importance of controlling environmental conditions, such as temperature and humidity, in tray bioreactors (Sentís-Moré et al., 2023; Samadi et al., 2016).

As explained in detail in Chapter 4 and Chapter 5, IAA production through SSF has been less explored compared to liquid and submerged methods. Compared to the few similar studies that have been described previously, IAA can be produced in varying quantities depending on the substrate, the producer microorganisms, and the fermentation method. To the best of the authors' knowledge, this work is the first attempt to use a tray bioreactor to produce biostimulants using GW under realistic conditions. Moreover, introducing a temperature regimen as a new effective strategy to keep the IAA levels high is a great achievement. Therefore, the results obtained in this study represent a significant advance in promoting sustainable GW valorization within the framework of a circular economy.

#### **6.4 The comparison of the results obtained in 22 L packed bed reactor and tray reactor**

Table 6.5 compares data obtained from SSF in the tray reactor and the 22 L packed bed reactor for the production of IAA and conidial spores. The results using tray reactors ( $201.3 \mu\text{g g}^{-1} \text{DM}$ ) show an almost two-fold increase in IAA production compared to the results from the 22 L packed bed reactor, which was  $119.9 \mu\text{g g}^{-1} \text{DM}$ . While the maximum sporulation was similar in both reactor configurations, a wider range of variation was observed in the tray bioreactor. The fermentation duration was longer in trays, with maximum IAA production occurring later, between days 5 to 10 of fermentation. In contrast, the 22 L reactor process was shorter, with maximum IAA production achieved on day 3. This means that the time for maximum production of IAA and is not similar causing higher productivity for IAA in 22 L reactor with a maximum value of  $40 \mu\text{g g}^{-1} \text{DM d}^{-1}$ , while the productivity of IAA in the tray is maximum  $29 \mu\text{g g}^{-1} \text{DM d}^{-1}$ . The maximum productivity observed in the 22 L reactor and tray reactor is in a similar range with a lower minimum value in the tray reactor. The difference in the timing of the process is likely due to the different configurations and temperature strategy. In trays, the temperature remained low even when not controlled, owing to different aeration. The airflow for the reactors was selected based on the superficial velocity per dry mass, which was similar for both configurations, ranging from  $2.0 \times 10^{-3}$  to  $3.3 \times 10^{-3} \text{ cm g}^{-1} \text{DM min}^{-1}$ . However, in tray reactors, the specific airflow was  $2.9\text{--}3.7 \text{ mL min}^{-1} \text{ g}^{-1} \text{DM}$ , which was higher than in the 22 L reactor ( $0.9\text{--}1.1 \text{ mL min}^{-1} \text{ g}^{-1} \text{DM}$ ). A higher specific airflow indicates that more air is provided per unit of dry mass. Additionally, in the tray reactors it is easier to main the porosity as the final porosity of the materials is more in tray than in the 22 L reactor.

## Chapter 6

The maximum sOUR obtained in the tray bioreactor was much lower than in the 22 L reactor, possibly due to the lower activity of TH at lower temperatures and due to the difficulty in measuring oxygen consumption with lower airflow. It is important to note that the sensor for measuring oxygen in trays was different from that used in the 22 L reactor, which may be a reason for some of the sOUR differences.

The final pH in trays was lower with less variation, while in the 22 L reactor, the pH was higher with a wider range of alteration. The final moisture content in the tray reactor was low with high variation probably due to the different aeration system, whereas the 22 L reactor had high final moisture with less variation. The initial moisture content for both reactors was similar, around 72-73%. The temperature in the tray reactor (when not controlled) did not increase significantly, while the 22 L reactor exhibited higher temperatures during the process.

Table 6.5 Values obtained from fermentations conducted in the tray reactor and the 22 L reactor.

	<b>Tray Reactor</b>	<b>22L Reactor</b>
<b>IAA (<math>\mu\text{g g}^{-1}\text{DM}</math>)</b>	110-201	62-120
<b>IAA productivity (<math>\mu\text{g g}^{-1}\text{DM d}^{-1}</math>)</b>	19-29	20-40
<b>Spores (spores <math>\text{g}^{-1}\text{DM}</math>)</b>	$9.0 \times 10^7 - 1.1 \times 10^9$	$9.5 \times 10^8 - 1.3 \times 10^9$
<b>Spores' productivity (spores <math>\text{g}^{-1}\text{DM d}^{-1}</math>)</b>	$1.6 \times 10^7 - 1.6 \times 10^8$	$1.4 \times 10^8 - 4.3 \times 10^8$
<b>Maximum sOUR (<math>\text{g O}_2 \text{kg}^{-1}\text{DM h}^{-1}</math>)</b>	0.5-1.4	0.9-1.8
<b>Airflow (<math>\text{mL min}^{-1}</math>)</b>	500-1000	1000
<b>Specific airflow (<math>\text{mL min}^{-1} \text{g}^{-1}\text{DM}</math>)</b>	2.9-3.7	0.9-1.1
<b>Superficial velocity (<math>\text{cm min}^{-1}</math>)</b>	0.46-0.91	2.12
<b>Specific superficial velocity (<math>\text{cm g}^{-1}\text{DM min}^{-1}</math>)</b>	$2.6 \times 10^3 - 3.3 \times 10^3$	$2.0 \times 10^3 - 2.4 \times 10^3$
<b>Fermentation duration (day)</b>	7-10	3-7
<b>Maximum production of IAA (day)</b>	5-10	3
<b>Final pH</b>	7.7-8.0	7.7-8.6
<b>Final moisture (%)</b>	50-65	72-79
<b>Final Porosity (%)</b>	84-89	62-69
<b>Temperature (<math>^{\circ}\text{C}</math>)</b>	17-23.5	24-37

These findings suggest that the tray bioreactor is a more adequate configuration for producing IAA by TH using GW. As previously mentioned, the tray bioreactor is a popular configuration for conducting an SSF process at a pilot scale, especially when working with fungi as the inoculum. Numerous studies document the use of tray bioreactors for producing various enzymes, biofuels, and other products through SSF. Some studies have indicated that using a tray bioreactor enhances yield. For example, one study reported a 2.5-fold increase in xylanase production by *Aspergillus*

*niger* when using tray reactors compared to SSF in flasks (Khanahmadi et al., 2018). Sala et al. (Sala et al., 2022) compared different reactor configurations for producing biopesticides using beer draff and rice husk with two strains, *Trichoderma hazianum*, and *Beauveria bassiana*. They showed that tray bioreactors can increase production due to more effective heat removal compared to compact bed reactors. More efficient heat removal is another appealing advantage offered by tray reactors (Arora et al., 2018). As the outcome of this work indicates, low temperature improves IAA production. Therefore, using a tray bioreactor that maintains a temperature as low as 18°C (with the help of a cooling system) is crucial to prevent IAA degradation and enhance yield. This configuration facilitates scale-up by increasing the number of trays while maintaining the same bed height. Moreover, this reactor design is functional for experimental setups, allowing for multiple tests to be performed simultaneously, saving time and energy. Hence, it can be inferred that a well-designed reactor with the right configuration could play a decisive role in the successful large-scale production of IAA through SSF.

However, at research level studies, despite the advantages of tray reactors inside an incubator, some drawbacks have been observed. One drawback is that gas measurement cannot be done independently for each tray if there is more than one tray in the incubator. Another disadvantage observed in this work was the variation in results from the tray reactor. To address this, it was suggested to keep the temperature low, and this strategy proved successful. However, when the process temperature was controlled, the ventilation system of the incubator worked to keep the temperature low, resulting in moisture loss in the material despite periodic moisturizing during fermentation. As is presented in Table 6.6, the initial moisture content for all experiments ranged from 68% to 72%. When the temperature was controlled, the final moisture content was reduced

to 49-56%. However, when the temperature was not controlled, the final moisture content was higher, ranging from 60% to 65%.

Table 6.6 The moisture content of all the tray experiments.

Experiment	Temperature	Day 0	Day 2	Day 3	Day 5	Day 7	Day 10
	controlled						
<b>A</b>	No	69.1 ± 0.3	68.8 ± 0.6	67.0 ± 0.3		60.4 ± 1.4	
<b>B</b>	No	72.7 ± 2.1		70.5 ± 0.7	67.9 ± 3.8	74.3 ± 0.4	61.8 ± 0.4
<b>C</b>	No	72.7 ± 2.1		74.3 ± 1.7	66.5 ± 1.2	71.5 ± 3.1	65.4 ± 1.5
<b>D</b>	No	71.6 ± 0.4		69.8 ± 0.1	68.0 ± 1.6	63.2	65.7 ± 1.6
<b>No Trp</b>	No	69.9 ± 4.1		72.2 ± 0.6	65.6 ± 0.1	70.9 ± 2.4	63.2 ± 1.2
<b>Regimen 1 (0.43% Trp)</b>	Yes	69.4 ± 0.1			57.7		50.3
<b>Regimen 1 (0.2% Trp)</b>	Yes	69.1 ± 1.8			58.3		49.1
<b>Regimen 2</b>	Yes	71.1 ± 0.7		66.6 ± 0.0	60.3 ± 0.4	62.7 ± 0.8	56.2 ± 2.6

Altogether, controlling the temperature in the current tray bioreactor design appeared to lead to other parameters, such as moisture, becoming more difficult to control. Therefore, it is recommended to develop more effective strategies for moisturizing the material, such as automatic watering, or to use incubators that can control the temperature and humidity. Despite the disadvantages of the current ventilation system, the existing setup remains functional.

## **6.5 Conclusion**

The outcome of SSFs in a tray reactor for producing IAA and TH conidial spores using GW suggested a highly productive process. PCA analysis showed that the variation in the final products was related to the temperature in the latter part of the process. Therefore, a low-temperature regimen was recommended to increase IAA production and prevent its degradation, and this strategy proved effective. This reactor design allows for maintaining a low process temperature, thereby preventing IAA degradation and increasing production.

The tray bioreactor showed a more advantageous configuration for SSF biostimulant production compared to the 22 L packed bed reactor to produce IAA providing an aeration system to reduce heat removal. The results of this study present an innovative approach to increase the efficiency of SSF for producing biostimulants and biopesticides, as well as valorizing GW.



## Chapter 7

# Conclusions and Future Remarks

---

## 7.1 General conclusions

- This is the first work that valorizes green waste through solid-state fermentation at the laboratory scale and bench-scale to produce biostimulant (Indole-3-acetic acid) and biopesticide (conidial spores).
- Solid-state fermentation was conducted successfully using green waste as substrate to produce IAA and conidial spores of *Trichoderma harzianum*.
- Simple and low-cost conditioning was found to facilitate the use of green waste for *T. harzianum*.
- The effect of moisture of the substrate, the grass and pruning waste content, and the amount of added Trp was analyzed, and a model was developed to optimize the simultaneous production of IAA and conidial spores. The results showed that the optimized parameters for maximum production of IAA and spores are different.
- The effect of other parameters including temperature and time of fermentation also confirmed the different conditions to have maximum IAA and spores. According to the results of the time course experiment, the maximum IAA level was observed at day 3 of fermentation ( $101.4 \mu\text{g g}^{-1} \text{DM}$ ) while the maximum spore count was at day 7 of fermentation ( $3.0 \times 10^9 \text{ spores g}^{-1} \text{DM}$ ).
- The application of SSF product (as a liquid extract) on the germination of cucumber seeds suggested the positive effect of the SSF liquid extract on seed germination.
- IAA and conidial spore were produced successfully  $119.9 \mu\text{g g}^{-1} \text{DM}$  of IAA and  $1.3 \times 10^9$  spores  $\text{g}^{-1} \text{DM}$  of spores in a 22 L packed bed reactor using green waste as substrate at the optimal conditions determined at lab scale.

- Porosity was found to be a key factor in performing a successful SSF obtained by using a suitable bulking agent (wood chips).
- Green waste was found to be a challenging substrate to perform sequential batch operation due to the contamination issues arising from its complex composition.
- The effect of different concentrations of Trp and IAA on spore germination of *T. harzianum* was studied, revealing that lower concentrations of IAA and Trp positively influence spore germination, while higher concentrations have a negative effect.
- The SSF with green waste to produce IAA and spores was studied in a tray bioreactor. Despite variations in the results, the highest IAA production in this study was achieved in tray configuration with the value of 201.3  $\mu\text{g g}^{-1}$  DM.
- PCA and regression analysis indicated a negative relationship between the final IAA concentration and the final Trp consumed, the final spore count, and the maximum process temperature. Conversely, a positive relationship was found between spore count, Trp consumption, and maximum temperature. Therefore, the final concentrations of IAA and spores are specially influenced by temperature, which in turn affects the activity of *T. harzianum*.
- Based on the results of multiple tray experiments and the findings from PCA and regression analysis, a new strategy was developed to maintain high IAA production and prevent its degradation. This strategy involves starting the process at a temperature of around 21-25°C, which is subsequently controlled to a lower temperature (18°C) to reduce the activity of *T. harzianum*, thereby preventing the fungus from degrading and consuming IAA.

- Comparing the outcomes of 22 L and tray reactors, a tray reactor appeared to be a more advantageous configuration to produce IAA through SSF. This is due to the different system that the tray configuration offers, which particularly affects porosity, humidity and air distribution inside the reactor, making it more suitable for fermentation using fungi that produce aerial spores. different aeration system that is more suitable for the fermentations applying fungi that produce aerial spores.

### **7.2 Future Works**

Since this was the first work using green waste to produce biostimulants at GICOM research group, the focus of the work was on the fermentation process and its optimization. Therefore, further research is needed to gain a deeper understanding of the downstream processes and the application of SSF products:

- Further studies are required to provide more knowledge to overcome the problems of using GW in larger scales of SSF.
- It is recommended to scale up IAA and spore production using a new design of tray bioreactor that simultaneously controls temperature and moisture, with the capability to increase the number of trays.
- The recovery of IAA should be improved, and its stability should be determined under different conditions.
- It is recommended to investigate different application methods of SSF products, specially the fermented solid containing IAA on plants to assess the effects of IAA on plant growth and to develop an efficient formulation.

# Chapter 8

## References

---

## References

- Abraham J, Gea T, Komilis D, Sánchez A, 2017. Reproducibility of solid-state fermentation at bench-scale: the case of protease production. *Glob. NEST J.* 19, 183–190.
- Adav, S.S., Chao, L.T., Sze, S.K., 2012. Quantitative secretomic analysis of *Trichoderma reesei* strains reveals enzymatic composition for lignocellulosic biomass degradation. *Mol. Cell. Proteomics* 11, M111.012419-1. <https://doi.org/10.1074/mcp.M111.012419>
- Apine, O.A., Jadhav, J.P., 2011. Optimization of medium for indole-3-acetic acid production using *Pantoea agglomerans* strain PVM. *J. Appl. Microbiol.* 110, 1235–1244. <https://doi.org/10.1111/j.1365-2672.2011.04976.x>
- Arora, S., Rani, R., Ghosh, S., 2018. Review Bioreactors in solid state fermentation technology: Design, applications and engineering aspects. <https://doi.org/10.1016/j.jbiotec.2018.01.010>
- Ballardo, C., Barrena, R., Artola, A., Sánchez, A., 2017. A novel strategy for producing compost with enhanced biopesticide properties through solid-state fermentation of biowaste and inoculation with *Bacillus thuringiensis*. *Waste Manag.* 70, 53–58. <https://doi.org/10.1016/j.wasman.2017.09.041>
- Baltazar, M., Correia, S., Guinan, K.J., Sujeeth, N., Bragança, R., Gonçalves, B., 2021. Recent Advances in the Molecular Effects of Biostimulants in Plants: An Overview. *Biomolecules* 11, 1096. <https://doi.org/10.3390/BIOM11081096>
- Barrena, R., Gea, T., Ponsá, S., Ruggieri, L., Artola, A., Font, X., Sánchez, A., 2011. Categorizing Raw Organic Material Biodegradability Via Respiration Activity Measurement: A Review. *Compost Sci. Util.* 19, 105–113. <https://doi.org/10.1080/1065657X.2011.10736985>

- Betiku, E., Ishola, M.M., 2023. Bioethanol: A Green Energy Substitute for Fossil Fuels.  
<https://doi.org/10.1007/978-3-031-36542-3>
- Bharucha, U., Patel, K., Trivedi, U.B., 2013. Optimization of Indole Acetic Acid Production by *Pseudomonas putida* UB1 and its Effect as Plant Growth-Promoting Rhizobacteria on Mustard (*Brassica nigra*). *Agric. Res.* 2, 215–221. <https://doi.org/10.1007/S40003-013-0065-7/TABLES/2>
- Blasi, A., Verardi, A., Lopresto, C.G., Siciliano, S., Sangiorgio, P., 2023. Lignocellulosic Agricultural Waste Valorization to Obtain Valuable Products: An Overview. *Recycl.* 2023, Vol. 8, Page 61 8, 61. <https://doi.org/10.3390/RECYCLING8040061>
- Boonmahome, P., Mongkoltharuk, W., 2023. Characterization of indole-3-acetic acid biosynthesis and stability from *Micrococcus luteus*.  
<https://doi.org/10.7324/JABB.2023.117202>
- Bunsangiam, S., Thongpae, N., Limtong, S., Srisuk, N., 2021. Large scale production of indole-3-acetic acid and evaluation of the inhibitory effect of indole-3-acetic acid on weed growth. *Sci. Reports* 2021 11 11, 1–13. <https://doi.org/10.1038/s41598-021-92305-w>
- C. Solano, G. Ghoreishi, A. Sanchez, R. Barrena, X. Font, C. Ballardo, A.A., 2024. Solid-state fermentation of green waste for the production of biostimulants to enhance lettuce (*Lactuca sativa* L.) cultivation under water stress: closing the organic waste cycle.
- Casciadori, F.P., Laurentino, C.L., Taboga, S.R., Casciadori, P.A., Thoméo, J.C., 2014. Structural properties of beds packed with agro-industrial solid by-products applicable for solid-state fermentation: Experimental data and effects on process performance. *Chem. Eng. J.* 255, 214–224. <https://doi.org/10.1016/J.CEJ.2014.06.040>
- Castiglione, A.M., Mannino, G., Contartese, V., Berteà, C.M., Ertani, A., 2021. Microbial

Biostimulants as Response to Modern Agriculture Needs: Composition, Role and Application of These Innovative Products. *Plants* 2021, Vol. 10, Page 1533 10, 1533.

<https://doi.org/10.3390/PLANTS10081533>

Cavalcante, R.S., Lima, H.L.S., Pinto, G.A.S., Gava, C.A.T., Rodrigues, S., 2008. Effect of moisture on trichoderma conidia production on corn and wheat bran by solid state fermentation. *Food Bioprocess Technol.* 1, 100–104. <https://doi.org/10.1007/S11947-007-0034-X/TABLES/3>

Cerda, A., Gea, T., Vargas-García, C., Sánchez, A., 2017. Towards a competitive solid state fermentation: Cellulases production from coffee husk by sequential batch operation and role of microbial diversity. *Sci. Total Environ. J.* 589, 56–65.

<https://doi.org/10.1016/j.scitotenv.2017.02.184>

Chen, Y., Wu, C., Fan, X., Zhao, Xinqing, Zhao, Xihua, Shen, T., Wei, D., Wang, W., 2020. Engineering of *Trichoderma reesei* for enhanced degradation of lignocellulosic biomass by truncation of the cellulase activator ACE3. *Biotechnol. Biofuels* 13, 1–14.

<https://doi.org/10.1186/S13068-020-01701-3/FIGURES/6>

Chilakamarry, C.R., Sakinah, A.M.M., Zularisam, A.W., Sirohi, R., Khilji, I.A., Ahmad, N., Pandey, A., 2022. Advances in solid-state fermentation for bioconversion of agricultural wastes to value-added products: Opportunities and challenges. *Bioresour. Technol.* 343, 960–8524. <https://doi.org/10.1016/j.biortech.2021.126065>

Daize, E., Dallastra, G., Caroline, A., Dias, P., Benevides De Morais, P., Fonseca Moreira Da Silva, J., Casciadori, F.P., Grajales, L.M., 2023. Development of a novel pilot-scale tray bioreactor for solid-state fermentation aiming at process intensification Solid-State Fermentation (SSF) processes have high contamination and low productivity rates, since it



- involves batch processes with multiple manual stages. *Chem. Eng. Process. Process Intensif.* 193, 109526. <https://doi.org/10.1016/j.cep.2023.109526>
- de Rezende, L.C., de Andrade Carvalho, A.L., Costa, L.B., de Almeida Halfeld-Vieira, B., Silva, L.G., Pinto, Z.V., Morandi, M.A.B., de Medeiros, F.H.V., Mascarin, G.M., Bettioli, W., 2020. Optimizing mass production of *Trichoderma asperelloides* by submerged liquid fermentation and its antagonism against *Sclerotinia sclerotiorum*. *World J. Microbiol. Biotechnol.* 36, 1–14. <https://doi.org/10.1007/s11274-020-02882-7>
- du Jardin, P., 2015. Plant biostimulants: Definition, concept, main categories and regulation. *Sci. Hortic. (Amsterdam)*. 196, 3–14. <https://doi.org/10.1016/j.scienta.2015.09.021>
- Duca, D.R., Glick, B.R., 2020. Indole-3-acetic acid biosynthesis and its regulation in plant-associated bacteria. *Appl. Microbiol. Biotechnol.* 2020 10420 104, 8607–8619. <https://doi.org/10.1007/S00253-020-10869-5>
- Engin, A., Basak, A., Editors, E., 2015. *Molecular and Integrative Toxicology Tryptophan Metabolism: Implications for Biological Processes, Health and Disease*, Humana Press.
- Eras-Muñoz, E., Gea, T., Font, X., 2023. Carbon and nitrogen optimization in solid-state fermentation for sustainable sophorolipid production using industrial waste. *Front. Bioeng. Biotechnol.* 11, 1252733. <https://doi.org/10.3389/FBIOE.2023.1252733/BIBTEX>
- Figueroa-Montero, A., Esparza-Isunza, T., Saucedo-Castañeda, G., Huerta-Ochoa, S., Gutiérrez-Rojas, M., Favela-Torres, E., 2011. Improvement of heat removal in solid-state fermentation tray bioreactors by forced air convection. *J. Chem. Technol. Biotechnol.* 86, 1321–1331. <https://doi.org/10.1002/JCTB.2637>
- Ghoreishi, G., Barrena, R., Font, X., 2023. Using green waste as substrate to produce biostimulant and biopesticide products through solid-state fermentation. *Waste Manag.* 159,

84–92. <https://doi.org/10.1016/j.wasman.2023.01.026>

Giri, R., Sharma, R.K., 2020. Fungal pretreatment of lignocellulosic biomass for the production of plant hormone by *Pichia fermentans* under submerged conditions. *Bioresour. Bioprocess.* 7, 1–11. <https://doi.org/10.1186/S40643-020-00319-5/FIGURES/5>

Goswami, D., Thakker, J.N., Dhandhukia, P.C., 2015. Simultaneous detection and quantification of indole-3-acetic acid (IAA) and indole-3-butyric acid (IBA) produced by rhizobacteria from l-tryptophan (Trp) using HPTLC. *J. Microbiol. Methods* 110, 7–14. <https://doi.org/10.1016/j.mimet.2015.01.001>

Gravel, V.V., Antoun, H., Tweddell, R.J., 2007. Growth stimulation and fruit yield improvement of greenhouse tomato plants by inoculation with *Pseudomonas putida* or *Trichoderma atroviride*: Possible role of indole acetic acid (IAA). *Soil Biol. Biochem.* 39, 1968–1977. <https://doi.org/10.1016/j.soilbio.2007.02.015>

Gujarathi, A.M., Sadaphal, A., Bathe, G.A., 2015. Multi-Objective Optimization of Solid State Fermentation Process. *Mater. Manuf. Process.* 30, 511–519. <https://doi.org/10.1080/10426914.2014.984209>

Guo, S., Dong, X., Liu, K., Yu, H., Zhu, C., 2015. Chemical, energetic, and structural characteristics of hydrothermal carbonization solid products for lawn grass. *BioResources* 10, 4613–4625. <https://doi.org/10.15376/biores.10.3.4613-4625>

Hamrouni, R., Molinet, J., Dupuy, N., Taieb, N., Carboue, Q., Masmoudi, A., Roussos, S., 2020. The Effect of Aeration for 6-Pentyl-alpha-pyrone, *Conidia* and Lytic Enzymes Production by *Trichoderma asperellum* Strains Grown in Solid-State Fermentation. *Waste and Biomass Valorization* 11, 5711–5720. <https://doi.org/10.1007/S12649-019-00809-4/FIGURES/3>

Illescas, M., Pedrero-Méndez, A., Pitorini-Bovolini, M., Hermosa, R., Monte, E., 2021.

- Phytohormone Production Profiles in Trichoderma Species and Their Relationship to Wheat Plant Responses to Water Stress. *Pathogens* 10, 991.  
<https://doi.org/10.3390/PATHOGENS10080991>
- Inghels, D., Dullaert, W., Bloemhof, J., 2016. A model for improving sustainable green waste recovery. *Resour. Conserv. Recycl.* 110, 61–73.  
<https://doi.org/10.1016/j.resconrec.2016.03.013>
- Jiménez-Peñalver, P., Rodríguez, A., Daverey, A., Font, X., Gea, T., 2019. Use of wastes for sophorolipids production as a transition to circular economy: state of the art and perspectives. *Rev. Environ. Sci. Biotechnol.* 18, 413–435. <https://doi.org/10.1007/s11157-019-09502-3>
- Karimi, A., Shojaosadati, S.A., Hejazi, P., Vasheghani-Farahani, E., Hashemi, M., 2014. Porosity changes during packed bed solid-state fermentation. *J. Ind. Eng. Chem.* 20, 4022–4027. <https://doi.org/10.1016/j.jiec.2014.01.001>
- Keswani, C., Singh, Satyendra Pratap, Cueto, L., García-Estrada, C., Mezaache-Aichour, S., Glare, T.R., Borriss, R., Singh, Surya Pratap, Blázquez, M.A., Sansinenea, E., 2020. Auxins of microbial origin and their use in agriculture. *Appl. Microbiol. Biotechnol.* 104, 8549–8565. <https://doi.org/10.1007/S00253-020-10890-8/FIGURES/3>
- Khanahmadi, M., Arezi, I., Amiri, M. sadat, Miranzadeh, M., 2018. Bioprocessing of agro-industrial residues for optimization of xylanase production by solid- state fermentation in flask and tray bioreactor. *Biocatal. Agric. Biotechnol.* 13, 272–282.  
<https://doi.org/10.1016/j.bcab.2018.01.005>
- Kucharska, K., Rybarczyk, P., Hołowacz, I., Łukajtis, R., Glinka, M., Kamí Nski, M., 2018. molecules Pretreatment of Lignocellulosic Materials as Substrates for Fermentation

Processes 23(11), 2937. <https://doi.org/10.3390/molecules23112937>

Kulkarni, G., Nayak, A., Sajjan, S., 2013. Indole-3-acetic acid biosynthetic pathway and aromatic amino acid aminotransferase activities in *Pantoea dispersa* strain GPK. *Artic. Lett. Appl. Microbiol.* 56, 340–347. <https://doi.org/10.1111/lam.12053>

Kumar, V., Bahuguna, A., Ramalingam, S., Kim, M., 2021. Developing a sustainable bioprocess for the cleaner production of xylooligosaccharides: An approach towards lignocellulosic waste management. *J. Clean. Prod.* 316, 128332. <https://doi.org/10.1016/J.JCLEPRO.2021.128332>

Kumla, J., Suwannarach, N., Matsui, K., Lumyong, S., 2020. Biosynthetic pathway of indole-3-acetic acid in ectomycorrhizal fungi collected from northern Thailand. *PLoS One* 15, e0227478. <https://doi.org/10.1371/JOURNAL.PONE.0227478>

Langsdorf, A., Volkmar, M., Holtmann, D., Ulber, R., 2021. Material utilization of green waste: a review on potential valorization methods. *Bioresour. Bioprocess* 8, 19. <https://doi.org/10.1186/s40643-021-00367-5>

Leasure, C.D., Chen, Y.-P., He, Z.-H., 2013. Enhancement of Indole-3-Acetic Acid Photodegradation by Vitamin B6. <https://doi.org/10.1093/mp/sst089>

Leite, P., Sousa, D., Fernandes, H., Ferreira, M., Rita Costa, A., Filipe, D., Gonçalves, M., Peres, H., Belo, I., Salgado, J.M., 2020. Recent advances in production of lignocellulolytic enzymes by solid-state fermentation of agro-industrial wastes. <https://doi.org/10.1016/j.cogsc.2020.100407>

Li, W., Zhao, L., He, X., 2022. Degradation potential of different lignocellulosic residues by *Trichoderma longibrachiatum* and *Trichoderma afroharzianum* under solid state fermentation. *Process Biochem.* 112, 6–17.

- <https://doi.org/10.1016/J.PROCBIO.2021.11.011>
- Liu, X., Xie, Y., Sheng, H., 2023. Green waste characteristics and sustainable recycling options. *Resour. Environ. Sustain.* 11, 100098. <https://doi.org/10.1016/J.RESENV.2022.100098>
- Lopes Perez, C., Casciatori, F.P., Cláudio Thoméo, J., 2018. Strategies for scaling-up packed-bed bioreactors for solid-state fermentation: The case of cellulolytic enzymes production by a thermophilic fungus. <https://doi.org/10.1016/j.cej.2018.12.169>
- López-Bucio, J., Pelagio-Flores, R., Herrera-Estrella, A., 2015. Trichoderma as biostimulant: Exploiting the multilevel properties of a plant beneficial fungus. *Sci. Hortic. (Amsterdam)*. 196, 109–123. <https://doi.org/10.1016/j.scienta.2015.08.043>
- López-Gómez, J.P., Venus, J., 2021. Potential role of sequential solid-state and submerged-liquid fermentations in a circular bioeconomy. *Fermentation* 7. <https://doi.org/10.3390/fermentation7020076>
- Luo, J., Zhou, J.J., Zhang, J.Z., 2018. Aux/IAA Gene Family in Plants: Molecular Structure, Regulation, and Function. *Int. J. Mol. Sci.* 19, 259. <https://doi.org/10.3390/IJMS19010259>
- Luo, Y., Liang, J., Zeng, G., Chen, M., Mo, D., Li, G., Zhang, D., 2018. Seed germination test for toxicity evaluation of compost : Its roles , problems and prospects. *Waste Manag.* 71, 109–114. <https://doi.org/10.1016/j.wasman.2017.09.023>
- Luziatelli, F., Ficca, A.G., Bonini, P., Muleo, R., Gatti, L., Meneghini, M., Tronati, M., Melini, F., Ruzzi, M., 2020. A Genetic and Metabolomic Perspective on the Production of Indole-3-Acetic Acid by *Pantoea agglomerans* and Use of Their Metabolites as Biostimulants in Plant Nurseries. *Front. Microbiol.* 11, 547862. <https://doi.org/10.3389/FMICB.2020.01475/BIBTEX>
- Madrini, B., Shibusawa, S., Kojima, Y., Hosaka, S., 2016. Effect of natural zeolite

(Clinoptilolite) on ammonia emissions of leftover foodrice hulls composting at the initial stage of the thermophilic process. *J. Agric. Meteorol.* 72, 12–19.

<https://doi.org/10.2480/agrmet.D-15-00012>

Malécange, M., Sergheraert, R., Teulat, B., Mounier, E., Lothier, J., Sakr, S., 2023. Biostimulant Properties of Protein Hydrolysates: Recent Advances and Future Challenges. *Int. J. Mol. Sci.* 2023, Vol. 24, Page 9714 24, 9714. <https://doi.org/10.3390/IJMS24119714>

Malleswari. D and Bagyanarayana. G, 2013. *Pantoea eucrinalis* (Cf 7) a novel plant growth promoting rhizobacterium from India | Abstract. *Ann. Biol. Res.* 139–144.

Manzo-Valencia, M.K., Valdés-Santiago, L., Sánchez-Segura, L., Guzmán-De-Peña, D.L., 2016. Naphthalene Acetic Acid Potassium Salt (NAA-K<sup>+</sup>) Affects Conidial Germination, Sporulation, Mycelial Growth, Cell Surface Morphology, and Viability of *Fusarium oxysporum* f. sp. *radici-lycopersici* and *F. oxysporum* f. sp. *cubense* in Vitro. *J. Agric. Food Chem.* 64, 8315–8323. <https://doi.org/10.1021/acs.jafc.6b03105>

Maria, A., Galletti, R., Antonetti, C., De Luise, V., Licursi, D., Nassi, N., Nasso, D., 2012. Levulinic acid from waste. *BioResources* 7, 1824–1835.

Martínez-Avila, O., Sánchezsánchez, A., Font, X., Barrena, R., 2019. Fed-Batch and Sequential-Batch Approaches To Enhance the Bioproduction of 2-Phenylethanol and 2-Phenethyl Acetate in Solid-State Fermentation Residue-Based Systems. *J. Agric. Food Chem.* 67, 3389–3399. <https://doi.org/10.1021/acs.jafc.9b00524>

Maulini-Duran, C., Abraham, J., Rodríguez-Pérez, S., Cerda, A., Jiménez-Peñalver, P., Gea, T., Barrena, R., Artola, A., Font, X., Sánchez, A., 2015. Gaseous emissions during the solid state fermentation of different wastes for enzyme production at pilot scale. *Bioresour. Technol.* 179, 211–218. <https://doi.org/10.1016/J.BIORTECH.2014.12.031>

- Maulini-Duran, C., Artola, A., Font, X., Sánchez, A., 2014. Gaseous emissions in municipal wastes composting: Effect of the bulking agent. *Bioresour. Technol.* 172, 260–268. <https://doi.org/10.1016/J.BIORTECH.2014.09.041>
- Mehmood, A., Hussain, A., Irshad, M., Hamayun, M., Iqbal, A., Khan, N., 2019. In vitro production of IAA by endophytic fungus *Aspergillus awamori* and its growth promoting activities in *Zea mays*. *Symbiosis* 77, 225–235. <https://doi.org/10.1007/S13199-018-0583-Y/FIGURES/6>
- Mejias, L., Cerda, A., Barrena, R., Gea, T., Sánchez, A., 2018. Microbial strategies for cellulase and xylanase production through solid-state fermentation of digestate from biowaste. *Sustain.* 10. <https://doi.org/10.3390/su10072433>
- Melini, F., Luziatelli, F., Bonini, P., Ficca, A.G., Melini, V., Ruzzi, M., 2023. Optimization of the growth conditions through response surface methodology and metabolomics for maximizing the auxin production by *Pantoea agglomerans* C1. *Front. Microbiol.* 14, 1022248. <https://doi.org/10.3389/FMICB.2023.1022248/BIBTEX>
- Mitchell, D.A., Pandey, A., Sangsurasak, P., Krieger, N., 1999. Scale-up strategies for packed-bed bioreactors for solid-state fermentation. *Process Biochem.* 35, 167–178. [https://doi.org/10.1016/S0032-9592\(99\)00048-5](https://doi.org/10.1016/S0032-9592(99)00048-5)
- Molina-Peñate, E., Del, M., Vargas-García, C., Artola, A., Sánchez, A., 2023. Filling in the gaps in biowaste biorefineries: The use of the solid residue after enzymatic hydrolysis for the production of biopesticides through solid-state fermentation. *Waste Manag.* 161, 92–103. <https://doi.org/10.1016/j.wasman.2023.02.029>
- Molina, R., Rivera, D., Mora, V., Gastón López, ·, Rosas, S., Spaepen, S., Vanderleyden, J., Cassán, · Fabricio, 2018. Regulation of IAA Biosynthesis in *Azospirillum brasilense* Under

## Chapter 8

Environmental Stress Conditions. *Curr. Microbiol.* 75, 1408–1418.

<https://doi.org/10.1007/s00284-018-1537-6>

Mujtaba, M., Fernandes Fraceto, L., Fazeli, M., Mukherjee, S., Savassa, S.M., Araujo de Medeiros, G., do Espírito Santo Pereira, A., Mancini, S.D., Lipponen, J., Vilaplana, F., 2023. Lignocellulosic biomass from agricultural waste to the circular economy: a review with focus on biofuels, biocomposites and bioplastics. *J. Clean. Prod.* 402, 136815.

<https://doi.org/10.1016/J.JCLEPRO.2023.136815>

Napitupulu, T.P., Kanti, A., Sudiana, I.M., 2019a. IOP Conference Series: Earth and Environmental Science Evaluation of the Environmental Factors Modulating Indole-3-acetic Acid (IAA) Production by *Trichoderma harzianum* InaCC F88. *Earth Environ. Sci. Pap.* 308. <https://doi.org/10.1088/1755-1315/308/1/012060>

Napitupulu, T.P., Kanti, A., Sudiana, I.M., 2019b. Evaluation of the Environmental Factors Modulating Indole-3-acetic Acid (IAA) Production by *Trichoderma harzianum* InaCC F88. *IOP Conf. Ser. Earth Environ. Sci.* 308, 012060. <https://doi.org/10.1088/1755-1315/308/1/012060>

Ningsih Susilowati, D., Ida Riyanti, E., Setyowati, M., Mulya, K., 2002. Indole-3-acetic acid producing bacteria and its application on the growth of rice □ Indole-3-Acetic Acid Producing Bacteria and Its Application on the Growth of Rice. *AIP Conf. Proc* 20016. <https://doi.org/10.1063/1.5050112>

Nutaratat, P., Monprasit, A., Srisuk, N., 2017. High-yield production of indole-3-acetic acid by *Enterobacter* sp. DMKU-RP206, a rice phyllosphere bacterium that possesses plant growth-promoting traits. *3 Biotech* 7, 1–15. <https://doi.org/10.1007/S13205-017-0937-9/FIGURES/6>



- Nutaratat, P., Srisuk, N., Arunrattiyakorn, P., Limtong, S., 2016. Fed-batch fermentation of indole-3-acetic acid production in stirred tank fermenter by red yeast *Rhodospiridium paludigenum*. *Biotechnol. Bioprocess Eng.* 21, 414–421. <https://doi.org/10.1007/S12257-015-0819-0/METRICS>
- Oiza, N., Moral-Vico, J., Sánchez, A., Oviedo, E.R., Gea, T., 2022. Solid-State Fermentation from Organic Wastes: A New Generation of Bioproducts. *Processes* 10, 2675. <https://doi.org/10.3390/PR10122675>
- Pallín, M.Á., González-Rodríguez, S., Eibes, G., López-Abelairas, M., Moreira, M.T., Lema, J.M., Lú-Chau, T.A., 2022. Towards industrial application of fungal pretreatment in 2G biorefinery: scale-up of solid-state fermentation of wheat straw. *Biomass Convers. Biorefinery* 1, 1–13. <https://doi.org/10.1007/S13399-022-02319-1/FIGURES/6>
- Patten, C.L., Blakney, A.J.C., Coulson, T.J.D., 2013. Activity, distribution and function of indole-3-acetic acid biosynthetic pathways in bacteria. *Crit. Rev. Microbiol.* 39, 395–415. <https://doi.org/10.3109/1040841X.2012.716819>
- Paul, S., Dutta, A., 2017. Challenges and opportunities of lignocellulosic biomass for anaerobic digestion. *Resour. Conserv. Recycl.* 130, 164–174. <https://doi.org/10.1016/j.resconrec.2017.12.005>
- Puyuelo, B., Gea, T., Sánchez, A., 2010. A new control strategy for the composting process based on the oxygen uptake rate. *Chem. Eng. J.* 165, 161–169. <https://doi.org/10.1016/J.CEJ.2010.09.011>
- Ramawat, N., Bhardwaj, V., 2022. *Biostimulants: Exploring Sources and Applications BOOK.*
- Ramprakash, B., Incharoensakdi, A., 2022. Dark fermentative hydrogen production from pretreated garden wastes by *Escherichia coli*. *Fuel* 310, 122217.

<https://doi.org/10.1016/J.FUEL.2021.122217>

Rayhane, H., Josiane, M., Gregoria, M., Yiannis, K., Dupuy, N., Ahmed, M., Sevastianos, R., 2019. From flasks to single used Bioreactor: Scale-up of solid state fermentation process for metabolites and conidia production by *Trichoderma asperellum*. *J. Environ. Manage.* 252, 109496. <https://doi.org/10.1016/j.jenvman.2019.109496>

Reineke, G., Heinze, B., Schirawski, J., Buettner, H., Kahmann, R., Basse, C.W., 2008. Indole-3-acetic acid (IAA) biosynthesis in the smut fungus *Ustilago maydis* and its relevance for increased IAA levels in infected tissue and host tumour formation. *Mol. Plant Pathol.* 9, 339–355. <https://doi.org/10.1111/J.1364-3703.2008.00470.X>

Reyes-Torres, M., Oviedo-ocaña, E.R., Dominguez, I., Komilis, D., Sánchez, A., 2018. A systematic review on the composting of green waste : Feedstock quality and optimization strategies. *Waste Manag.* 77, 486–499. <https://doi.org/10.1016/j.wasman.2018.04.037>

Rodríguez-Durá, L. V., Michel, M.R., Pichardo, A., Aguilar-Zárate, P., 2023. Microbial bioreactors for secondary metabolite production. *Microb. Bioreact. Ind. Mol.* 275–296. <https://doi.org/10.1002/9781119874096.CH13>

Rouphael, Y., Cardarelli, M., Bonini, P., Colla, G., 2017. Synergistic action of a microbial-based biostimulant and a plant derived-protein hydrolysate enhances lettuce tolerance to alkalinity and salinity. *Front. Plant Sci.* 8, 1–12. <https://doi.org/10.3389/fpls.2017.00131>

Rouphael, Y., Colla, G., 2020. Toward a sustainable agriculture through plant biostimulants: From experimental data to practical applications. *Agronomy* 10. <https://doi.org/10.3390/agronomy10101461>

Rouphael, Y., Colla, G., 2018. Synergistic biostimulatory action: Designing the next generation of plant biostimulants for sustainable agriculture. *Front. Plant Sci.* 871, 1–7.

- <https://doi.org/10.3389/fpls.2018.01655>
- Ruggieri, L., Gea, T., Artola, A., Sánchez, A., 2009. Air filled porosity measurements by air pycnometry in the composting process: A review and a correlation analysis. *Bioresour. Technol.* 100, 2655–2666. <https://doi.org/10.1016/j.biortech.2008.12.049>
- Ruggieri, L., Gea, T., Mompeó, M., Sayara, T., Sá Nchez, A., 2008. Performance of different systems for the composting of the source-selected organic fraction of municipal solid waste. *Biosyst. Eng.* 101, 78–86. <https://doi.org/10.1016/j.biosystemseng.2008.05.014>
- Rupal K, S., Raval, V.H., Saraf, M., 2020. Biosynthesis and purification of indole-3-acetic acid by halotolerant rhizobacteria isolated from Little Runn of Kachchh. *Biocatal. Agric. Biotechnol.* 23, 101435. <https://doi.org/10.1016/J.BCAB.2019.101435>
- Sala, A., Artola, A., Sánchez, A., Barrena, R., 2020. Rice husk as a source for fungal biopesticide production by solid-state fermentation using *B. bassiana* and *T. harzianum*. *Bioresour. Technol.* 296, 122322. <https://doi.org/10.1016/j.biortech.2019.122322>
- Sala, A., Barrena, R., Artola, A., Sánchez, A., 2019. Current developments in the production of fungal biological control agents by solid-state fermentation using organic solid waste. *Crit. Rev. Environ. Sci. Technol.* 49, 655–694. <https://doi.org/10.1080/10643389.2018.1557497>
- Sala, A., Barrena, R., Sánchez, A., Artola, A., 2021a. Fungal biopesticide production: Process scale-up and sequential batch mode operation with *Trichoderma harzianum* using agro-industrial solid wastes of different biodegradability. *Chem. Eng. J.* 425, 131620. <https://doi.org/10.1016/j.cej.2021.131620>
- Sala, A., Echegaray, T., Palomas, G., Boggione, M.J., Tubio, G., Barrena, R., Artola, A., 2022. Insights on fungal solid-state fermentation for waste valorization: *Conidia* and chitinase production in different reactor configurations. <https://doi.org/10.1016/j.scp.2022.100624>

## Chapter 8

- Sala, A., Vittone, S., Barrena, R., Antoni, S., Artola, A., 2021b. Scanning agro-industrial wastes as substrates for fungal biopesticide production : Use of *Beauveria bassiana* and *Trichoderma harzianum* in solid-state fermentation. *J. Environ. Manag. J.* 295. <https://doi.org/10.1016/j.jenvman.2021.113113>
- Salmenperä, H., Pitkänen, K., Kautto, P., Saikku, L., 2021. Critical factors for enhancing the circular economy in waste management. *J. Clean. Prod.* 280, 124339. <https://doi.org/10.1016/J.JCLEPRO.2020.124339>
- Samadi, S., Mohammadi, M., Najafpour, G.D., 2016. *Saccharomyces cerevisiae* in Tray Bioreactor. *Int. J. Eng.* 29, 1029–1036. <https://doi.org/10.5829/idosi.ije.2016.29.08b.01>
- Sentís-Moré, P., Romero-Fabregat, M.P., Rodríguez-Marca, C., Guerra-Sánchez, A.J., Ortega-Olivé, N., 2023. Design Optimization of a Tray Bioreactor for Solid-State Fermentation: Study of Process Parameters through Protein Modification of By-Products. *Fermentation* 9, 921. <https://doi.org/10.3390/FERMENTATION9100921>
- Shoebitz, M., Ribaudó, C.M., Pardo, M.A., Cantore, M.L., Ciampi, L., Curá, J.A., 2009. Plant growth promoting properties of a strain of *Enterobacter ludwigii* isolated from *Lolium perenne* rhizosphere. *Soil Biol. Biochem.* 41, 1768–1774. <https://doi.org/10.1016/J.SOILBIO.2007.12.031>
- Sible, C.N., Seebauer, J.R., Below, F.E., 2021. Plant Biostimulants: A Categorical Review, Their Implications for Row Crop Production, and Relation to Soil Health Indicators. *Agron.* 2021, Vol. 11, Page 1297 11, 1297. <https://doi.org/10.3390/AGRONOMY11071297>
- Singh, I., Solomon, S., Gopalakrishnan, V.A.K., Ghosh, A., 2023. Environmental benefits of an alternative practice for sugarcane cultivation using *Gracilaria*-based seaweed biostimulant. *Sugar Tech* 25, 440–452. <https://doi.org/10.1007/S12355-022-01217-0/FIGURES/5>

- Sofokleous, M., Christofi, A., Malamis, D., Mai, S., Barampouti, E.M., 2022. Bioethanol and biogas production: an alternative valorisation pathway for green waste. *Chemosphere* 296, 133970. <https://doi.org/10.1016/J.CHEMOSPHERE.2022.133970>
- Solano Porras, R.C., Artola, A., Barrena, R., Ghoreishi, G., Ballardo Matos, C., Sánchez, A., 2023. Breaking New Ground: Exploring the Promising Role of Solid-State Fermentation in Harnessing Natural Biostimulants for Sustainable Agriculture. *Processes* 11, 1–27. <https://doi.org/10.3390/pr11082300>
- Spaepen, S., Vanderleyden, J., Remans, R., 2007. Indole-3-acetic acid in microbial and microorganism-plant signaling. *FEMS Microbiol. Rev.* 31, 425–448. <https://doi.org/10.1111/j.1574-6976.2007.00072.x>
- Subash, M., Rafath, H., Lalitha, J., 2015. Influence of GA 3 and IAA and their frequency of application on seed germination and seedling quality characters. *Int. Lett. Nat. Sci.* 30, 44–48. <https://doi.org/10.56431/p-30x529>
- Suleimanova, A., Bulmakova, D., Sokolnikova, L., Egorova, E., Itkina, D., Kuzminova, O., Gizatullina, A., Sharipova, M., 2023. Phosphate Solubilization and Plant Growth Promotion by *Pantoea brenneri* Soil Isolates. *Microorganisms* 11, 1136. <https://doi.org/10.3390/MICROORGANISMS11051136/S1>
- Sun, P.-F., Fang, W.-T., Shin, L.-Y., Wei, J.-Y., Fu, S.-F., Chou, J.-Y., 2014. Indole-3-Acetic Acid-Producing Yeasts in the Phyllosphere of the Carnivorous Plant *Drosera indica* L. *PIOS* 1–22. <https://doi.org/10.1371/journal.pone>
- Tabatabaei, S., Ehsanzadeh, P., Etesami, H., Alikhani, H.A., Glick, B.R., 2016. Indole-3-acetic acid (IAA) producing *Pseudomonas* isolates inhibit seed germination and  $\alpha$ -amylase activity in durum wheat (*Triticum turgidum* L.). *Spanish J. Agric. Res.* 14, e0802–e0802.

<https://doi.org/10.5424/SJAR/2016141-8859>

Tan, E.C.D., Lamers, P., 2021. Circular Bioeconomy Concepts—A Perspective. *Front. Sustain.* 2, 701509. <https://doi.org/10.3389/FRSUS.2021.701509/BIBTEX>

Tang, J., Li, Y., Zhang, L., Mu, J., Jiang, Y., Fu, H., Zhang, Y., Cui, H., Yu, X., Ye, Z., 2023. Biosynthetic Pathways and Functions of Indole-3-Acetic Acid in Microorganisms. *Microorganisms* 11. <https://doi.org/10.3390/microorganisms11082077>

Templeton, S., Gresnigt, M.S., Krappmann, S., Keller, N.P., Choera, T., Zelante, T., Romani, L., 2018. A Multifaceted Role of Tryptophan Metabolism and indoleamine 2,3-Dioxygenase Activity in *Aspergillus fumigatus*-Host interactions. *Front. Immunol* 8, 22. <https://doi.org/10.3389/fimmu.2017.01996>

Terezinha Jung Finkler, A., Fernando de Lima Luz Jr, L., Krieger, N., Alexander Mitchell, D., Mário Jorge, L., 2021a. A model-based strategy for scaling-up traditional packed-bed bioreactors for solid-state fermentation based on measurement of O<sub>2</sub> uptake rates. *Biochem. Eng. J.* 166, 107854. <https://doi.org/10.1016/j.bej.2020.107854>

Terezinha Jung Finkler, A., Zanlorenzi Weber, M., Alexandre Fuchs, G., Aluisio Scholz, L., Fernando de Lima Luz Jr, L., Krieger, N., Alexander Mitchell, D., Mário de Matos Jorge, L., 2021b. Estimation of heat and mass transfer coefficients in a pilot packed-bed solid-state fermentation bioreactor. *Chem. Eng. J.* 408, 1385–8947. <https://doi.org/10.1016/j.cej.2020.127246>

Tomberlin, J.K., Crippen, T.L., Wu, G., Griffin, A.S., Wood, T.K., Kilner, R.M., 2017. Indole: An evolutionarily conserved influencer of behavior across kingdoms. *BioEssays* 39, 1–12. <https://doi.org/10.1002/bies.201600203>

Walterson, A.M., Stavrinides, J., 2015. *Pantoea*: insights into a highly versatile and diverse

- genus within the Enterobacteriaceae. *FEMS Microbiol. Rev.* 027, 968–984.  
<https://doi.org/10.1093/femsre/fuv027>
- Wang, Z., Piao, Y., Zhang, · Fugui, Hu, Y., Zeng, J., Nan, J., 2019. Promoting Effects on Watermelon and Fermentation Optimization of Plantibacter sp. WZW03. *J. Plant Growth Regul.* 39, 970–980. <https://doi.org/10.1007/s00344-019-10037-8>
- Woo, S.L., Pepe, O., 2018. Microbial Consortia: Promising Probiotics as Plant Biostimulants for Sustainable Agriculture. *Front. Plant Sci.* 9, 1801. <https://doi.org/10.3389/fpls.2018.01801>
- Yang, W., Zhang, L., 2022. Addition of mature compost improves the composting of green waste. *Bioresour. Technol.* 350, 126927. <https://doi.org/10.1016/j.biortech.2022.126927>
- Yazid, N.A., Barrena, R., Komilis, D., Sánchez, A., 2017. Solid-state fermentation as a novel paradigm for organic waste valorization: A review. *Sustain.* 9, 1–28.  
<https://doi.org/10.3390/su9020224>
- Yue, T., Jiang, D., Zhang, Z., Zhang, Y., Li, Y., Zhang, T., Zhang, Q., 2021. Recycling of shrub landscaping waste: Exploration of bio-hydrogen production potential and optimization of photo-fermentation bio-hydrogen production process. *Bioresour. Technol.* 331, 125048.  
<https://doi.org/10.1016/j.biortech.2021.125048>
- Zanoni do Prado, D., Okino-Delgado, C.H., Zanutto-Elgui, M.R., Silva, R.B.G. da, Pereira, M.S., Jahn, L., Ludwig-Müller, J., Silva, M.R. da, Velini, E.D., Fleuri, L.F., 2019a. Screening of *Aspergillus*, *Bacillus* and *Trichoderma* strains and influence of substrates on auxin and phytases production through solid-state fermentation. *Biocatal. Agric. Biotechnol.* 19, 101165. <https://doi.org/10.1016/j.bcab.2019.101165>
- Zanoni do Prado, D., Oliveira, S.L., Okino-Delgado, C.H., Auer, S., Ludwig-Müller, J., Ribeiro da Silva, M., Júnior da Costa Fernandes, C., Carbonari, C.A., Zambuzzi, W.F., Fleuri, L.F.,

- 2019b. *Aspergillus flavipes* as a novel biostimulant for rooting-enhancement of *Eucalyptus*. *J. Clean. Prod.* 234, 681–689. <https://doi.org/10.1016/j.jclepro.2019.06.211>
- Zhang, J., Yang, Q., 2015. Optimization of solid-state fermentation conditions for *Trichoderma harzianum* using an orthogonal test. *Genet. Mol. Res.* 14, 1771–1781. <https://doi.org/10.4238/2015.March.13.4>
- Zhang, N., Xu, H., Xie, J., Cui, J.Y., Yang, J., Zhao, J., Tong, Y., Jiang, J., 2021. Screening of Cucumber Fusarium Wilt Bio-Inhibitor: High Sporulation *Trichoderma harzianum* Mutant Cultured on Moso Bamboo Medium. *Front. Microbiol.* 12. <https://doi.org/10.3389/fmicb.2021.763006>
- Zhang, Y., Wang, L., Chen, H., 2017. Correlations of medium physical properties and process performance in solid-state fermentation. *Chem. Eng. Sci.* 165, 65–73. <https://doi.org/10.1016/J.CES.2017.02.039>
- Zhao, G., Zhong, T., 2013. Influence of exogenous IAA and GA on seed germination, vigor and their endogenous levels in *Cunninghamia lanceolata*. *Scand. J. For. Res.* 28, 511–517. <https://doi.org/10.1080/02827581.2013.783099>
- Zhao, L., Sun, Z.F., Zhang, C.C., Nan, J., Ren, N.Q., Lee, D.J., Chen, C., 2022. Advances in pretreatment of lignocellulosic biomass for bioenergy production: Challenges and perspectives. *Bioresour. Technol.* 343, 126123. <https://doi.org/10.1016/J.BIORTECH.2021.126123>
- Zhu, C., Zhang, R., Zhu, L., Zhu, R., Jiang, Y., Ni, Y., Fan, M., Li, Q., 2024. A green biomass pretreatment using iron ion-catalyzed hydrogen peroxide for lignocellulose fermentation and biofuel production. *Cellulose*. <https://doi.org/10.1007/s10570-024-06054-w>